Reviews in Mineralogy & Geochemistry
Vol. 88 pp. 809–876, 2022

Carbon and Nitrogen in Mantle-Derived Diamonds

Thomas Stachel

Earth and Atmospheric Sciences
University of Alberta
Edmonton, AB T6G 2E3, Canada

tstachel@ualberta.ca

Pierre Cartigny

Institut de physique du globe de Paris
Université de Paris
CNRS, F-75005 Paris, France

cartigny@ipgp.fr

Thomas Chacko, D. Graham Pearson

Earth and Atmospheric Sciences
University of Alberta
Edmonton, AB T6G 2E3, Canada

tchacko@ualberta.ca; gdpearso@ualberta.ca

INTRODUCTION

This chapter is devoted to the carbon and nitrogen stable isotope compositions of terrestrial diamonds with a strong focus on monocrystalline diamonds formed in Earth's mantle. The wealth of C- and N-stable isotope studies forces us to make some choices to keep this chapter within an acceptable length. Here, we focus on both the ground-breaking early diamond stable isotope studies as well as the latest developments in the field. Using a comprehensive database of diamond stable isotope data compiled from literature, we examine key constraints on diamond-forming processes, the origins of diamond growth media and the cycling of C and N through shallow and deep Earth reservoirs.

Diamond as a unique probe to study mantle carbon and nitrogen cycles

Given its inert and resistant nature, diamond can be preserved during and following ascent from its primary stability field, located at depths > 110 km in ancient cratonic roots or the sublithospheric mantle beneath. As discussed elsewhere in this volume, through micro-scale inclusions of minerals, primarily silicates, oxides and sulfides (Stachel et al. 2022, this volume; Walter et al. 2022, this volume), and fluids (Weiss et al. 2022, this volume) entrapped during diamond growth, diamond provides unique information on the physical and chemical processes responsible for its genesis, the mineralogy of Earth's mantle, and the evolution of the lithospheric and the convecting sublithospheric mantle. Mineral- and fluid-inclusion-bearing diamonds are, however, rare, constituting only a few percent of typical mine productions.

This chapter focusses instead on the information that is carried by every diamond, i.e., its carbon (Lavoisier 1776, p. 615) and, with the exception of rare Type II diamonds, its main substitutional impurity nitrogen (Kaiser and Bond 1959). The definition of Type II diamond as containing N below the limit of detection is method-dependent but for the commonly

1529-6466/22/0088-0015$10.00 (print)
1943-2666/22/0088-0015$10.00 (online)
http://dx.doi.org/10.2138/rmg.2022.88.15

applied technique of micro-infrared spectroscopy implies N-contents below about 10 atomic ppm (at.ppm). Other substitutional or interstitial impurities, including H, B, and O, have not been applied in a consistent way to understand diamond formation and consequently are not considered here.

A diamond's journey to the surface is *unpleasant* and *unsafe* and, in some instances, only a small percentage of the original diamond load in the transporting magma may be preserved. Transport of diamond in hot, potentially oxidizing and fluid-rich kimberlite magma at depths outside its primary stability field may lead to graphitization, resorption to rounded dodecahedra, or etching (Robinson et al. 1989; Harris et al. 2022, this volume). Xenoliths and xenocrysts from the deep lithospheric mantle are often affected by alteration, re-equilibration or kimberlite metasomatism (e.g., Richardson et al. 1985; Boyd et al. 1997) and any carbonate minerals present would typically break down during final ascent. Other carbon hosts, such as graphite or carbide, cannot be unambiguously ascribed to a particular depth (Shiryaev and Gaillard 2014). Consequently, when dealing with the deep carbon cycle, diamond represents a unique probe into Earth's mantle with respect to both depth (down to ~ 800 km) and time (formation ages up to 3.5 Ga; see Smit et al. 2022, this volume). Carbon-bearing magmas, such as kimberlites, carbonatites, mid-ocean ridge basalts and ocean island basalts represent complementary sources of information but they sample/average much larger mantle volumes. Degassing and low-temperature alteration of samples are also major concerns when aiming to address, e.g., the C-isotope variability and the origin of carbon in such magmas. This explains why diamond, which retains its original isotopic composition, is a particularly valuable source of information in the study of the deep carbon cycle.

On Earth, diamond has been reported from a wide variety of geological contexts, some not relevant to this review. Meteorites can contain substantial amounts (~ 1500 ppm) of nanometer-sized diamonds: some of these nano-diamonds formed from material originally present in the solar nebula and some are of pre-solar origin (Huss 2005). The occurrence of diamond in meteorites does not necessarily require the high pressure and temperature conditions under which mantle diamonds typically grow. Considering surface energy minimization, even at low P and T conditions it is energetically more favorable to grow nanometer-sized diamond instead of graphite or other polycyclic aromatics (Badziag et al. 1990). This metastable formation mechanism allows for the precipitation of diamond from a gas phase under low-vacuum conditions (0.01–0.27 atmospheric pressure; diamond synthesis through chemical vapor deposition (CVD)). A metastable formation mechanism may also apply to nano-diamonds in melt inclusions in xenoliths from Hawaii (Wirth and Rocholl 2003) and, possibly some metamorphic diamonds, found in subducted and exhumed metamorphic rocks (Simakov 2011). At least some metamorphic diamonds, including those from the Kokchetav massif in Kazakhstan (Sobolev and Shatsky 1990), however, grew in their primary stability field, as supported by several independent geobarometers (see Chopin 2003 for review). Impact diamonds, occasionally up to 1 cm in size, occur, for example, in the Popigai and Ries impact craters (Hough et al. 1995; Koeberl et al. 1997) and are also commonly considered as being formed in their primary stability field. Impact diamonds, however, differ from mantle and metamorphic diamonds by being formed through solid state conversion of a graphite-rich target whereas mantle and metamorphic diamonds likely grow from C-rich fluids/melts (see below and Luth et al. 2022, this volume). Nano-diamonds found in uranium-rich carbonaceous sediments probably also form in the solid state but under crustal P and T conditions, through alpha particle-induced transitioning of graphite sp^2-bonds into diamond sp^3-bonds (Daulton and Ozima 1996). Among the many other forms of natural diamond, carbonado, a sintered type of polycrystalline diamond, remains the most enigmatic. Carbonados may form during meteorite impact, in Earth's mantle or in extraterrestrial environments (see Garai et al. 2006; Kagi and Fukura 2008; Cartigny 2010; Haggerty 2014 and reference therein).

Diamond types

Here we focus on the C- and N-stable isotope geochemistry of mantle-derived diamonds, which include a number of subdivisions. Not considering orogenic peridotite massifs, mantle-derived diamonds are transported to Earth's surface by kimberlites or, less commonly, by lamproites, ultramafic lamprophyres and, in one instance, komatiite (see Kjarsgaard et al. 2022, this volume).

Under the generic term '*smooth-surfaced monocrystalline diamonds*' we include smooth-faced monocrystalline diamonds that crystallized as primary octahedra, macles or cuboids and their resorption forms. All these diamonds formed prior to kimberlite activity and were therefore xenocrysts in their host kimberlite, with mantle residence times varying from several b.y. to a few hundred m.y. (Smit et al. 2022; Green et al. 2022, both this volume). The xenocrystic nature of smooth-surfaced monocrystalline diamonds is supported by advanced nitrogen aggregation states (typically Type IaAB, see Green et al. 2022, this volume) but the reverse is not true (i.e., a diamond with poorly aggregated nitrogen is not necessarily young). Based on the study of their mineral inclusions (typically about 1% of diamonds contain inclusions ≥ 100 μm in size, Stachel and Harris 2008), smooth-surfaced monocrystalline diamonds can be assigned to three particular mantle depth intervals:

1. *Lithospheric mantle (110–250 km)*. Based on their mineral inclusions, (smooth-surfaced monocrystalline) lithospheric diamonds grow in peridotitic, eclogitic or more rarely webstertic (pyroxenitic) substrates. On the basis of garnet composition and the presence of clinopyroxene, the peridotitic diamond substrates can be further subdivided into dunites-harzburgites, lherzolites, and wehrlites (Sobolev 1977; Meyer 1987; Stachel et al. 2021). Being both the most abundant and most studied type of diamond, the vast majority (> 90%) of C- and N-isotope data originate from lithospheric diamonds. Sulfide inclusion-bearing diamonds, assigned to either the peridotitic or eclogitic suite based on sulfide Ni-contents, may show geochemical characteristics, such as higher N-contents and lower N-aggregation states, that are distinct from other peridotitic or eclogitic diamonds from the same kimberlite (Cartigny et al. 2009; Thomassot et al. 2009). In such cases, a distinct diamond-forming event, possibly from a different growth medium, for sulfide-included diamonds may be invoked.

2. *Asthenosphere and transition zone (250–660 km)*. Such diamonds can be identified from the mineralogy and chemical composition of their inclusions, in particular the occurrence of majoritic garnet inclusions (Moore and Gurney 1985; Walter et al. 2021). Most diamonds of this type have silicate inclusions indicative of metabasaltic to metapyroxenitic substrates. Diamonds containing inclusions (e.g., ringwoodite; Pearson et al. 2014) indicative of a meta-peridotitic paragenesis are extremely rare. There are no mantle xenoliths that are directly derived from sublithospheric depth (see Sautter et al. 1991; Deines and Haggerty 2000 for descriptions of retrogressed, originally sublithospheric xenolith samples) and therefore, transition-zone diamonds represent a unique source of information. Although rare, nearly every available *asthenospheric and transition-zone* diamond has been studied for its stable isotopic composition.

3. *Lower mantle (> 660 km)*. Diamonds from the lower mantle can be identified from their co-existing silicate (bridgmanite and CaSi-perovskite) and oxide (ferropericlase) inclusions (see Walter et al. 2021). Although diamond sustains high-internal pressures, these are generally not sufficient to preserve the original high-pressure crystallographic structure of the inclusion. A lower mantle origin is thus usually inferred from the chemical composition of the inclusions and associations that cannot occur under equilibrium conditions at lower pressures (e.g., combinations of ferropericlase with bridgmanite or CaSi-perovskite). Most lower mantle diamonds derive from meta-peridotitic substrates, with meta-basaltic associations being rare

(see Stachel et al. 2005; Thomson et al. 2014; Walter et al. 2021). Of the three principal minerals constituting lower mantle associations, only bridgmanite is exclusively restricted to depth exceeding the 660 km seismic discontinuity. This creates some uncertainty when assigning diamonds containing bridgmanite-free associations (e.g., CaSi-perovskite ± ferropericlase) to the lower mantle, as a transition-zone origin may also be possible. The recently recognized superdeep origin of an inclusion-bearing subset of so-called CLIPPIR (nitrogen-free, large, resorbed, inclusion-poor, and irregularly shaped) diamonds is characterized by phase assemblages that may occur in both the transition zone and the lower mantle (Smith et al. 2016).

Four additional groups of terrestrial diamonds occur that are not included in the data set reviewed here but are listed for completeness:

1. *Polycrystalline diamond aggregates (PDA).* Polycrystalline diamonds are a common component of kimberlite-hosted diamond populations, with typical abundances ranging from several percent to > 10% (e.g., at the Orapa and Jwaneng mines in Botswana; Harris et al. 1986). Their polycrystalline nature requires high supersaturation conditions leading to high nucleation rates (Sunagawa 1990). This type of diamond is addressed in detail by Jacob and Mikhail (2022, this volume).

2. *Fibrous diamonds, cloudy diamonds and diamond coats*. These diamond varieties commonly are associated with rough fibrous diamond growth occurring under extreme levels of supersaturation (Sunagawa 1990). Their typically opaque nature relates to abundant micrometer- to nanometer-sized inclusions of 'mantle fluids', trapped during diamond growth (Kamiya and Lang 1964; Navon et al. 1988). The chapter by Weiss et al. (2022, this volume) addresses these diamonds and the nature and composition of the '*fluids'* included in them.

3. *Metamorphic diamonds.* Such diamonds have been reported from various localities and are found in subducted rocks that subsequently experienced rapid exhumation to the surface (see Dobrzhinetskaya et al. 2022, this volume). Although there is an increasing number of ultra-high-pressure (UHP) metamorphic terranes being recognized (through the presence of coesite, diamond or other high-pressure indicators), some described localities remain contentious and may relate to sample contamination (see Howell et al. 2015a), misidentification (e.g., Beyssac and Chopin 2003) or metastable diamond formation (e.g., Simakov 2010, 2011). Due to the typically very small diamond size (often ≤ 10 μm) in these occurrences, C- and N-isotope data remain scarce, with the Kokchetav massif in Kazakhstan representing the best studied locality (Sobolev and Shatsky 1990; De Corte et al. 1998, 1999).

4. *Graphitized octahedra after diamond in high-temperature peridotite massifs.* Graphite crystals up to 2 cm have been identified in pyroxenite dikes within the high-temperature peridotite massifs of Beni-Boussera (Morroco) and Ronda (Spain). The pyroxenite veins are typically ≤ 30 cm in width, though the C-rich varieties (up to 25 wt% locally) are commonly > 1 m thick. Graphite occurs as aggregates of distorted octahedra and/or in irregular habit. The occurrence of sharp-edged octahedra, a crystal form that is in the cubic system rather than the hexagonal system of graphite, is striking (see Fig. 1 in Pearson et al. 1989) and, along with the orientation of the graphite relative to the octahedral form, constitute the primary basis of their identification as graphitized diamonds (Slodkevich 1980, 1983; Pearson et al. 1989; Davies et al. 1993). On the basis of paleogeothermal gradients, the presence of diamond pseudomorphs requires exhumation of these mantle sections from depths in excess of 200 km (e.g., Davies et al. 1993). Little work has subsequently been devoted to this type of occurrence, but available studies still support the concept that graphitized diamonds do occur and, accordingly, that sections of both the crust and the mantle can be exhumed from the diamond stability field in orogenic cycles (e.g., Leech and Ernst 1998; Korsakov et al. 2019).

We will not venture into a detailed discussion of two complex topics related to diamond formation: the composition of diamond-forming fluids/melts and the role of oxygen fugacity in diamond stability. The following statements summarize our view on these two topics:

1. Terrestrial diamonds, with the exception of impact diamonds, form from a 'mobile phase' commonly refered to as 'diamond growth medium', 'carbon-bearing fluid/melt' or 'COH-fluid'. This deliberately vague wording illustrates that little is known about the exact chemical composition or redox state (i.e., whether it is oxidized or reduced) of this mobile phase. Other wording includes 'CO_2-bearing fluids' or 'CH_4-bearing fluids', in which cases the redox state of the fluid and the diamond-forming meachanism via either either reduction or oxidation are specified, but again the fluids overall chemical composition is not specified. High-density-fluids (HDFs) of 'saline', 'hydrous–silicic' and 'carbonatitic' character are directly observed in fluid-rich *fibrous* diamonds (see Weiss et al. 2021) and clearly form an important part of the spectrum of diamond-forming fluids/melts.
2. Diamond is an allotrope of elemental carbon (C^0) with a stability field that is not only restricted by pressure and temperature but also limited to a narrow range of redox conditions (oxygen fugacities or fO_2). At fO_2 conditions more oxidizing than the enstatite–magnesite–olivine–diamond (EMOD) buffer, carbon is stored in the form of carbonate rather than as diamond (Eggler and Baker 1982). For the strongly reducing conditions prevailing in Earth's mantle beyond about 300 km depth, where fO_2 is buffered by the Fe–FeO (IW) equilibrium, carbon either dissolves in an Fe–Ni metal phase or occurs as carbides or methane rather than as diamond (Frost and McCammon 2008; Rohrbach et al. 2014). Thus when a diamond originates from these great depths, e.g., from the transition zone (410–660 km depth), then it must have either formed in substrates more oxidized than the ambient mantle at those depths or been infiltrated by an oxidizing agent such as a carbonated melt. During the infiltration of metasomatic fluids in the lithospheric mantle, the fO_2 of the diamond substrate must remain in the sweet spot between the IW and EMOD buffers or diamond destruction will occur. For further reading into this aspect of diamond formation/survival and oxygen fugacity, we refer the reader to Luth (1993), O'Neill et al. (1993), Frost and McCammon (2008), Rohrbach and Schmidt (2011), Stagno et al. (2013), Stachel and Luth (2015), and Luth et al. (2022, this volume).

A brief history of diamond stable isotope studies (1940–2000)

By convention, the stable isotope composition of carbon is expressed using the delta-notation, where the isotope ratio is stated as relative deviation to an international standard, which is generally taken to be a belemnite from the Peedee Formation of South Carolina, USA[1].

$$\delta^{13}C = \left(\frac{\left(\frac{^{13}C}{^{12}C}\right)\text{sample}}{\left(\frac{^{13}C}{^{12}C}\right)\text{VPDB}} - 1 \right) \times 1000 [‰]$$

By definition, the Vienna-Pee Dee Belemnite has a $\delta^{13}C_{VPDB}$ = 0‰. Expressed differently, a diamond with $\delta^{13}C$ = −40‰ has a $^{13}C/^{12}C$ ratio (0.01078771) that is 40 parts per thousand (i.e., 4%) lower than the $^{13}C/^{12}C$ ratio of the VPDB standard (0.01123720).

[1] Note that this is the 'old' way of expressing the δ-notation, the 'new' and actually more rigorous way of expressing δ is omitting the '× 1000' which is already included when using the '‰'. We retained the old notation to avoid any misunderstanding with the literature that has and mostly still uses the 'old' notation. Importantly, this has no influence on the C- and N-isotope data reported here or in any previous or future papers.

Consisting of pure carbon, diamond was among the first materials to be analyzed for $^{13}C/^{12}C$ (Nier and Gulbransen 1939) but the measurements were still imprecise until the advent of dual-inlet mass spectrometers (Nier 1947). The first systematic C-isotope study of diamonds was conducted by Craig (1953) on six octahedral diamonds from Kimberley, South Africa (*'De Beers Pool'*—Bultfontein, De Beers, Dutoitspan, Wesselton). He reported $\delta^{13}C$-values ranging from –4.7 to –2.7‰. Subsequently, Wickman (1956) analyzed 37 diamonds from kimberlites from central and southern Africa with $\delta^{13}C$-values ranging from –9.6 to –3.2‰ and concluded that diamonds have a globally homogenous C-isotope composition. Actually, Wickman discarded a value of –13.9‰ measured on one of the diamonds, the sample being, according to him, contaminated with organic matter, while another sample from New South Wales (Australia) had a $\delta^{13}C$-value of +2.7‰. Vinogradov et al. (1965) reported $\delta^{13}C$-values ranging from –8.8 to –5.6‰ on diamonds from Yakutia (Siberia) and confirmed the previous conclusions. These early studies used diamonds to characterize the isotopic composition and variability of mantle carbon rather than aiming to understand the origin of diamond itself. The first three studies all suggested that mantle carbon has a $\delta^{13}C$-value of ~ –6 to –5‰. This was an important outcome that allowed the average C-isotope composition of surface carbon to be established. Preceding the theory of plate tectonics, the $\delta^{13}C$-value of bulk surface carbon was presumed to be the same as that of the mantle. With sedimentary carbonate and organic matter having $\delta^{13}C$-values of ~ 0‰ and ~ –25‰, respectively, a mantle value of –6 to –5‰ implies that these two surface carbon reservoirs are in about 80:20 proportions (e.g., Javoy et al. 1982). This estimate is still valid globally today, although it is now well documented that large heterogeneities exist among different subduction zones (e.g., Plank and Manning 2019). From a diamond perspective, during the 1950s and 1960s, Earth's mantle was seen as being isotopically homogeneous.

The first strongly negative $\delta^{13}C$-values for diamond were obtained by Vinogradov et al. (1966) but determined on carbonados, whose origin (Earth's mantle or extraterrestrial) is still debated. Subsequently, Koval'skiy et al. (1972) measured $\delta^{13}C$-values between –22.2 and –21.4‰ on diamonds from Yakutian placer deposits and Smirnov et al. (1979) obtained values down to –20.5‰ in diamonds from kimberlites in Lesotho, demonstrating that the assumption of C-isotope homogeneity among diamonds was invalid. By the end of the 1970s, a considerable amount of additional data were obtained, primarily by Russian groups (mostly published in Russian, with some papers translated in Geochemistry International). These data are not all easily accessible but it is worth noting that the histogram for the C-isotope composition of diamonds compiled by Deines (1980; his Fig. 4) was primarily built on data produced by Russian laboratories. By the end of the 1970s it had become clear that diamond can be strongly depleted in ^{13}C, down to –35‰ (today, the lowest known value in a terrestrial natural diamond is –41.4‰; De Stefano et al. 2009). The study of Sobolev et al. (1979) was seminal in demonstrating that diamonds belonging to the peridotitic suite have a narrower range in $\delta^{13}C$-values than those belonging to the eclogitic suite. This finding paved the way for a series of studies examining the C-isotope composition of diamond in relation to source paragenesis, inclusion mineralogy and chemistry, and other physical characteristics (e.g., shape or color) of diamond, most notably through the systematic studies of Peter Deines and coworkers (e.g., Deines et al. 2009 and references therein). The original finding of Sobolev et al. (1979) was generally confirmed, although not every diamond mine studied contained eclogitic diamonds with $\delta^{13}C$-values < –10‰ (e.g., the Finsch Mine; Deines et al. 1989) and the abundance of eclogitic diamonds with low $\delta^{13}C$-values was found to be variable (ranging from 0 to 100% of the eclogitic diamond population). Sobolev et al. (1979) suggested that the non-mantle like C-isotope compositions of eclogitic diamonds derive from surface 'sedimentary' signatures subducted into the mantle, making diamond a tracer of plate tectonics. Milledge et al. (1983) observed that Type II diamonds from the Cullinan Mine (formerly known as Premier) cover a large range of $\delta^{13}C$-values (from ~ –32 to ~ 0‰, i.e., almost the entire $\delta^{13}C$-range known at that time) and attributed this finding also to variations in the *nature of the carbon reservoir source*. Nisbet et al. (1994) expressed this differently as

'*Can* [eclogitic] *diamond be dead bacteria*?'. This model has profound implications: suggesting the possibility that sediments may be subducted without drastic (isotope) re-equilibration with their surrounding environment so as to preserve low $\delta^{13}C$-values.

With the improvement of analytical techniques, the study of diamond internal variability became viable. This occurred first by analyzing laser-cut sections of diamonds (cubes < 0.25 mm in each dimension, weighting as little as 0.05 mg; e.g., Swart et al. 1983; Boyd et al. 1987) and subsequently using secondary ion mass spectrometry (SIMS) with a spatial resolution of 10–20 µm in diameter and 1–5 µm in depth (Harte et al. 1992, 1999; Hauri et al. 1999; Fitzsimons et al. 2000). These studies typically showed little diamond-internal variability (generally < 3‰ and often < 1‰; see Fig. 7 in Galimov 1991; Fig. 4 in Cartigny et al. 2004; and Harte et al. 1999 for the first SIMS-based assessment) compared to the worldwide diamond $\delta^{13}C$-range. These intra-grain variations in isotopic composition are discussed further below with respect to the negligible diffusion of carbon and nitrogen in diamond and models of diamond formation.

Although the content and speciation of nitrogen in diamond is not the focus of this review, nitrogen forms the basis of diamond classification and thus a brief summary is given here (for details and appropriate references, see Green et al. 2022, this volume). Based on FTIR (Fourier transform infrared) analyses, Robertson et al. (1934) recognized two types of diamond (Type I and II), the former displaying extra-absorption in the 1400–900 cm^{-1} region. Only in 1959 was it understood that this extra absorption relates to nitrogen defects (Kaiser and Bond 1959). Nitrogen and carbon have similar ionic radii and charge, enabling nitrogen to substitute as an impurity into the diamond lattice. Nitrogen concentrations reach up to 3800 at.ppm in mantle-derived diamonds (Donnelly et al. 2007) but typically are much lower (median value of 160 at.ppm; see Stachel 2014 and Cartigny et al. 2014 for reviews). Based on the infrared characteristics of diamond and without necessarily understanding the nature of the underlying defect(s), further work (for details see Green et al. 2022) led to a subdivision into Type Ib (single N-impurities, typical of synthetic diamonds and occurring in < 0.1% of natural diamonds), Type Ia (aggregated nitrogen impurities), Type IIa (no nitrogen, no boron) and Type IIb (no nitrogen, boron-bearing). Type Ia diamonds were subsequently subdivided in IaA (N-pairs) and IaB (4 N-atoms around a vacancy). Nitrogen is a substitutional defect (Kaiser and Bond 1959) being strongly bonded to C-atoms. The occurrence of the various N-defects in diamond is not arbitrary and follows a well-accepted sequence of aggregation, starting from single N-atoms (Ib diamond) to N-pairs (IaA diamonds) to 4 N-atoms around a vacancy (IaB diamonds). The aggregation sequence follows a second-order kinetic diffusion process (Chrenko et al. 1977; Evans and Qi 1982) and allows constraints to be placed on either the residence time or the residence temperature of diamond in the mantle. Because of the high activation energy of the IaA to IaB conversion, N-aggregation is, however, primarily used as a geothermometer (Evans and Harris 1989; Taylor et al. 1990). Since the early 1980s, infrared spectroscopy has been the main method to determine diamond N-content and aggregation state (e.g., Milledge et al. 1983; Deines et al. 1984). Given typical infrared beam sizes of ~ 100 µm and thickness of analyzed diamond fragments up to 1 mm, these analyses correspond to bulk measurements. SIMS analyses now determine nitrogen contents (but not aggregation state) in diamond to sub-ppm levels and with high spatial resolution. Both methods show that the abundance of N in superdeep (asthenosphere to lower mantle) diamonds is low and, from FTIR data, associated with advanced aggregation (typically < 100 ppm in IaB state; e.g., Tappert et al. 2005; Palot et al. 2012 and reference therein). Fibrous diamonds are N-rich with little N-aggregation (~ 1000 ppm and IaA, e.g., Cartigny et al. 2003 and reference therein). The abundance of N in eclogitic and peridotitic diamonds, for which the largest number of data are available, can be variable across locations and across diamond size classes (with diamonds < 1 mm often showing a high abundance of Type II diamonds; Tolansky and Komatsu 1967). On average, peridotitic diamonds have lower N-contents (mean: 219 at.ppm; median: 109 at.ppm) than eclogitic diamonds (mean: 472 at.ppm; median: 454 at.ppm; see supplementary data set).

In some locations, sulfide-bearing diamonds have higher N-content and lower N-aggregation states than silicate-included diamonds belonging to the same paragenesis. Metamorphic diamonds can have much higher N-contents (up to 10,000 at.ppm) and are invariably low in aggregation state (Ib-IaA) (Xu et al. 2018 and references therein).

The first systematic N-isotope[2] study was undertaken on fibrous diamonds from Mbuji Mayi (Democratic Republic of the Congo) using conventional dual-inlet techniques and thus requiring large (0.87 to 1.55 g) amounts of diamond (Javoy et al. 1984). Although fibrous diamonds constitute only a few percent of the worldwide production, these diamonds have the advantage of being N-rich (average ~ 1000 at.ppm N) and, at least at this locality, are in part quite large (up to a few cm). This paper was seminal for several reasons: first, it demonstrated that fibrous diamonds record ^{15}N-depleted isotope compositions (average $\delta^{15}N$ of ~ −5‰ relative to atmospheric nitrogen taken as the reference, i.e., standard value), which was unexpected, and secondly, it demonstrated the viability of using N-isotopes as a tracer of crustal recycling (see below). Javoy et al. (1984) explained the observed variations in C- and N-isotope compositions by open-system fractionation of kimberlite volatiles (through Rayleigh distillation, a model that was imposed by the most extreme sample (D3), which was actually not a fibrous diamond). Importantly, their model seemed to imply that fibrous diamonds are 'young', having roughly the age of the kimberlite. In the same year, Richardson et al. (1984) reported the first Sm–Nd isotope model ages of ~ 3.2 Ga for non-fibrous, garnet-included diamonds from the Finsch mine and the pooled production of the four mines in Kimberley (*'De Beers Pool'*), establishing that monocrystalline diamond formation predated kimberlite magmatism by several billion years. These Archean diamond ages for non-fibrous diamonds are probably the main reason why the model of Javoy et al. (1984), linking fibrous diamond formation to (proto)-kimberlite derived volatiles, received little attention although it has been supported through a number of subsequent studies (for early studies see Boyd et al. 1987, 1994; Navon et al. 1988; Akagi and Masuda 1998; for a different viewpoint, see Klein-BenDavid et al. 2010; Timmerman et al. 2019). These early C- and N-isotope data on fibrous diamonds from Mbuji Mayi were subsequently confirmed and extended worldwide (Boyd et al. 1987, 1992; Burgess et al. 2009; Klein-BenDavid et al. 2010; Timmerman et al. 2019). What remains striking in all these studies is the small C- and N-isotope variability of fibrous diamonds, with values nearly identical to mid-ocean ridge basalts (see Fig. 1 in Cartigny and Marty 2013); this observation is commonly used to argue that fibrous diamonds, and by inference kimberlites, form from volatiles derived from the convecting mantle. The studies of Boyd et al. (1987, 1992) were also important because they introduced the use of static vacuum mass spectrometry (the same type of instrument used for the analysis of noble gases), allowing the analysis of three orders of magnitude smaller (sub-mg, a 1 mm^3 diamond is 3.5 mg) or much more N-poor samples. Based on this technical break-through, the diamond internal variability of N-isotope compositions could be studied together with N-content and C-isotope compositions. The first systematic study of smooth-surfaced monocrystalline diamonds was undertaken by Boyd and Pillinger (1994) on samples of unknown paragenesis, followed by a series of studies (starting with Cartigny et al. 1997) on diamonds containing mineral inclusions of known paragenesis (peridotitic or eclogitic) and derived from known localities (see reference list associated with the supplementary data set).

The fine-scale C- and N-isotope variability of diamonds became truly open to study with use of ion microprobes (Fitzsimons et al. 1999; Harte et al. 1999; Bulanova et al. 2002; Zedgenizov and Harte 2004; Craven et al. 2009; Smart et al. 2011; Peats et al. 2012; Palot et al. 2014, 2017; Howell et al. 2015b; Petts et al. 2015; Smit et al. 2016, 2019a), although not every study using MC-SIMS (multi-collector secondary ion mass spectrometer) actually focused on detailed C- and N-mapping (e.g., Johnson et al. 2012; Krebs et al. 2016; Howell et al. 2020). It should be noted that the later (2009 onwards) studies in this list achieved a factor of 2 to 5 improvement

[2] $\delta^{15}N_{diamond} = [(^{15}N/^{14}N)_{diamond}/(^{15}N/^{14}N)_{AIR}-1] \times 1000$ (in ‰)

in analytical precision of the isotopic analyses relative to the earlier studies, which permitted more subtle internal variations to be detected. Although limited to a few multi-collector SIMS instruments worldwide configured to do these isotopic analyses and requiring very good sample preparation, SIMS analysis nowadays represents a powerful way to investigate the internal C- and N-isotope variability of diamonds. Below ~ 100 ppm (using Faraday cups), the precision on δ^{15}N-measurements on SIMS instruments is still limited by counting statistics and bulk techniques—despite being destructive—remain central; e.g., Palot et al. (2012) reported the nitrogen isotopic composition of a lower mantle diamond containing only 6 ppm nitrogen.

Early models: some still in consideration

Primordial heterogeneity. Until the acquisition of larger datasets, no one had made a serious attempt to differentiate diamond sub-populations based on paragenesis, C- and N-isotope composition or aggregation state. Primarily relying on statistical analysis, Deines et al. (1984) used a data set of 66 diamonds from Cullinan and 91 diamonds from Finsch to determine that many sub-populations of diamond exist (for example, McDade and Harris 1999 identified 10 sub-populations among 48 studied diamonds from the Letseng Mine in Lesotho). From this original and subsequent studies, Deines et al. (1984) favored a model where the C-isotope variability observed in diamond is primordial, i.e., inherited from the heterogeneity of Earth's accretionary building blocks - represented by chondritic meteorites. This primordial heterogeneity would have needed to survive the formation of magma oceans early in Earth's history and the subsequent differentiation, stirring and homogenization of bulk silicate Earth that is documented in many geochemical proxies, among them the observation of consistent mass-dependent ^{17}O/^{16}O–^{18}O/^{16}O signatures (e.g., Robert et al. 1992; Rumble et al. 2007). From a diamond perspective, the primordial heterogeneity model also fails to demonstrate why strongly negative δ^{13}C-values mostly occur among eclogitic diamonds; the model of Deines and coworkers actually predicts that peridotitic rather than eclogitic diamonds should display the largest δ^{13}C-variability. Today, this model is generally no longer considered a valid hypothesis and evidence for primordial stable isotopic heterogeneity was subsequently only proposed for very few diamonds (Cartigny et al. 1997; Palot et al. 2012), based on extremely low δ^{15}N-values (down to –40‰) that were actually accompanied by mantle-like δ^{13}C-values (around –4‰).

In retrospect, Deines et al. (1984) probably considered too many parameters in distinguishing diamond sub-populations. For example, nitrogen aggregation is very sensitive to mantle residence temperature (besides N-content and residence time) and consequently, in hindsight, dividing diamond populations based on N-aggregation state was not the best choice. Like N-aggregation, plastic deformation and associated brown coloration postdate diamond formation; in addition, the shear stresses leading to plastic deformation may be highly localized. Distinguishing diamond sub-populations based on evidence for plastic deformation, therefore, was not pertinent. Finally, the assumption that diamond with a low nitrogen content formed in a N-poor mantle environment was subsequently contradicted by observations that diamonds from a single mantle xenolith (Thomassot et al. 2007) and growth zones within single diamonds (e.g., Fitzsimons et al. 1999; Smart et al. 2011) can vary in N-content by several orders of magnitude, illustrating that partitioning of nitrogen between diamond and its growth medium is an additional, very important parameter to consider.

High temperature stable isotope fractionation. As discussed in detail below (see section *Origin of covariations among δ^{13}C, δ^{15}N and nitrogen content*), the high temperatures of mantle processes generally result in small equilibrium isotope fractionation factors. As such, the generation of large stable isotope variations in mantle samples either requires very extensive Rayleigh fractionation or derivation of the element in question from multiple sources with widely different isotopic compositions. The models described in this section call for Rayleigh fractionation to produce the observed isotopic variations.

Early contributions (e.g., Javoy et al. 1986) proposed a possible role for within-mantle isotope fractionation processes in producing large ranges of $\delta^{13}C$-values from a single, homogenous, starting composition with a mantle-like $\delta^{13}C$-value of ~ −5‰. However, these studies did not point to a specific process that would account for the distinct $\delta^{13}C$-distributions of eclogitic versus peridotitic diamonds. Instead, they considered the frequency distribution of diamonds worldwide without paying attention to source paragenesis, despite the earlier evidence of the difference in diamond paragenesis (Sobolev et al. 1979). Javoy et al. (1986) proposed that large carbon isotope fractionation between CO_2 and magma could lead to the observed large variability in diamond $\delta^{13}C$-values. This model is analogous to CO_2 degassing during volcanic eruptions, which has been shown to produce up to 12‰ range in the $\delta^{13}C$-values of the evolved CO_2 (e.g., Aubaud et al. 2006). Criticism of this model focusses on the large (> 4‰) isotope fractionation factors used by Javoy et al. (1986) in their calculations, which rely on a *preliminary* value determined by Javoy et al. (1978). More recent experiments indicate somewhat smaller CO_2–melt C-isotope fractionation factors (at 1200 °C) of ~ 2.0–2.4‰ for basalt and soda-melilite melts (Mattey et al. 1990; Mattey 1991) and 3.0‰ for alkali (Li–Na–K) carbonate melts (Appora-Gnekindy 1998). Smaller fractionation factors would lead to less dispersion of $\delta^{13}C$-values during Rayleigh fractionation. Some additional empirical evidence from kimberlites and carbonatites can also be considered. Carbonatites and kimberlites show restricted variation in $\delta^{13}C$, i.e., 95% of values being between −8 and −2‰ (e.g., Wilson et al. 2007; Giuliani et al. 2012), yet in some rare cases, $\delta^{13}C$ is reported to spread over −35 to +35‰ (Galimov 1991).

Galimov (1991) was the first to address differences in $\delta^{13}C$-distribution among eclogitic and peridotitic diamonds, which he related again to Rayleigh fractionation in the mantle but without identifying a specific reaction. Importantly, Javoy et al. (1986) and Galimov (1991) both realized that the carbon stable isotope variability of diamond cannot relate to the crystallization process itself but instead must be produced prior to diamond formation, with diamond largely behaving as a *passive recorder*, which faithfully logs but does not significantly contribute to C-isotope variations in the mantle. Otherwise, peridotitic and eclogitic diamonds would display the same $\delta^{13}C$-distributions. Building on these two previous models, the new observation of negative $\delta^{15}N$-values for most eclogitic diamonds (see also below), and the experimental work of Luth (1993) and Knoche et al. (1999) on the poor CO_2-buffering capacity of olivine-free mantle lithologies, Cartigny et al. (1998) proposed that the distinct $\delta^{13}C$-distributions of eclogitic and peridotitic diamonds record characteristic pathways in the chemical and isotopic evolution of initially isotopically indistinguishable, oxidized melts/fluids. In this model, the differences in evolution ultimately reflect the role of olivine in peridotites in buffering CO_2 through carbonation reactions, whereas in olivine-free eclogites decarbonation and CO_2-escape from carbonated fluids/melts is permissible. Such decarbonation of fluids/melts in eclogite would allow the escape of ^{13}C-enriched CO_2, leaving a ^{13}C-depleted residue from which eclogitic diamonds could crystallize.

Rayleigh fractionation predicts $\delta^{13}C$ frequency distributions varying with the logarithm of the residual carbon fraction. Consequently, even for large fractionation factors (e.g., 5‰) only a very small fraction of diamond (1%) will reach isotopic compositions < −27‰, based on an initial $\delta^{13}C$ of −5‰ for the diamond-forming medium. In other words, to derive $\delta^{13}C$-distributions as observed in specific cases such as at Argyle (Australia) or Dachine (French Guiana) from a starting composition at $\delta^{13}C$ ~ −5‰, over 99% of the fractionated carbon reservoir must remain 'unsampled'; either the diamonds were not sampled/preserved or the bulk of the carbon did not crystallize as diamond. Such a possibility is, however, unlikely and for these and similar cases (e.g., diamonds from Jagersfontein, New South Wales and Jericho as extreme examples) an initial $\delta^{13}C$-value less than −5‰ is required.

Forming diamond from subducted carbon (isotope fingerprinting). In isotope forensics, the isotopic compositions of two *compounds* (a bulk sample, or specific molecules, or even the intra-molecular composition of a single molecule) are compared to constrain whether these are the same or not, in order to understand, for example, whether this is *real tequila*, or whether an *orange juice contains added sugar*. The principle of relating eclogitic diamond formation to recycled sedimentary carbon follows the same approach, best illustrated in Nisbet et al. (1994) and McCandless and Gurney (1997). In order to demonstrate diamond formation from recycled organic matter and sedimentary carbonate carbon with typical δ^{13}C-values of −25 and 0‰, respectively (e.g., Plank and Manning 2019; their Fig. 2a and references therein), Nisbet et al. pointed to the observation that the δ^{13}C ranges covered by diamond and these sedimentary carbon sources are very similar and predicted that even lower δ^{13}C-values would be found in diamond to achieve a perfect match (i.e., the authors addressed the range of values, not the resulting distributions). This agreement between δ^{13}C ranges has been a central argument for the formation of eclogitic diamond from recycled carbon (see section *Origin of large ranges in* $\delta^{13}C$ *and* $\delta^{15}N$) and is supported by the indisputably recycled nature of most eclogite xenoliths.

The key difference between isotope forensics and diamond geology, however, lies in the metamorphic history of the carbon and nitrogen source rocks preceding diamond formation, which may include processes (e.g., re-equilibration with other carbon phases in the rock, devolatilization, melting) that shift the isotope compositions of the C- and N-bearing phases relative to their original values. A straight comparison between subducted carbon, hosted in sediments and in altered oceanic crust (organic carbon with δ^{13}C ~ −25‰, with or without associated carbonates), and diamond assumes that the original isotopic compositions are preserved during subduction and associated metamorphism. Yet, when in direct contact, carbonate and organic carbon (graphite) undergo recrystallization and associated C-isotope exchange at a temperature of ≥ ~ 600 °C (e.g., Valley and O'Neil 1981), i.e., at less than 100 km depth along a typical subduction geotherm. This is supported by the observation that the C-isotope composition of CO_2 at arcs covers only a restricted range of δ^{13}C-values (from −8 to 0‰; Fig. 2 of Plank and Manning 2019). Furthermore, to preserve the extreme δ^{13}C-values present in subducted organic carbon and biogenic carbonate, an additional pre-requisite is that no significant mixing with mantle carbon must occur. The suggestion of eclogitic diamond formation *exclusively* from recycled organic carbon thus relies on several assumptions that often are not explicitly considered (e.g., Nisbet et al. 1994; Tappert et al. 2005).

The present-day budget of subducted sedimentary carbon illustrates a large variability in the ratio of carbonate/organic carbon (with a relative proportion of organic carbon from 0 to 80%, averaging close to 20%; see Plank and Manning 2019); therefore, the opportunity to subduct sediment with a high ratio of organic carbon to carbonate (implying low bulk δ^{13}C) exists, but is compensated by higher average δ^{13}C-values in other subduction settings. The most recent development (Li et al. 2019) emphasizes that the altered igneous portion of oceanic crust (AOC) has a total carbon content of similar magnitude to that of subducted sediments and the combined δ^{13}C range (−24 to +11‰) of normal and biogenic carbonate and organic matter in AOC is of similar extent to diamond (−41 to +3‰). An AOC origin of carbon in eclogitic diamonds (inferred from δ^{13}C outside the mantle range) is consistent with the observation that eclogite xenoliths and eclogitic inclusions in diamonds differ significantly from sedimentary protolith compositions. An important role of mantle-derived carbon-bearing fluids during diamond formation in AOC-derived substrates was highlighted by Ickert et al. (2013), with the observed "mixing" relationship implying low carbon contents in most of the AOC-derived substrates, with the exception of the originally shallowest and most altered sea floor basalts. With a mean δ^{13}C of about −5‰, AOC and in particular its organic matter and biogenic carbonate components must still escape metamorphic homogenization, at least locally, to impart the prominent ^{13}C-depleted tail to the eclogitic diamond population. Melting of subducted oceanic crust in the Archean is often invoked to account for the occurrence of TTG magmas and the magnesian character of cratonic eclogite xenoliths. The behavior of carbon during melting is however difficult to predict, as carbon may behave both compatibly or incompatibly in the melting residue, depending on various parameters—in particular speciation, chemical composition and CO_2/SiO_2 ratio (see Yaxley et al. 2019 for a review); we will return to this aspect further below, but it is clear that models relating diamond formation to subducted carbon require that carbon must survive devolatilization, decarbonation and melting.

Negligible diffusion and homogenization of C and N in diamond

The fairly homogenous C-isotope composition of individual diamond crystals does not reflect diffusion and homogenization over time. This is implicit from fine scale (down to at least 1 μm) zoning in cathodoluminescence (CL) images and sharp contrasts in N-content and stable isotopic composition (down to the analytical resolution limit of ~ 10 μm), and was ultimately experimentally demonstrated for C and N (Koga et al. 2003, 2005; Harte et al. 2009). Put simply, diffusion of C and N in diamond on the millimeter scale may only be possible for mantle residence times corresponding to the age of the Earth at *very high* temperatures (> 2000 °C), such as those expected in the lower mantle. In other words, the limited C-isotope variability of most diamonds—which form in the lithospheric upper mantle at mean temperatures of ~ 1150–1200 °C (Stachel and Luth 2015)—is a primary feature that directly relates to diamond formation, not its post-crystallization history. Nitrogen diffuses in the diamond lattice, allowing it to aggregate over time, but only on the nanometer level. For diamonds from the lower mantle, significant diffusion is possible but again not supported by the observation of fine-scale features in CL images and abrupt changes in carbon isotope composition and nitrogen concentration along SIMS transects (e.g., Palot et al. 2014).

Database and methods

As the basis for this review, we compiled an analytical database for 5115 diamonds from literature. Of these samples, 4307 were analyzed for their carbon isotope composition, 840 for their nitrogen isotope composition and all 5115 for their nitrogen content. The emphasis in compiling the database was on inclusion-bearing diamonds of known paragenesis (3474 diamonds), but an additional 1541 diamonds of unknown paragenesis are included (also in the statistical analysis of "all diamonds" in Figs. 1 and 6). For the vast majority of diamonds, analyses either are single bulk combustion analyses or represent averages of multiple bulk combustion or MC-SIMS analyses. For a small number of samples, where SIMS profiles revealed distinct growth events and, consequently, average values are not representative of real compositions, individual growth zones where averaged as "core" and "rim" (76 averages for 38 diamonds) and sometimes additionally as "middle" (for 23 diamonds). Note that "core" and "rim" of diamond fragments may not correspond to true centers and rims of the original crystals. The full database, a list of references and a "dictionary" explaining data columns and abbreviations are available online at https://doi.org/10.7939/DVN/B8VYHV. For the sake of readability of this chapter, the data sources referenced online are not duplicated here.

Raleigh isotope fractionation during diamond precipitation can be modeled assuming either a single carbon species or two carbon species in the fluid. The modeling spreadsheets (DiaRIF.xlsx and RIFMS.xlsx, respectively) used by us to calculate fractionation trends are provided online at https://doi.org/10.7939/DVN/JAEQKZ. Temperature dependent carbon isotope fractionation factors for diamond–$CaCO_3$, diamond–CO_2 and diamond–CH_4 are based on calculations or experimental data reported in Richet et al. (1977), Chacko et al. (1991), Polyakov and Kharlashina (1995), and Horita (2001). See also Table 1 in Stachel et al. (2017). As detailed in a later section, C-isotope fractionation factors are relatively well established for many systems relevant to diamond formation but there is considerably more uncertainty associated with N-isotope fractionation factors for diamond, which, for the most part, have only been investigated empirically based on fractionation trends observed in natural diamonds.

For data presentation we chose to employ kernel density estimation, a non-parametric approach, where kernel density plots (KDPs) visualize the density over which a large population is distributed, based on the assumption that the data represent a random sample of the overall population. For the C-isotope database investigated here, at the individual deposit scale, this underlying assumption might be debatable, but it is likely true when considering the large overall population of diamonds analyzed globally. KDPs use a uniform bandwidth that should be calculated objectively from the data, by the adopted program, rather than by the user. Unlike histograms, KDPs do not require the user to choose end-point bins which can create spurious features to the plots. When used in an objective way, KDPs are thus less subject to the creation of artificial peaks in the visualized distribution. In a kernel density estimate, each data point in the sample population is featured as a Gaussian curve centered on the data point value, whose standard deviation is given by the bandwidth. The smooth curve of the KDP is then the sum of the individual Gaussian distributions.

To assess the proportion of data that may be contained within the various peaks in the data distributions, we use a mixture modeling approach. Mixture modeling (e.g., Fraley and Raftery 2002), is a parametric approach that typically assumes that the population density is the sum of a small number of Gaussian distributions. The key goal of the approach, for a given sample, is to identify the number of components, their means, standard deviations and proportions of the components making up the overall populations. Where large distributions approach a Gaussian form, this approach is usually more successful than other approaches, such as feature recognition, in identifying the main features of the population (see Rudge 2008 for more detail).

Here, we compute Kernel density estimations and mixture models using the program DensityPlotter (Vermeesch 2012). The kernel width (bandwidth) is calculated in an adaptive approach based on local density, rather than determined by analytical uncertainty (Vermeesch 2012). Mixture modeling of stable isotope data with DensityPlotter uses the algorithm of Galbraith (2005) to assess the number of components that may constitute a given distribution of data. The program calculates peak locations for each "component" and their proportions.

Statistical tests were calculated using the Real Statistics Resource Pack (Excel Add-in) written by Charles Zaiontz (*http://www.real-statistics.com*). Two-tailed Student's *t-tests* for equality of means of two independent samples were performed assuming unequal variances and an alpha-value of 5% (i.e., a decision not to reject the null hypothesis of equal means carries 95% confidence). Normality of sample distributions was assessed using both the Shapiro–Wilk and d'Agostino-Pearson (Omnibus version) tests, again using an alpha-value of 5%. Both tests are robust with symmetric and long-tailed distributions that feature in several of our datasets. The Shapiro-Wilk test is vulnerable to losing power in data sets with a significant number of identical values with small standard deviations, which are present in some C-isotope datasets. In these cases, the d'Agostino–Pearson test is favoured as it is less susceptible to identical values. This test first calculates skewness and kurtosis to examine how far the distribution is from Gaussian, then it calculates how far each of these parameters differs from the expected value for a Gaussian distribution, computing a P value from the sum of these differences.

CARBON ISOTOPE COMPOSITION OF DIAMOND AND ITS RELATIONSHIP TO INCLUSION PARAGENESIS

On the $\delta^{13}C$ scale, the carbon isotope composition of Earth's mantle, based on analyses of carbonatites, kimberlite carbonates, mantle xenoliths and volcanic CO_2, is about −5‰ (Deines 2002). The median value (−5.2‰) and the main mode in the kernel density estimation of mantle-derived diamonds (−5.1‰; Fig. 1; Table 1) coincide with this mantle value (c.f., Deines 1980; Galimov 1991). Defining the $\delta^{13}C$ mantle array as −5 ± 2‰ (Cartigny et al. 2014) includes the

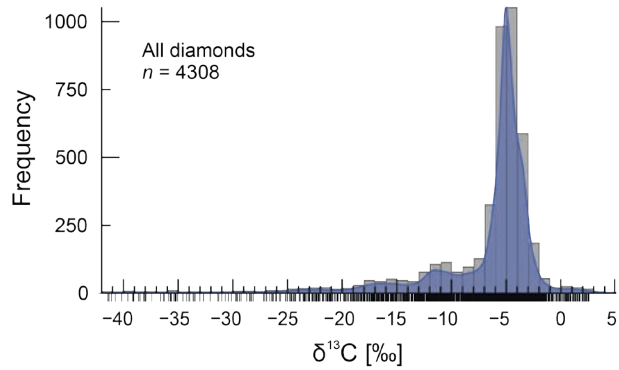

Figure 1. Distribution in carbon isotope composition ($\delta^{13}C$) for (mostly) inclusion-bearing diamonds worldwide. The blue curve is a Kernel density estimation, shown in the background is a histogram with a 1‰ binning interval. **Black dashes** below the *x*-axis indicate individual data points.

Table 1. The carbon isotope compositions ($\delta^{13}C$) of inclusion-bearing diamonds from worldwide sources.

Suite	All diamonds	Peridotitic			Eclogitic	Websteritic	Asthenospheric-TZ "Eclogitic"	Lower Mantle
Paragenesis		All	Lherzolitic	Harzburgitic				
n	4308	1906	216	503	1204	58	55	154
Min (‰)	–41.4	–34.5	–11.8	–26.4	–40.7	–41.3	–24.8	–28.3
Max (‰)	2.5	2.3	0.3	2.3	2.5	–3.7	0.9	0.7
Average (‰)	–6.9	–4.9	–4.5	–5.1	–9.4	–11.5	–14.5	–6.1
SD (‰)	5.5	1.9	1.5	1.7	6.7	9.1	7.2	5.6
Median (‰)	–5.2	–4.9	–4.8	–5.1	–6.5	–6.0	–15.3	–4.6
MAD (‰)	1.1	0.8	0.7	0.7	2.3	2.2	6.5	0.7
Q1 (‰)	–6.8	–5.5	–5.3	–5.7	–11.9	–17.9	–21.2	–5.2
Q3 (‰)	–4.2	–4.0	–3.7	–4.2	–5.0	–4.8	–8.5	–3.8
IQR (‰)	2.6	1.5	1.6	1.5	6.9	13.1	12.7	1.4
Mode (‰)	–5.1	–5.2	–5.2	–5.3	–5.0	–4.9		–4.9

Note: Statistical parameters quoted are: *n*—number of samples; Min—lowest values; Max—highest values; Average—arithmetic mean; SD—1 standard deviation calculated based on a sample; Median—median value; MAD—median absolute deviation; Q1—25th percentile; Q3—75th percentile; IQR—interquartile range (IQR = Q3–Q1); Mode—maximum value of the kernel density estimation.

majority of diamonds (69%) but the total distribution extends far beyond this range, from –41.4 to +2.5‰. To further evaluate the origin of this variability, we split mantle-derived diamonds into suites and further into parageneses based on their mineral inclusion content.

Peridotitic suite

The carbon isotope composition of lithospheric diamonds with peridotitic inclusions forms a narrow distribution about the mantle value (median $\delta^{13}C$-value of –4.9‰; mode at –5.2‰; Fig. 2), with 85% of samples falling between −7 and –3‰ and 95% of samples between −8 and −2‰. Only 1% of samples fall below −10‰ (extending down to –34.5‰) and only four samples (0.2%) exceed 0‰ (Table 1). The distribution is non-normal (Shapiro-Wilk and d'Agostino-Pearson tests) though the strong negative skewness value (–4.6) is due to a significant number of outliers biasing the value: 18 samples or 1.1% of the entire population have $\delta^{13}C$-values three

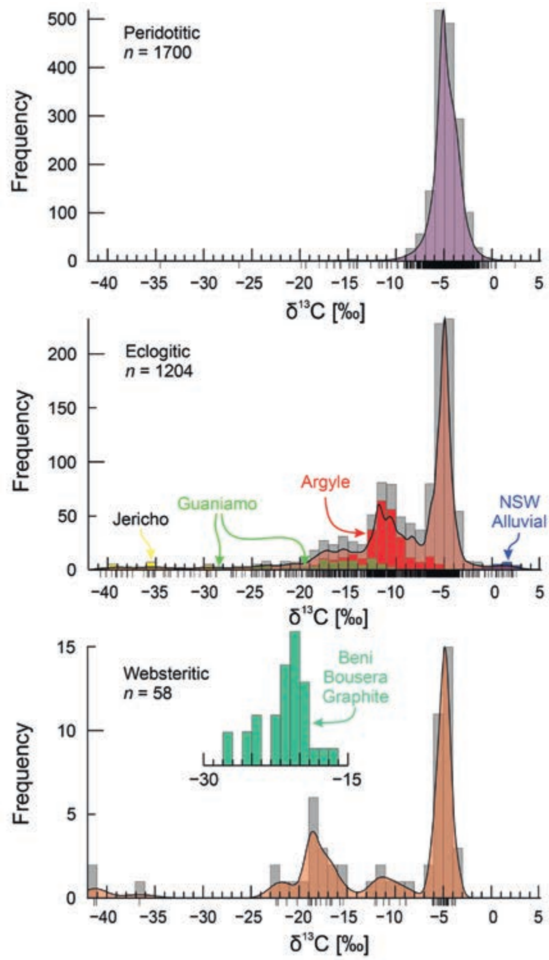

Figure 2. Distribution in carbon isotope composition for diamonds with peridotitic **(top)**, eclogitic (**middle**) and websteritic **(bottom)** suite inclusions. The **colored curves** are Kernel density estimations, shown in the background are histograms with a 1‰ binning interval. **Black dashes** below the *x*-axis indicate individual data points. For the distribution of eclogitic diamonds, four locations with distinctly non-mantle-like distributions (Jericho in the Northern Slave Craton, Guaniamo on the Amazon Shield, Argyle on the Kimberley Craton and the New South Wales alluvials) are highlighted. The insert above the websteritic diamond distribution shows the carbon isotope composition of graphite pseudomorphs after diamond in pyroxenite layers (dikes) in the Beni Bousera peridotite complex (Pearson et al. 1991) for comparison.

standard deviations below the mean (i.e., < −10.7‰; see Table 1), versus the 5 expected at the 99.7 probability level. These outliers thus likely represent a separate population of peridotitic diamonds. Through the presence of clinopyroxene and garnet inclusions, for close to half of the peridotitic samples a specific paragenesis, harzburgitic (–dunitic) or lherzolitic, can be assigned. Diamonds containing wehrlitic inclusions are rare (0.6% of inclusion-bearing diamonds; Stachel and Harris 2008) and consequently are ignored here. For the harzburgitic paragenesis, the median value of −5.1‰ is well within the Median Absolute Deviation (MAD[3]) about the median of the peridotitic distribution as a whole. The kernel density plot, however, reveals a

[3] In statistics MAD is considered a more robust measure of variability than standard deviation because the former does not rely on the assumption of a normal distribution.

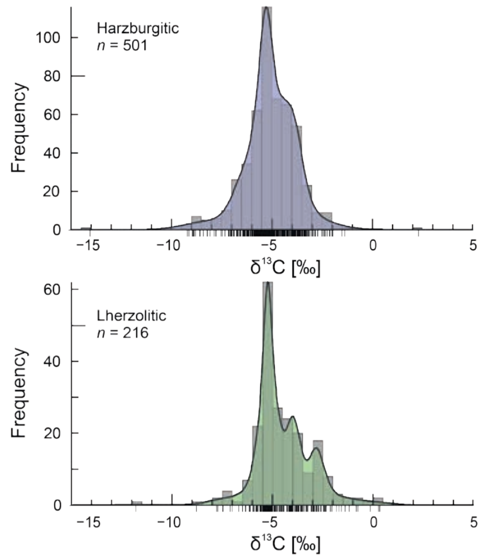

Figure 3. Distribution in carbon isotope composition for diamonds with peridotitic inclusions of harzburgitic **(top)** and lherzolitic **(bottom)** paragenesis. The **colored curves** are Kernel density estimations, shown in the background are histograms with a 1‰ binning interval. **Black dashes** below the x-axis indicate individual data points.

minor peak on the ^{13}C-enriched side of the distribution (Fig. 3) reflecting the contribution of diamond populations from Akwatia in Ghana and Boa Vista in Brazil (alluvial deposits), both with median values of −3.9‰, Williamson (formerly Mwadui) in Tanzania, with a median of −3.8‰, and Pipe 50 in China, at −3.5‰ (c.f., Stachel et al. 2009, their Fig. 2). This skewness is even more pronounced in the distribution for lherzolitic diamonds (Fig. 3), with the appearance of distinct secondary modes at −4.0 and −2.8‰. The two secondary modes principally reflect a bimodal distribution of lherzolitic diamonds at Cullinan (formerly Premier) Mine in South Africa, with a subordinate contribution of overall ^{13}C-enriched lherzolitic diamonds from Kankan and Akwatia in West Africa and Williamson in Tanzania. Although it is important to note the mildly ^{13}C-enriched nature of peridotitic diamonds from the West African and Tanzania cratons and of the potentially Bushveld event-associated lherzolitic diamonds from Cullinan Mine (Richardson et al. 1993) on the Kalahari Craton, the principal observation for peridotitic diamonds is their tight distribution about the mantle value of −5‰.

Eclogitic suite

Most of the variability in carbon isotope composition seen in the worldwide diamond distribution derives from samples with eclogitic (meta-basaltic) inclusions. The eclogitic suite of lithospheric diamonds shows a prominent mode at −5.0‰ but is distinctly skewed towards more negative values extending to −40.7‰, with a second mode at −11.8‰ (Fig. 2). The record for eclogitic diamonds is dominated by samples from the Kalahari Craton of Southern Africa (603 of 1204 analyses), which together with diamonds from the Central Slave Craton, the Siberian Platform and the Ural alluvials account for the prominent mode at -5‰. A dominance of mantle-like carbon is, however, not a universal feature of eclogitic diamonds, with datasets, e.g., for the deposits at Argyle (Kimberley Craton), Guaniamo (Amazon Craton) and Jericho (Northern Slave Craton) having overall ^{13}C-depleted distributions with an almost complete absence of mantle-like carbon (see Cartigny et al. 2014, their Fig. 5). The large analytical data set for Argyle (221 analyses) is responsible for the second mode at −11.8‰ in the eclogitic distribution (Fig. 2). To limit the influence of localities that are overrepresented in the worldwide database (Argyle and Premier/Cullinan), Cartigny et al. (2014) adjusted each locality to have the same statistical weight but still obtained the same second mode at ~ −11‰. $\delta^{13}C$-values above 0‰ are restricted to diamonds from the New South Wales alluvial deposits (Fig. 2), with an unusually Ca-rich inclusion suite that may relate to meta-rodingites as diamond substrates (Davies et al. 2003). The most ^{13}C-depleted values among eclogitic diamonds, down to −40.7‰, are reported from the former Jericho mine (Northern Slave Craton).

Websteritic (pyroxenitic) suite

Based on the chemistry of websteritic inclusions in lithospheric diamonds, the websteritic (or more general, pyroxenitic) suite forms in substrates that are intermediate between those of the eclogitic and peridotitic suites (Gurney et al. 1984, Stachel and Harris 2008). Despite a much smaller sample number, websteritic diamonds have a very similar $\delta^{13}C$-distribution to eclogitic diamonds, with a prominent mode at −4.9‰ and a tail towards ^{13}C-depleted compositions extending to −41.3‰ (again a diamond from Jericho), with secondary modes peaking at −11.2 and −18.5‰ (Fig. 2). The key difference to the eclogitic diamond distribution is an absence of ^{13}C-enriched websteritic diamonds, with the maximum $\delta^{13}C$-value being −3.7‰. A further distinguishing criterion is that websteritic diamonds from individual deposits generally either all fall into the mantle range (e.g., Venetia on the Kalahari Craton, the Namibian coast, A154 at Diavik on the Central Slave Craton) or are all distinctly depleted in ^{13}C ($\delta^{13}C < -10$‰; e.g., Jagersfontein and the Orapa Cluster on the Kalahari Craton and Jericho).

Graphite pseudomorphs after diamond in pyroxenites (garnet–clinopyroxenites) from Beni Bousera (Morocco) provide an additional data set for the carbon isotope composition of "websteritic diamonds". The Beni Bousera pseudomorphs range in $\delta^{13}C$ from −27.6 to −16.4‰ (Fig. 2), with a median at −21.0‰, and fall into the ^{13}C-depleted group of websteritic diamonds.

Asthenospheric and transition zone suite

Only very few diamonds have been described that contain majoritic garnet inclusions of harzburgitic, lherzolitic or wehrlitic paragenesis. In all cases, these peridotitic majoritic garnet inclusions carry a signature of depleted lithospheric substrates, by either being subcalcic (having CaO contents below the lherzolitic Ca-Cr array, indicative of clinopyroxene-free substrates; see Sobolev et al. 1973), or through high Cr_2O_3 contents (≥ 4 wt%), i.e., their compositions are not consistent with an origin in fertile convecting mantle but instead point to their derivation from either over-thickened subcratonic lithospheric mantle (Pokhilenko et al. 2004) or deeply subducted oceanic lithospheric mantle. In total, carbon isotope analyses are available for eight such diamonds and range from −12.2 to −2.7‰, with a median of −5.2‰. Due to their rarity, uncertain origin and low number of analyses, these samples are not further considered here.

Far more common in asthenosphere- and transition zone-derived diamonds are inclusions with "eclogitic" (meta-basaltic) compositions, mostly low-Cr (below detection to 0.37 wt% Cr_2O_3) majoritic garnets. The carbon isotope compositions of these sublithospheric diamonds cover a wide range from −24.8 and +0.9‰ (Fig. 4; Table 1), similar to lithospheric eclogitic and websteritic diamonds. Individual localities seem to carry specific carbon isotope signatures. Diamonds from the Juina area in Brazil fall into two clusters, one with strongly negative values (−24.8 to −23.4‰) and the other with moderate to no ^{13}C depletion (−15.3 to −4.6‰) relative to the canonical mantle value. Other localities have much narrower ranges, with, e.g., Jagersfontein diamonds being strongly ^{13}C-depleted ($\delta^{13}C$ between −23.0 and −17.2‰), Koffiefontein (Kalahari Craton) diamonds showing less negative $\delta^{13}C$ (−18.6 to −15.4‰) and Kankan (W. African Craton) diamonds being ^{13}C-enriched (−3.1 to +0.9‰). Overall, these "eclogitic" sublithospheric diamonds are unlike any of the other suites discussed here, showing a relatively flat $\delta^{13}C$ frequency distribution, with no mode near the mantle value, and high variance. This characteristic is, however, shared with a small number of individual deposits (Argyle, Guaniamo, Jericho, NSW alluvials) contributing to the eclogitic diamond population (see Fig. 2).

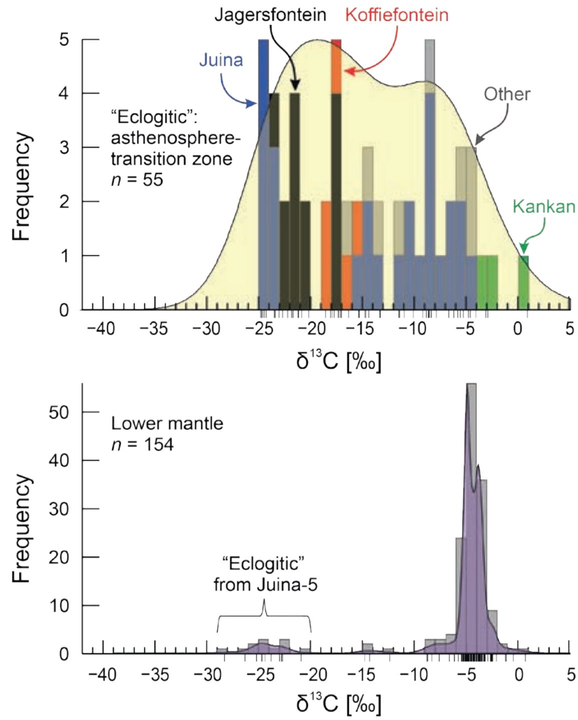

Figure 4. Distribution in carbon isotope composition for diamonds with superdeep inclusions. The distribution for diamonds from the asthenosphere and transition zone **(top)** is entirely based on samples containing inclusions with "eclogitic" (meta-basaltic) mineral compositions, mostly low-Cr majoritic garnets. Most of these inclusions are derived from four deposits, Juina (Amazon Craton), Jagersfontein and Koffiefontein (Kalahari Craton) and Kankan (West African Craton). Lower mantle diamonds **(bottom)** generally derive from meta-peridotitic substrates, with the exception of a small number of samples from the Juina-5 kimberlite containing inclusions with re-constructed bulk compositions that document metabasaltic ("eclogitic") diamond substrates (Thomson et al. 2014). The **colored curves** are Kernel density estimations, shown in the background are histograms with a 1‰ binning interval. **Black dashes** below the *x*-axis indicate individual data points.

Lower mantle suite

The bulk of diamonds with an assigned lower mantle origin carries associations including the mineral ferropericlase. These diamonds are generally assigned to "meta-peridotitic" substrates and predominantly come from the Juina area, Kankan and the DO27 kimberlite from the Central Slave Craton. A definitive lower-mantle paragenesis of ferropericlase-bearing diamonds is only substantiated by co-existence with $MgSiO_3$, with the appropriate Ni partitioning for equilibration at lower mantle pressures (Stachel et al. 2000b), or $CaSiO_3$. For diamonds carrying ferropericlase inclusions only, a shallower origin (Brey et al. 2004) is possible but, for the purpose of this review, such an origin is considered unlikely as long as other diamonds from the same locality contain associations unique to the lower mantle. For a small subgroup of Juina diamonds, exclusively recovered from the Juina 5 kimberlite, Thomson et al. (2014) reconstructed inclusion compositions indicative of a meta-basaltic ("eclogitic") association. The meta-peridotitic diamonds have a $\delta^{13}C$-distribution focused on a prominent mode at –4.9‰, with an associated secondary mode at –3.9‰, and a range from −14.8 to +0.7‰ (Fig. 4). The distribution is non-normal (Shapiro-Wilk and d'Agostino-Pearson tests) and has a negative skewness (–2.5). The meta-basaltic diamonds are all strongly depleted in ^{13}C ($\delta^{13}C$ between −28.3 to −20.9‰; Fig. 4).

The δ^{13}C-distributions of meta-peridotitic lower mantle diamonds and peridotitic lithospheric diamonds are a close match. Using a Student's *t-test*, equality of means between metaperidotitic lower mantle diamonds and peridotitic lithospheric diamonds cannot be rejected; on the paragenesis level the same is true for lherzolitic but not for harzburgitic lithospheric diamonds. With the lherzolitic paragenesis (Fig. 3) the lower mantle diamonds share a rapid drop-off in abundance at δ^{13}C below –6‰ and a secondary mode at about –4‰. The secondary mode for meta-peridotitic lower mantle diamonds is caused by samples from Kankan (West African Craton), which also contribute to the secondary mode at –4‰ for lithospheric lherzolitic diamonds. This documents that lower mantle and lithospheric peridotitic (lherzolitic) diamonds not only share the same principal mode but also subtle isotopic shifts typical for a particular cratonic region.

Commonalities and differences of the isotopic composition of diamond carbon across mantle reservoirs

The carbon isotope compositions of the four principal diamonds suites (peridotitic, eclogitic, asthenosphere-transition zone, and lower mantle) are compared in Figure 5. Peridotitic lithospheric and meta-peridotitic lower mantle diamonds share a narrow principal mode and median value close to or at the mantle value, as defined by other mantle-derived samples such as carbonatites, kimberlites, mid-ocean ridge and ocean-island basalts. This strong similarity is particularly true for the lherzolitic paragenesis of lithospheric diamonds, whilst harzburgitic diamonds have a statistically different mean than meta-peridotitic lower mantle diamonds. The peridotitic lithospheric and metaperidotitic lower mantle diamond suites evidently tap the same mantle carbon reservoir and the observation of common minor isotopic shifts for lower mantle and lithospheric diamonds from the West African Craton documents a vertical flux of carbon between superdeep and shallow diamond substrates.

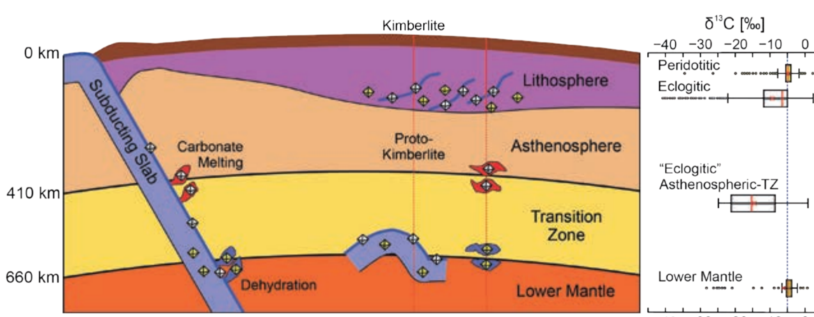

Figure 5. Environment of formation and carbon isotope composition for the four principal diamond suites. Lithospheric diamonds of the peridotitic (**yellow**) and eclogitic (**white**) suites grow in depleted peridotitic (purple) and meta-basaltic (eclogitic; **dark blue**) substrates (e.g., Meyer and Boyd 1972; Sobolev 1977). In the asthenosphere and transition zone, diamonds form in subducting oceanic crust (**dark blue**; Stachel et al. 2000a) or in reaction zones between slab-derived carbonatitic melts and pyrolytic wall rock (**red**; Walter et al. 2008; Thomson et al. 2016). Inclusions in these diamonds (**white**) have meta-basaltic ("eclogitic") affinity. In the lowermost transition zone and the lower mantle, diamonds may form in the meta-peridotitic (**light blue with yellow diamonds**) or meta-basaltic (**dark blue with white diamonds**) portions of subducting slabs, or in adjacent pyrolytic wall rock (**blue jets with yellow diamonds**), driven by dehydration reactions (Harte 2010) and the associated expulsion of oxidized fluids into ambient mantle (Stachel et al. 2005; Regier et al. 2020). Sampling of superdeep diamonds likely occurs through ascending proto-kimberlite magma (**red dotted lines**), either from stagnant slabs (megaliths; **light and dark blue**) or from remnant reaction zones between slab-derived hydrous fluids (**blue**) or carbonatitic melts (**red**) and pyrolytic wall rock. Lithospheric diamonds are collected during rapid final ascent of kimberlite magma (**red line**) through subcratonic lithospheric mantle. The carbon isotopic composition (δ^{13}C in ‰) of the four principal diamond suites is given in the right-hand column as median values (**red lines**), averages (**red crosses**), 25th to 75th percentiles (interquartile range; **boxes**) and ranges (**whiskers**). Outliers are indicated as **small circles** (**white** for meta-basaltic and **yellow** for meta-peridotitic affinity). The **blue dashed line** indicates the assumed mantle value of –5‰ (Deines 2002).

Diamonds formed in meta-basaltic substrates in the lithosphere and in the asthenosphere-transition zone have similar ranges (Fig. 5) but clearly differ through the strong dominance of mantle-like carbon in lithospheric eclogitic diamonds that is not as evident in the sub-lithospheric diamonds (Fig. 2). This not only documents that mantle-derived carbon is negligible for diamond formation associated with subducting slabs in the asthenosphere and transition zone but also suggests a common origin of both ^{13}C-depleted and ^{13}C-enriched diamond carbon for meta-basaltic environments in lithospheric and sublithospheric substrates. This aspect will be discussed further below.

NITROGEN ISOTOPE COMPOSITION OF DIAMOND AND ITS RELATIONSHIP TO INCLUSION PARAGENESIS

The nitrogen isotope composition of Earth's mantle, based on analyses of mid-ocean ridge basalts and fibrous diamonds, is −5 ± 2‰ (Cartigny and Marty 2013). The nitrogen isotope composition of diamond has a unimodal distribution with minor skewness to positive values and a range over 56‰ (from −39.4 to +16.9‰, Fig. 6). Compared to the mantle value, the mode (−3.5‰) and median (−2.1‰) are shifted to slightly higher values (Table 2). The range from −8.5 to +1.5‰ (i.e., the mode of −3.5 ± 5‰) contains about 2/3 of the data. The specific nitrogen isotope distributions of the various suites and parageneses of mantle-derived inclusion-bearing diamonds are discussed in detail below.

Peridotitic suite

The $\delta^{15}N$-distribution of diamonds with peridotitic inclusions has a principal mode at +2.0‰ with a secondary mode (or shoulder; Fig. 7) at −4.1‰. This Kernel density estimation can be approximated as a mixture of two Gaussian distributions with modes at −7.5‰ (44%) and +3.4‰ (56%; see section Database and Methods), which may or may not reflect geological reality. The peridotitic $\delta^{15}N$-distribution principally results from different modes in $\delta^{15}N$ for different localities, with ^{15}N-depleted diamond populations, e.g., at Pipe 50 (Liaoning, China) and the Victor Mine (Superior Craton), and ^{15}N-enriched populations, e.g., at the Kimberley mines ('*De Beers Pool*'), Cullinan Mine (both Kalahari Craton) and Ellendale (Kimberley Craton).

Broken down further by paragenesis, diamonds with harzburgitic inclusions have a mode at +2.1‰, coinciding with the upper mode for the peridotitic suite, and a distribution that is skewed towards more negative values (Fig. 8; Table 2). Lherzolitic diamonds show a distribution with two pronounced modes (−6.3 and +2.9‰), which can be largely resolved into two Gaussian distributions with modes at −5.9‰ (42%) and +3.9‰ (58%)—suggesting two overlapping distributions rather than a continuous but under-sampled population. Similar to the entire peridotitic suite, the two lherzolitic sub-populations largely reflect isotopically light nitrogen in diamonds from Victor and isotopically heavy nitrogen in diamonds from Cullinan Mine. The distribution of diamonds with lherzolitic inclusions (−11.7 to +9.6‰, Fig. 8) lacks the tail to strongly ^{15}N-depleted samples seen for harzburgitic diamonds (−24.1 to +12.4‰). The peridotitic diamond with the lowest $\delta^{15}N$-value (−39.4‰; diamond KK-21 from Kankan) cannot be further classified, containing olivine inclusions only (see Stachel et al. 2022, this volume).

Eclogitic suite

Diamonds with eclogitic inclusions show a nitrogen isotope distribution with a mode at −6.2‰, a shoulder at about −2.0‰, and a skewness towards high values (Fig. 7). Breaking the $\delta^{15}N$-distributions down by carbon isotope composition reveals a hitherto unrecognized systematic shift (Fig. 9): diamonds with a carbon isotope composition close to the mantle value ($\delta^{13}C$ between −7 and −3‰) are very similar to the overall eclogitic distribution in terms of their $\delta^{15}N$-values (same mode at −6.2‰ and a similar shoulder at about -2.0‰), with the exception of an absence of values greater than +11.1‰. Diamonds with distinctly ^{13}C-depleted isotope compositions ($\delta^{13}C \leq -15$‰) are ^{15}N-enriched, with a near normal distribution about

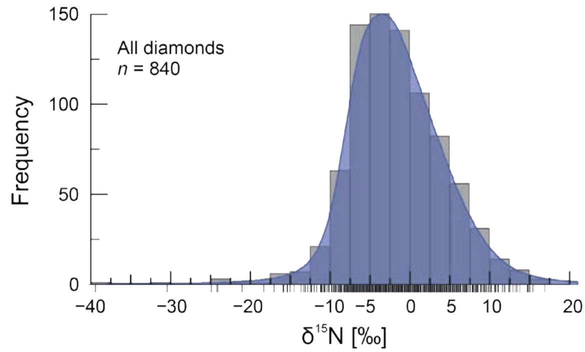

Figure 6. Distribution in nitrogen isotope composition ($\delta^{15}N$) for (mostly) inclusion-bearing diamonds worldwide. The **blue curve** is a Kernel density estimation, shown in the background is a histogram with a 1‰ binning interval. **Black dashes** below the *x*-axis indicate individual data points.

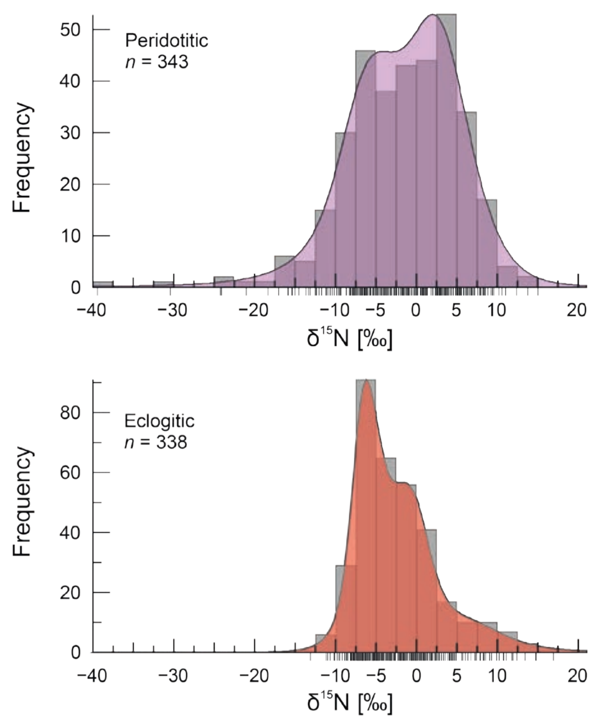

Figure 7. Distribution in nitrogen isotope composition for diamonds with peridotitic **(top)** and eclogitic suite **(bottom)** inclusions. The **colored curves** are Kernel density estimations, shown in the background are histograms with a 1‰ binning interval. **Black dashes** below the *x*-axis indicate individual data points.

a mode at +1.3‰ and a range from −5.3 to +14.8‰ (Fig. 9; Table 2). The data set for the ^{13}C-depleted diamonds is small ($n = 22$) but derives from seven different locations (Jwaneng, Orapa, Namibian southern coastal mines, Kimberley [all from the Kalahari Craton], Ural alluvials, Panda [Ekati Mine, Central Slave Craton] and Chidliak [likely North Atlantic Craton]) and, therefore, represents more than just local variability.

Table 2. Statistical assessment of the nitrogen isotope composition ($\delta^{15}N$) of inclusion-bearing diamonds from worldwide sources.

Suite	All diamonds	Peridotitic			Eclogitic			Lower Mantle
Paragenesis		All	Lherzolitic	Harzburgitic	All	$\delta^{13}C$ –7 to –3‰	$\delta^{13}C$ ≤ –15‰	
n	840	343	76	102	338	239	22	29
Min (‰)	–39.4	–39.4	–11.7	–24.1	–13.1	–13.1	–5.3	–24.9
Max (‰)	16.9	15.0	9.6	12.4	16.9	11.1	14.8	2.6
Average (‰)	–1.7	–1.7	–0.3	–0.1	–2.4	–3.6	2.6	–3.6
SD (‰)	6.0	7.0	5.5	6.8	5.2	4.1	5	4.9
Median (‰)	–2.1	–1.1	1.2	1.2	–3.4	–4.6	1.5	–2.8
MAD (‰)	3.9	4.8	4.5	4.1	3.2	2.7	3.2	1.7
Q1 (‰)	–5.8	–6.2	–5.7	–3.6	–6.4	–6.7	–1.7	–4.6
Q3 (‰)	2.1	3.2	3.7	4.9	0.1	0.6	6.1	–1.2
IQR (‰)	7.9	9.4	9.4	8.5	6.5	7.3	7.8	3.4
Mode (‰)	–3.5	2.0	2.9	2.1	–6.2	–6.2	1.3	–2.7

Note: Statistical parameters quoted are: *n*—number of samples; Min—lowest values; Max—highest values; Average—arithmetic mean; SD—1 standard deviation calculated based on a sample; Median—median value; MAD—median absolute deviation; Q1—25th percentile; Q3—75th percentile; IQR—interquartile range (IQR = Q3–Q1); Mode—maximum value of the kernel density estimation.

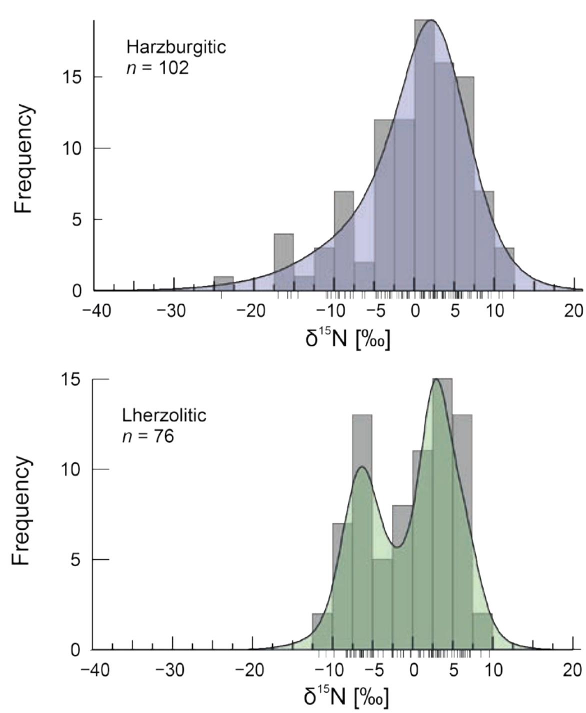

Figure 8. Distribution in nitrogen isotope composition for diamonds with peridotitic inclusions of harzburgitic **(top)** and lherzolitic **(bottom)** paragenesis. The **colored curves** are Kernel density estimations, shown in the background are histograms with a 1‰ binning interval. **Black dashes** below the *x*-axis indicate individual data points.

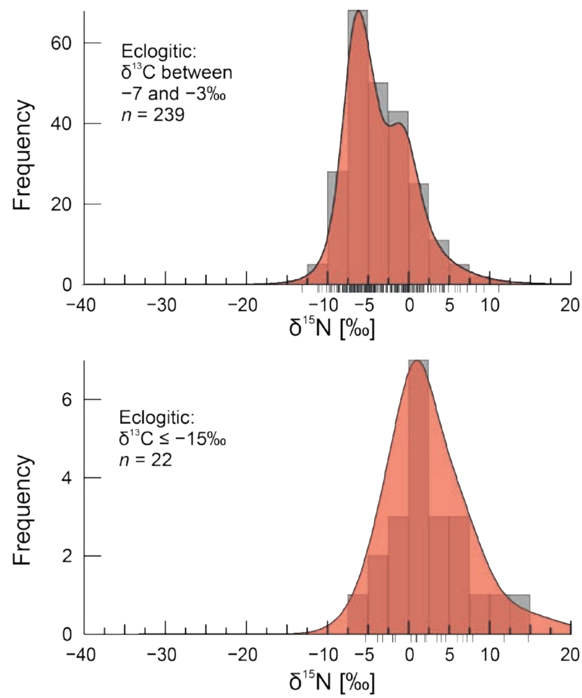

Figure 9. Distribution in nitrogen isotope composition for diamonds with eclogitic inclusions, split into two groups based on their carbon isotope composition: diamonds with δ^{13}C-values very close to the accepted mantle value (–5 ± 2‰; **top**) and with strongly ^{13}C-depleted compositions (≤ –15‰; **bottom**). The **colored curves** are Kernel density estimations, shown in the background are histograms with a 1‰ binning interval. **Black dashes** below the *x*-axis indicate individual data points.

Lower mantle suite

For superdeep diamonds, nitrogen contents that are typically either low or below the limit of detection lead to a small number of samples with associated nitrogen isotope analyses, which is only large enough for lower mantle diamonds (n = 29) to be included here. For a limited δ^{15}N dataset on asthenospheric and transition zone diamonds with "eclogitic" majorite inclusions, the reader is referred to Palot et al. (2012, 2017).

The analyzed diamonds with lower mantle inclusions (13 from Juina and 16 from Kankan) show a very tight normal distribution about a δ^{15}N mode of −2.7‰ (median −2.8‰; Fig. 10; Table 2). The diamonds have a δ^{13}C range from −7.6 to −1.3‰ and contain inclusions considered to reflect meta-peridotitic substrates. If we assume that nitrogen in the meta-peridotitic substrates for the analyzed lower mantle diamonds is not subduction-related, the narrow δ^{15}N-distribution of these diamonds may be used to bracket the nitrogen isotope composition of the lower mantle. For diamond formation at expected lower mantle temperatures in excess of 1600 °C (e.g., Stixrude and Lithgow-Bertelloni 2007), nitrogen fractionation factors between diamond and neutral to variably reduced nitrogen species (from N_2 through NH_3 and NH_4^+ to nitrides) will be fairly small (see Fig. 19), placing the nitrogen isotope composition of the lower mantle between about –4 and 0‰. This clearly supports the view of a convectively (largely) homogenized isotopic composition of nitrogen across the transition zone—lower mantle boundary (Palot et al. 2012).

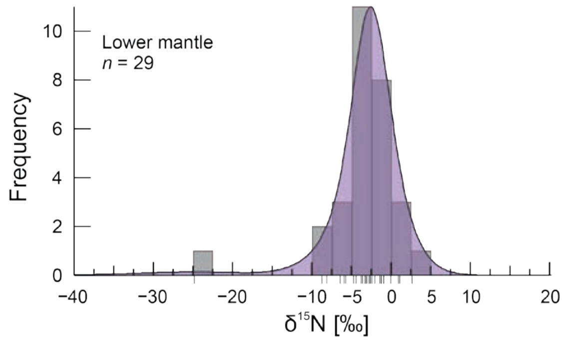

Figure 10. Distribution in nitrogen isotope composition for diamonds with lower mantle inclusions. Based on their inclusion assemblages (including the mineral ferropericlase in 22 of the 29 analyzed samples), derivation from principally meta-peridotitic substrates is inferred. The one outlier with a δ^{15}N-value of –24.9‰ also represents a diamond containing a ferropericlase inclusion. The **colored curve** is a Kernel density estimation, shown in the background is a histogram with a 1‰ binning interval. **Black dashes** below the *x*-axis indicate individual data points.

Commonalities and differences of the nitrogen isotope composition of diamond across mantle reservoirs

Comparing the δ^{15}N-distributions presented in Figures 6 to 10 reveals commonalities across diamond suites: (1) The ^{15}N-depleted peridotitic (mainly lherzolitic) diamond productions from Victor and Pipe 50 have a combined mode in δ^{15}N at –6.6‰, coinciding with the main mode for eclogitic diamonds (–6.2‰). This suggests derivation from a common nitrogen reservoir. (2) The main modes in nitrogen isotope composition for peridotitic diamonds, their harzburgitic and lherzolitic sub-divisions, and strongly ^{13}C-depleted ($\delta^{13}C \leq -15$‰) eclogitic diamonds fall in the δ^{15}N range +1 to +3‰, again suggesting tapping of a common nitrogen reservoir. (3) Lower mantle diamonds have a narrow distribution with a mode (–2.7‰) that falls between the two common modes for lithospheric diamonds, but coincides with the mode for all analyzed diamonds (–3.5‰). Given that the latter is a composite distribution of mostly peridotitic (41%) and eclogitic (40%) diamonds with distinct modes, this agreement may be purely coincidental.

The overall similarity in the nitrogen isotope compositions of peridotitic and eclogitic diamonds is further highlighted in Figure 11. The interquartile ranges and full ranges of eclogitic and lower mantle diamonds are contained within the peridotitic ranges and a

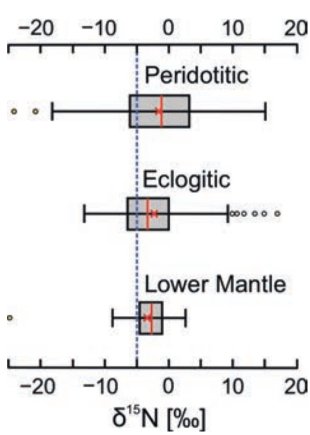

Figure 11. Nitrogen isotope composition (δ^{15}N) of peridotitic, eclogitic and lower mantle suite diamonds. Median values (**red lines**), averages (**red crosses**), 25th to 75th percentiles (interquartile range; **boxes**) and ranges (**whiskers**) are shown. Outliers are indicated as small circles (**white** for meta-basaltic and **yellow** for (meta-)peridotitic affinity). Two outliers for the peridotitic suite (at –39.4 and –30.4‰) are outside the δ^{15}N range shown. The **blue dashed line** indicates the assumed mantle value of –5 (± 2)‰ (Cartigny and Marty 2013).

single ^{15}N-enriched eclogitic diamond exceeds the peridotitic range. Based on the greatly expanded dataset presented here, the notion that positive δ^{15}N-values are a clear indication of subduction-related diamond associations cannot be maintained. In fact, δ^{15}N-values greater than 0‰ are more commonly observed among peridotitic (45% > 0‰) than among eclogitic (25%) diamonds. The main mode of peridotitic diamonds (δ^{15}N of +2‰) may instead indicate involvement of plume-derived nitrogen (δ^{15}N of +3 ±2‰; Dauphas and Marty 1999; Marty and Dauphas 2003). The fact that most eclogitic and peridotitic diamonds share similar δ^{15}N-values strongly suggests similar origins of their nitrogen (see also Cartigny 2005; Cartigny and Marty 2013; Smart et al. 2016 for further reviews and a discussions).

RELATIONSHIPS AMONG δ^{13}C, δ^{15}N AND NITROGEN CONTENT

δ^{13}C and nitrogen content

Nitrogen is the most abundant impurity in diamond (see *Introduction*), with average and median N-contents of 314 and 166 at.ppm (or 366 and 194 ppm on a weight basis), respectively, based on our worldwide database (n = 3899 for N_{FTIR}). Estimates of the nitrogen content of depleted (MORB source) mantle, based on ratios of nitrogen with noble gases and with carbon, range between 0.09 and 0.27 ppm (see review in Marty 2012). Accordingly, the average and median nitrogen content of diamond is 2100–4100 and 700–1400 times higher, respectively, than that of depleted mantle, which makes diamond an excellent target mineral for investigating the behavior of nitrogen in mantle processes.

Whether nitrogen preferentially partitions into diamond or the fluid/melt from which diamond precipitates is a subject of longstanding debate. One end-member view is that nitrogen is strictly incompatible in the diamond structure (i.e., $K_N = (C_{N\text{-diamond}}/\ C_{N\text{-fluid/melt}}) < 1$) but that kinetic effects play an important role. Specifically, rapidly-grown diamonds approach compatibility for nitrogen ($K_N \sim 1$) whereas slowly-grown diamonds largely exclude nitrogen (Boyd et al. 1994; Cartigny et al. 2001). The observation of sector zoning of nitrogen in diamond (Boyd et al. 1988)—during mixed habit growth octahedral sectors of natural diamonds incorporate about 12% more nitrogen than cuboid sectors (Howell et al. 2012 and reference therein)—clearly documents that kinetic effects play a role in controlling the partitioning behavior of nitrogen between diamond–fluid/melt. The opposite view, a compatible behavior of nitrogen in diamond ($K_N > 1$), is based on the observation of fractionation trends involving progressively decreasing N-contents in multiple diamonds from a single xenolith (Thomassot et al. 2007) and in individual diamonds from both natural occurrences (Smart et al. 2011; Wiggers de Vries et al. 2013; Petts et al. 2015; Smit et al. 2016, 2019a) and high-pressure/high-temperature diamond synthesis (Reutsky et al. 2008; Stachel et al. 2009). Mikhail and Howell (2016) suggested that nitrogen can partition either compatibly or incompatibly during diamond growth, depending on nitrogen speciation (N_2, NH_3 or NH_4^+) and how the different nitrogen species dissociate to create the transient monatomic nitrogen necessary for incorporation into the diamond lattice. Nitrogen speciation, in turn, depends on oxygen fugacity (Li and Keppler 2014) and, for aqueous diamond-forming fluids, on pH (Mikhail and Sverjensky 2014). Empirical evidence from fractionation trends, however, suggests that nitrogen is compatible under both strongly reducing (CH_4 as the principal carbon species: K_N = 2.0–3.5; Thomassot et al. 2007; Wiggers de Vries et al. 2013; Smit et al. 2019a) and more oxidizing conditions (carbonate or CO_2 as the principal carbon species: K_N = 2.0–4.4; Wiggers de Vries et al. 2013; Petts et al. 2015). The K_N-values in these studies were all estimated assuming diamond formation from fluids composed entirely of a single carbon species. Based on the speciation of fluids in the system COH (Zhang and Duan 2009) and the redox stability of pure carbonate melts versus dilute carbonate components (dilution extends stability to lower oxygen fugacities; Stagno and Frost 2010), diamond formation from a single pure carbon species is considered highly unlikely. As a consequence, the above values for K_N represent minimum estimates (Petts et al. 2015). For example, the water-rich (up to ~ 98% H_2O) COH fluids predicted to exist in diamond-stable subcratonic mantle near ~ 150 km depth require K_N-values > 70 to account for the observed N-content fractionation trends (Stachel et al. 2017). The extreme average enrichment of nitrogen in diamond relative to depleted mantle is also circumstantial evidence for the compatible nature of nitrogen in diamond.

Early SIMS-based studies of internal co-variations of $\delta^{13}C$ and N-content within individual diamonds (e.g., Fitzsimons et al. 1999; Harte et al. 1999; Zedgenizov and Harte 2004) principally focused on differences between successive growth zones and were limited by the comparatively low analytical precision (~0.6–1.4‰, 2 sigma) of $\delta^{13}C$ measurements using single-collector instruments. These studies indicated large variability in nitrogen content among different growth zones, accompanied by (within uncertainty) near constant or uncorrelated and abruptly changing carbon isotope compositions. With the advent of multi-collector SIMS (e.g., Craven et al. 2009; Smart et al. 2011) analytical uncertainty improved significantly (< 0.2‰, 2 sigma), allowing for subtle variations in carbon isotope composition to be detected, but the focus remained on tracing variations in $\delta^{13}C$-values and N-content from core to rim across multiple growth zones (e.g., Peats et al. 2012; Palot et al. 2013). Growth zone boundaries visible in cathodoluminescence (CL) images, however, represent discontinuities that may relate to abrupt fluctuations in fluid composition (fluid re-charge) and/or physical conditions during continued diamond growth. Alternatively, there may have been temporal gaps in diamond growth of unknown duration with re-initiation of diamond growth from new, potentially completely unrelated fluid pulses. Consequently, smooth continuous trends characterized by correlated, outward evolving carbon isotope compositions and nitrogen concentrations can typically only be detected on the level of individual growth zones with internally fairly homogenous appearance in CL images (first documented by Smart et al. 2011). Despite a series of subsequent studies, using multi-collector SIMS and also a step-wise oxidation approach (Mikhail et al. 2014), the number of samples with convincing continuous co-variations in $\delta^{13}C$ and N-content has remained extremely small, indicating that Rayleigh fractionation during the growth of individual diamonds is relatively rare. Nevertheless, smooth trends of both outward increasing (Smart et al. 2011; Wiggers de Vries et al. 2013; Smit et al. 2016) and decreasing (Wiggers de Vries et al. 2013; Reutsky et al. 2017; Smit et al. 2019a) $\delta^{13}C$-values associated with decreasing nitrogen contents have been documented. The interpretation of such trends is discussed further below (see section *Origin of covariations among* $\delta^{13}C$*,* $\delta^{15}N$ *and nitrogen content*).

On the level of our worldwide diamond database, $\delta^{13}C$ and nitrogen content are uncorrelated (Fig. 12). For the peridotitic suite, a comparatively small variance in carbon isotope composition relative to eclogitic diamonds creates a tight cluster with highly variable N-contents (below detection to 2390 at.ppm) mainly falling between −7 and −3‰ (Fig. 12). Over this $\delta^{13}C$-range, the moving median and average nitrogen contents drop by 80–90 at.ppm towards both sides of their respective maxima at ~ 5‰ (170 and 260 at. ppm nitrogen, respectively; see Fig. 13). If this drop was related to Rayleigh fractionation during diamond precipitation (Stachel et al. 2009), then based on the K_N-values discussed above, N-contents should fall more sharply (between 50 and 99%, depending on carbon speciation and exact choice of K_N; see fractionation trends in Fig. 12). If unrelated to fractionation, the maximum in median and average nitrogen content at $\delta^{13}C$ ~ 5‰ implies that fluids carrying the putative mantle carbon component are also the most enriched in nitrogen. For diamonds of the eclogitic suite, Stachel and Harris (1997) observed a decrease in maximum nitrogen content as $\delta^{13}C$ decreases away from the mantle value (−5‰). This relationship was subsequently formalized by Cartigny et al. (2001) as the "limit sector" and interpreted as resulting from Rayleigh fractionation during outgassing of CO_2 from carbonated melts (causing depletion of ^{13}C in the residual melt) and associated loss of nitrogen from the melt. Subsequent studies, e.g., on eclogitic suite diamonds from the Olenek River (Yakutia; Shatsky et al. 2014) and micro-diamonds from the Orapa Mine

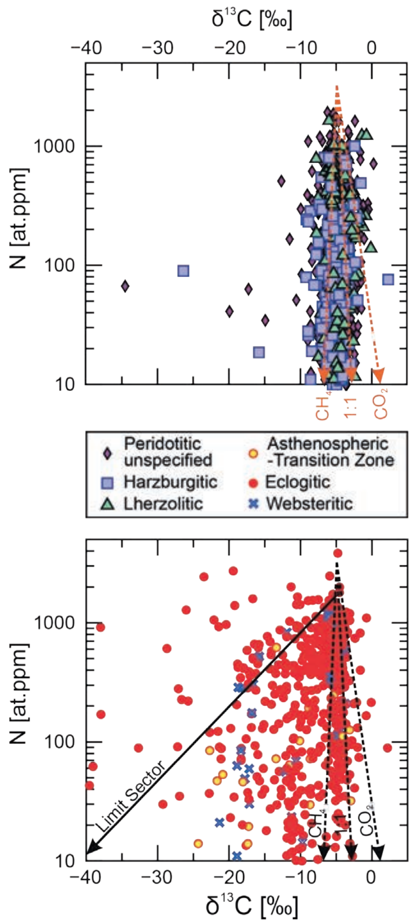

Figure 12. Nitrogen content (at.ppm) versus carbon isotope composition for inclusion-bearing diamonds **(top)** of the peridotitic suite (harzburgitic, lherzolitic and unspecified paragenesis shown separately) and **(bottom)** of the eclogitic, websteritic, and ("eclogitic") asthenospheric-transition zone suites. The **dashed lines** indicate Rayleigh fractionation trends calculated for fluids made up entirely of diamond-forming carbon species (pure CH_4, a 1:1 mix of CH_4 and CO_2, and pure CO_2), using diamond–fluid isotope fractionation factors appropriate for a temperature of 1150 °C (approximate average temperature of diamond formation) and a diamond–fluid nitrogen partition coefficient (K_N) of 4.4 (taken from Petts et al. 2015). The **solid black line** is the "limit sector" of Cartigny et al. (2001) and corresponds to a fractionation trend for a carbonated diamond-forming fluid/melt caused by fluid loss.

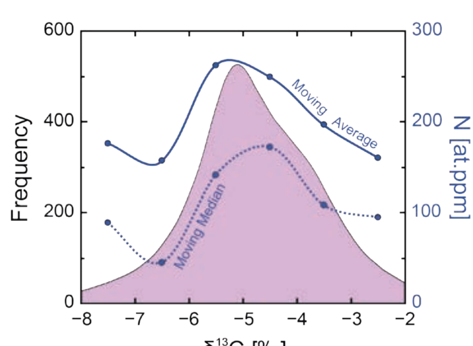

Figure 13. Kernel density estimation of the distribution in carbon isotope composition ($\delta^{13}C$) for diamonds worldwide containing inclusions of the peridotitic suite. The **blue curves** represent variations in nitrogen concentration (at.ppm, axis on right) with $\delta^{13}C$. The **solid curve** and **filled blue circles** are average values, the **dashed line** and **filled blue circles** are median values, calculated in one permille increments.

(Chinn et al. 2018; not included in Fig. 12), however, contradicted the limit sector relationship by showing high nitrogen contents (up to 3600 at.ppm) at δ^{13}C-values below −20‰. Overall, the lack of correlation between carbon isotope composition and nitrogen content for both the worldwide peridotitic and eclogitic suites suggests that either (1) carbon and nitrogen are at best weakly coupled in diamond-forming fluids, (2) variably evolved fluids carry distinct nitrogen contents, (3) a range of K_N-values exists, or (4) that precipitation/break-down of other N-bearing mantle phases (e.g., clinopyroxene or phlogopite) accompanies diamond growth.

δ^{15}N and nitrogen content

For the worldwide database, nitrogen in diamond and its isotopic composition (Fig. 14) show a surprising lack of coupling. Under the precondition that natural diamond-forming processes do not involve a highly variable elemental or isotopic partitioning behavior of nitrogen (i.e., large variations in K_N-value or N-isotope fractionation factor), this decoupling suggests that derivation of diamond-forming fluids from a single source (mantle or subducted crust), with constant nitrogen concentration and δ^{15}N-values, may be excluded. Additionally, if the large variability of nitrogen concentration and isotopic composition was due a single process, e.g., Rayleigh fractionation during diamond growth (see below), then a highly correlated behavior would be expected. A Rayleigh fractionation trend, induced by either diamond crystallization (Fig. 14) or nitrogen loss from a melt, clearly cannot explain the variability of diamonds of either the peridotitic or eclogitic suites.

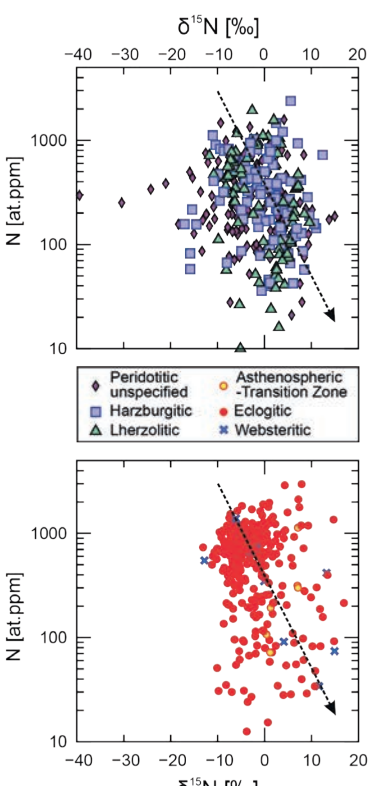

Figure 14. Nitrogen content (at.ppm) versus nitrogen isotope composition for inclusion-bearing diamonds **(top)** of the peridotitic suite (harzburgitic, lherzolitic and unspecified paragenesis shown separately) and **(bottom)** of the eclogitic, websteritic, and ("eclogitic") asthenospheric-transition zone suites. The **dashed line** indicates a Rayleigh fractionation trend using a diamond–fluid N-isotope fractionation factor appropriate for a temperature of 1150 °C (approximate average temperature of diamond formation) and a diamond–fluid nitrogen partition coefficient (K_N) of 4.4 (Petts et al. 2015).

For the peridotitic suite, the data form a cloud from low to high $\delta^{15}N$-values and nitrogen contents (Fig. 14). From this cloud extends an array of peridotitic diamonds of unspecified paragenesis with intermediate nitrogen contents (251 to 385 at.ppm) towards extremely ^{15}N-depleted compositions ($\delta^{15}N < 20‰$). If these isotopic compositions indeed represented mixing with a primordial component similar to enstatite chondrite (Cartigny et al. 1997; Palot et al. 2012), then this primordial component would be characterized by N-contents similar to the growth medium of "regular" diamonds.

For diamonds of the eclogitic suite, samples with broadly mantle-like $\delta^{15}N$ (−10 to 0‰) cluster at fairly high nitrogen concentrations, from which the data spread to higher $\delta^{15}N$ and/or lower N-contents. Two outliers, representing the highest nitrogen contents in the data set (~ 2900 at.ppm), are observed at $\delta^{15}N$ of +4.3‰ and +7.7‰ and relate to diamonds from Wellington (SE Australia) and Panda.

Considering diamonds for individual suites/parageneses on the level of individual mines does not significantly change this general picture, although, on the local level some eclogitic diamonds show a more consistent behavior in $\delta^{15}N$–N space with clear differences between certain occurrences (e.g., Jwaneng vs. Orapa mines). Hogberg et al. (2016) undertook a comprehensive SIMS-based study of 94 small diamonds from the Chidliak CH-6 and CH-7 kimberlites, producing 251 paired nitrogen content and $\delta^{15}N$ spot analysis. Although no mineral inclusions were recovered during this study, Chidliak diamonds are presumed to predominantly derive from eclogitic substrates. In diamonds with significant internal variations in nitrogen content and $\delta^{15}N$, subparallel trends of decreasing nitrogen content and increasing $\delta^{15}N$ were observed (Hogberg et al. 2016). Still, most of the population forms a cluster of mildly negative $\delta^{15}N$ at variable nitrogen contents and only a subset of diamonds fall on a positively correlated array in log(N)–$\delta^{15}N$ space. This latter group was interpreted to reflect limited degrees of Rayleigh fractionation during the waning stages of mantle fluid influx (Hogberg et al. 2016).

On the level of individual diamond plates, only two SIMS-based studies (Petts et al. 2015; Smit et al. 2016) observed smooth rim-ward trends of increasing $\delta^{15}N$ and decreasing nitrogen contents. The opposite observation, a trend of jointly decreasing $\delta^{15}N$ and nitrogen contents, was made for a set of cogenetic diamonds recovered from a single lherzolite xenolith from the Cullinan mine (Thomassot et al. 2007).

Based on the assumption that diamond nitrogen content decreases in the course of Rayleigh fractionation processes, associated with either melt degassing prior to diamond formation (Cartigny et al. 2001) or diamond formation in fluid-limited systems, high nitrogen concentrations in diamond should indicate primitive fluid compositions. The opposite, however, is not true and nitrogen-poor primitive components may exist but will exert only weak leverage on composite $\delta^{15}N$-values during fluid mixing. The variance in the nitrogen content of diamond at any given $\delta^{15}N$-value is large and, consequently, to reveal underlying trends we use both moving (1‰ steps) median N-contents calculated over 2‰ intervals in $\delta^{15}N$ and 5th- or 6th-order polynomials fitted through the nitrogen content versus $\delta^{15}N$ data (Fig. 15 and 16). The nitrogen isotope compositions of identified primitive (high-N) components as recorded by diamond are offset from the true value by the appropriate nitrogen isotope fractionation factors (depending on nitrogen speciation and temperature) and true values likely will be several permille higher (see section *Equilibrium nitrogen isotope fractionation factors related to diamond*).

For the peridotitic suite, a nitrogen-rich component with $\delta^{15}N$ ~ −3‰ is apparent, falling between the principal peak at +2.0‰ and the shoulder at −4.1‰ in the $\delta^{15}N$ kernel density distribution (Fig. 15). A second primitive component, with a $\delta^{15}N$ value of about −10 to −12‰, falls outside the principal $\delta^{15}N$-distribution and, consequently, is poorly represented in the data set. Analyzing the peridotitic data set on the paragenesis level, the nitrogen-rich component at about −3‰ (to −2‰) is also present in the lherzolitic diamonds while the ^{15}N-depleted component at about −10 to −12‰ is clearly seen in harzburgitic diamonds (Fig. 15). The polynomial fit of the harzburgitic N-content and δ^{15}N data suggests a second nitrogen-rich component at about +3‰, overlapping with the mode in the Kernel density distribution for harzburgitic diamonds at +2.1‰, but this component is not clearly evident in the moving medians. The lherzolitic diamond distribution suggests a further nitrogen-rich component at the ^{15}N-enriched end of the frequency distribution (> +7‰; Fig. 15). Combining the information on nitrogen-rich primitive components for the various groups of peridotitic diamonds, a low frequency ^{15}N-depleted component (−10 to −12‰), a higher frequency component with a δ^{15}N-value of about −3‰ and a possible strongly ^{15}N-enriched component (> +7‰) are indicated. The negatively skewed unimodal distribution in δ^{15}N of harzburgitic diamonds could be explained by a dominant nitrogen component at ~ +3‰ (coinciding with the δ^{15}N-value of plume derived nitrogen; Dauphas and Marty 1999), with the negative skew of the distribution resulting from mixing with a potentially primordial nitrogen-rich component with δ^{15}N < −10‰ (Cartigny et al. 1997). For the lherzolitic suite the nitrogen-rich component at about −3 to −2‰ falls between the two δ^{15}N modes, suggesting that the principal mode at +2.9‰ represents a nitrogen-poor component (in the +2 to +6‰ range, Fig. 15) with the ^{15}N-depleted smaller mode representing either a less N-rich component, defined by the moving medians to lie at −7‰, or fairly constant mixing between the nitrogen rich component at −3 to −2‰ with a dominant nitrogen poor component with low δ^{15}N (< −10‰).

For the eclogitic suite, a ^{15}N-depleted, nitrogen-rich component (localized at ~ −6‰ by the 5th order polynomial) and a much less abundant, even more nitrogen-rich component at ~ +7‰ are clearly present (Fig. 16).

δ^{13}C and δ^{15}N

For peridotitic suite diamonds worldwide, δ^{13}C-values fall mostly in the mantle range whilst δ^{15}N-values vary by almost 55‰, creating a near-horizontal array in Figure 17. The scatter in δ^{13}C at any given δ^{15}N is too large, even on the level of individual parageneses, to allow for statistically significant covariations between the two parameters to be determined; separate regressions for lherzolitic and harzburgitic paragenesis diamonds indicate shallow positive and negative (apparent) slopes, respectively, but with a low $r^2 = 0.14$ in both cases. The peridotitic data set can be interpreted in terms of two end-member models (or a combination thereof): (1) Rayleigh isotope fractionation of fluids carrying mantle-derived carbon and nitrogen creates the main portion of the array (see section *Origin of covariations among δ^{13}C, δ^{15}N and nitrogen content*). Especially for fluids carrying a CO_2–CH_4 mix or CH_4 as the diamond-forming carbon species, the effects of carbon isotope fractionation would disappear in the noise of the data set. The outliers with δ^{13}C-values below the mantle array and δ^{15}N-values below about −10‰, however, cannot be explained by this model (Fig. 17). (2) The δ^{13}C–δ^{15}N array represents mixing between several reservoirs (see section *Origin of large ranges in δ^{13}C and δ^{15}N*; see also Mikhail et al. 2014), involving a mantle component, several distinct subducted components (with low and high δ^{13}C and low and high δ^{15}N) and a potentially primordial component with extreme ^{15}N depletion (explaining values down to −39.4‰). To create large variations in δ^{15}N without much effect on δ^{13}C requires that the subducted components are nitrogen-rich, consistent with indications for nitrogen-rich components with positive δ^{15}N discussed in the preceding section. Considering individual mines would not change the above pictures. A SIMS-based study (Smit et al. 2016) of diamond plates of inferred peridotitic origin, however, revealed rare smooth internal trends of rim-ward increasing δ^{13}C and δ^{15}N. A fractionation trend of increasing δ^{15}N but decreasing δ^{13}C was observed for multiple lherzolitic diamonds from a single xenolith (Thomassot et al. 2007). In both cases, diamond precipitation is interpreted as driving the recorded N-content and isotope variability.

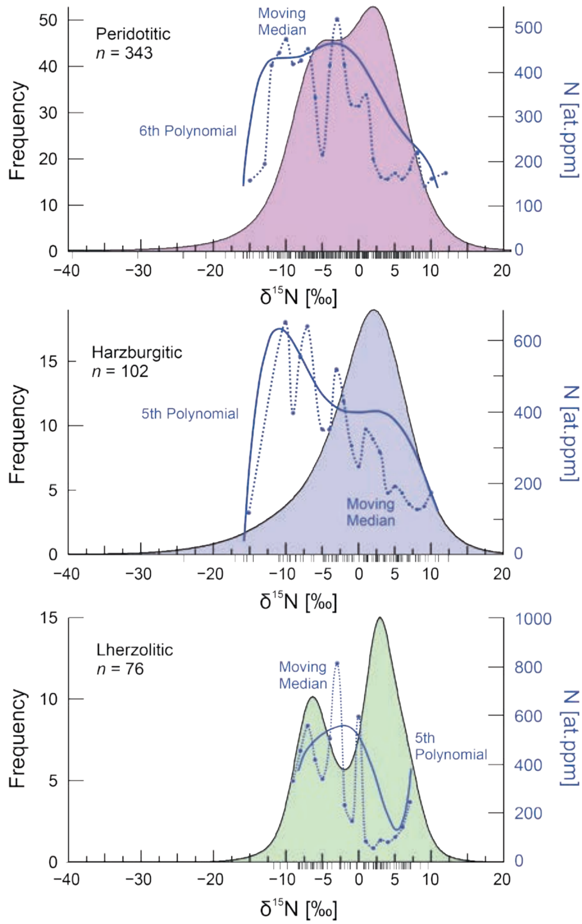

Figure 15. Kernel density estimation of the distribution in nitrogen isotope composition ($\delta^{15}N$) for diamonds worldwide containing inclusions of the peridotitic suite **(top)** and the harzburgitic (**middle**) and lherzolitic **(bottom)** parageneses (which both are also included in the peridotitic suite data set). The **blue curves** represent variations in nitrogen concentration (at.ppm, axis on right) with $\delta^{15}N$. The **solid curve** is a higher order polynomial fit; the **filled blue circles** connected by a **dashed line** are median values, typically calculated in one permille steps for increments that are two permille wide. Only at the two ends of the distributions, where data density strongly decreases, is a wider step and increment size used (typically steps of two and increments of four permille). **Black dashes** below the *x*-axis indicate individual data points and, together with the Kernel density estimations, indicate how robust median values and polynomial fits are in particular $\delta^{15}N$ ranges.

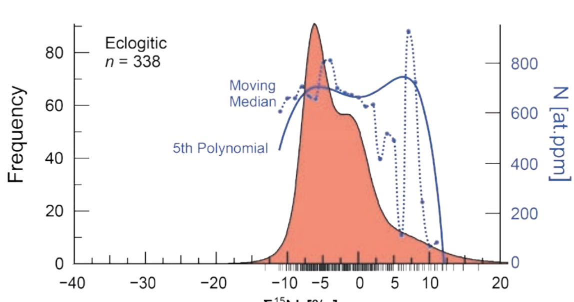

Figure 16. Kernel density estimation of the distribution in nitrogen isotope composition ($\delta^{15}N$) for diamonds worldwide containing inclusions of the eclogitic suite. The **blue curves** represent variations in nitrogen concentration (at.ppm, axis on right) with $\delta^{15}N$. The **solid curve** is a higher order polynomial fit; the **filled blue circles** connected by a **dashed line** are median values, calculated in one permille steps for bins that are two permille wide. **Black dashes** below the *x*-axis indicate individual data points and, together with the Kernel density estimations, indicate how robust median values and polynomial fits are in particular $\delta^{15}N$ ranges.

For diamonds of the eclogitic suite, similar to their peridotitic counter-parts, a near-horizontal array with mantle-like carbon isotope compositions and $\delta^{15}N$ ranging between about −10 and +5‰ is apparent (Fig. 17). In contrast to the peridotitic suite, however, there are a number of samples (including all "eclogitic" diamonds of sublithospheric origin) that are moderately to strongly ^{13}C-depleted. To explain this data distribution through mixing, requires a mantle-like component and a strongly ^{13}C-depleted and ^{15}N-enriched component with variable nitrogen contents (Fig. 17; see section *Origin of large ranges in $\delta^{13}C$ and $\delta^{15}N$* for details). On the level of individual mines, the large sample sets with paired $\delta^{13}C$-$\delta^{15}N$ analyses for Jwaneng (n = 129) and Orapa (n = 49) both display a continuum from low (~ −20‰) to mantle-like (−5 ± 2‰; Orapa) or slightly elevated (−2.0‰; Jwaneng) $\delta^{13}C$-values. For Jwaneng, however, there is only a mild overall increase in $\delta^{15}N$ from samples with mantle-like $\delta^{13}C$ (median $\delta^{15}N$-value −5.4‰, average −4.5‰) to strongly ^{13}C-depleted ($\delta^{13}C$ < −15‰; median $\delta^{15}N$-value −1.8‰, average −0.9‰) compared to Orapa (mantle-like samples: median $\delta^{15}N$-value −2.7‰, average 0.9‰; strongly ^{13}C-enriched samples: median +6.0‰, average +6.2‰). A SIMS-based study on a diamond plate of the eclogitic suite observed a smooth trend of rim-ward increasing $\delta^{13}C$ and $\delta^{15}N$ (combined with decreasing nitrogen content), which was interpreted as a Rayleigh fractionation trend (Petts et al. 2015). The study documented a one order of magnitude higher sensitivity of nitrogen isotopes compared to carbon isotopes to Rayleigh fractionation.

ORIGIN OF COVARIATIONS AMONG $\delta^{13}C$, $\delta^{15}N$ AND NITROGEN CONTENT

Correlated variations in C- and N-isotope composition and N-content observed within individual diamonds or within a suite of diamonds have been attributed to several different models:

1. An *equilibrium fractional crystallization model* whereby the precipitation of diamond and the attendant partitioning of isotopes or elements between the diamond and its parental fluid/melt causes progressive shifts in the isotopic and chemical composition of this fluid and, in turn, shifts in the composition of the later-formed diamond (i.e., a model where diamond precipitation induces significant isotope and chemical variability in the residual fluid, an active recorder). Notably, in this model, each growth zone of the diamond forms in isotopic and chemical equilibrium with the fluid present at the time of its growth.
2. A *kinetic fractional crystallization model*, which is analogous to the equilibrium model described above except that the isotopic and chemical partitioning between the diamond rim and growth medium reflects a kinetic fractionation rather than thermodynamic equilibrium.
3. A *mixing model* in which variations in the diamond's isotopic and elemental composition is attributed to the mixing of fluids derived from two or more sources with different isotopic compositions and N concentrations.

Which of these three models applies to a particular diamond or suite of diamonds affects interpretations regarding the nature of the diamond-forming fluid (e.g., was the fluid oxidizing or reducing?) and also affects inferences about the source(s) of these fluids. In this section, we begin with a detailed discussion of equilibrium C- and N-isotope partitioning between diamond and the likely diamond growth media and also summarize what we consider to be the best currently available diamond-related equilibrium fractionation factors for these two isotope systems. We then discuss kinetic isotope fractionation and whether isotope fractionation that occurs during the growth of natural diamonds more closely reflects an equilibrium or a kinetic process. Finally, we consider the role of fluid mixing in producing the isotopic and elemental variations observed in natural diamonds.

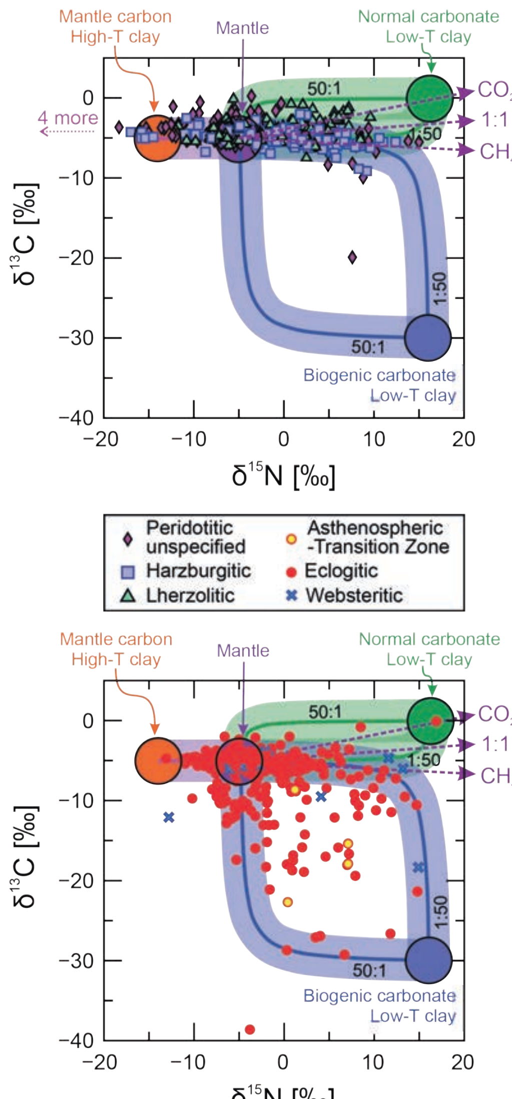

Figure 17. Carbon versus nitrogen isotope composition for inclusion-bearing diamonds **(top)** of the peridotitic suite (harzburgitic, lherzolitic and unspecified paragenesis shown separately) and **(bottom)** of the eclogitic, websteritic, and ("eclogitic") asthenospheric-transition zone suites. The four end-member components shown are taken from Li et al. (2019) and correspond to a mantle component and three components hosted in subducted former altered oceanic crust: (1) in normal marine carbonate, which precipitated in isotopic equilibrium with dissolved inorganic carbon (DIC) in seawater, and nitrogen in low-temperature clay; (2) in biogenic carbonate, again together with nitrogen in low-temperature clay; (3) in AOC that was altered at relatively high temperatures, containing negligible C but ^{15}N-depleted clay. Mixing lines between the mantle component and the AOC components correspond to high nitrogen content ($[N/C]_{Mantle}/[N/C]_{AOC}$ of 1:50) and low nitrogen content (50:1) in the subducted components (Li et al. 2019). The **purple dashed lines** indicate Rayleigh fractionation trends calculated for fluids made up entirely of diamond-forming carbon species (pure CH_4, a 1:1 mix of CH_4 and CO_2, and pure CO_2), using diamond–fluid isotope fractionation factors appropriate for a temperature of 1150 °C (approximate average temperature of diamond formation) and a diamond–fluid nitrogen partition coefficient (K_N) of 4.4 (taken from Petts et al. 2015).

High-temperature stable isotope fractionation

Only a brief introduction to equilibrium stable isotope fractionation theory is given here. The reader is referred to the seminal paper of Urey (1947) and the review papers by Richet et al. (1977) and Chacko et al. (2001) for a more detailed description of theory and the calculation of isotope reduced partition function ratios from which isotope fractionation factors can be calculated.

Chemical bonds involving the heavier and lighter stable isotopes of a particular element have slightly different vibrational energies, which cause co-existing C- or N-bearing phases or species (e.g., diamond and a fluid) to have distinct isotopic compositions. These differences in isotopic composition are expressed in terms of a fractionation factor, α. For example, the C-isotope fractionation between diamond and CO_2 can be expressed as $\alpha_{\text{diamond-}CO_2} = (^{13}C/^{12}C)_{\text{diamond}}/(^{13}C/^{12}C)_{CO_2} = (\delta^{13}C_{\text{diamond}} + 1000)/(\delta^{13}C_{CO_2} + 1000)$. Because α-values are numbers close to 1, fractionation factors are commonly reported in terms of $1000 \ln \alpha_{\text{diamond-}CO_2} = \Delta^{13}C_{\text{diamond-}CO_2}$. In this chapter, we will refer to fractionation factors in one of the latter two forms.

At high temperatures, where thermodynamic equilibrium is more likely to prevail, the fractionation factor, Δ, scales approximately linearly with $1/T^2$; the higher the temperature, the smaller the isotope fractionation, which eventually becomes zero at infinite temperature. Stable isotope fractionation is commonly assumed to be largely independent of pressure over the pressure ranges of the crust and upper mantle because the volume change associated with isotope substitution is small (Clayton et al. 1975). Fractionations at the extreme pressures of the lower mantle may in principle be somewhat different than those in the crust or upper mantle but the magnitude of any potential pressure effect decreases markedly with increasing temperature (Polyakov and Kharlashina 1994; Horita and Polyakov 2015). As such, extrapolation of fractionations determined for low-pressure conditions to deep mantle conditions is unlikely to lead to large errors because of the very high temperatures associated with the deeper parts of the mantle. Finally, chemical bonds in oxidized phases are generally stronger than those in reduced phases and the heavy isotope favours substances with stronger bonds. Consequently, at equilibrium, the most reduced species (carb<u>ides</u>, nitr<u>ides</u>) are more depleted in the heavy isotope of an element (^{13}C relative to ^{12}C, ^{15}N relative to ^{14}N) than more oxidized species (elemental forms such as diamond/graphite, N_2-gas), which in turn are more depleted than the most oxidized forms (carbon<u>ates</u>, CO_2, nitr<u>ates</u>).

Carbon and nitrogen isotope fractionation factors relevant to diamonds have been estimated using several different methods including laboratory experiments, theoretical calculations, and the analysis of natural samples. Each of these methods has advantages and disadvantages. Laboratory experiments are the most direct and in principle most reliable method for determining fractionation factors but are limited in a number of ways. Experiments can typically only be conducted over a restricted temperature range so as not to exceed the thermal stability limit of the phases of interest. At the same time, the experiments need to be carried out at temperatures high enough to permit significant isotopic exchange to occur between those phases. In many cases, these experimental fractionation data, obtained over a limited temperature range, must then be extrapolated outside that range for their application to natural samples. Another challenge for isotope exchange experiments, especially those involving the isotopically refractory mineral diamond, is the demonstration of the attainment of isotopic equilibrium during the course of the experiment.

Two criteria must be met to unequivocally prove that equilibrium was established:

Firstly, the same phases should be present at the start and end of the experiment, i.e., isotopic exchange should be accomplished either by diffusional processes or recrystallization of pre-existing phases in the experimental charges rather than by the growth of new phases. Although the synthesis of new phases during the experiment greatly facilitates isotopic exchange, the free energy changes associated with these synthesis reactions are orders of magnitude greater than those associated with isotope exchange reactions, which can result in unidirectional, kinetic isotope effects and produce spurious, non-equilibrium fractionations (Matsuhisa et al. 1978; O'Neil 1986; Chacko et al. 2001).

Secondly, experiments should be conducted in such a way that the equilibrium fractionation factor can be 'reversed'. That is, at any given temperature, two or more companion experiments should be carried out where the initial isotopic fractionations between the phases of interest lie on opposite sides of the equilibrium fractionation factor (i.e., initial fractionations both smaller and larger than the equilibrium value). Measuring the same final fractionation factor in all the companion experiments is the clearest demonstration possible that true isotopic equilibrium has been achieved.

It is important to note that fractionation factors obtained in experiments that do not meet these two criteria should be regarded with caution, as they may not record equilibrium values. To date, no carbon or nitrogen isotope exchange experiments directly involving diamond have met these criteria, which reflects the difficulty in conducting laboratory experiments with a mineral with such slow diffusion rates for C and N (Koga et al. 2003; Harte et al. 2009).

Theoretical methods, following the protocols originally developed by Urey (1947) for ideal gases and then later extended to solids (e.g., Bottinga 1968; Kieffer 1982), have also been used to determine diamond-related fractionation factors. Unlike experiments, the calculations are not restricted to a relatively narrow temperature range. However, the calculations, particularly for solid phases, require a number of simplifying approximations, the accuracy of which must be verified independently (e.g., through well-constrained experimental data). Despite this limitation, an especially useful aspect of theoretical calculations is their ability to accurately predict the temperature dependence of fractionation factors. Thus, although theory may or may not accurately capture the absolute magnitude of fractionation factors, it does provide robust constraints on the basic shape of fractionation factor versus temperature curves. As such, theoretical constraints are essential for reliable interpolation of fractionations within the temperature range of experimental studies and particularly the extrapolation of experimental data outside that temperature range.

A third method of obtaining fractionation factors related to diamonds is through the assessment of isotopic evolution trends measured in natural diamonds (e.g., Javoy et al. 1986; Thomassot et al. 2007; Petts et al. 2015). The distinct advantage of this approach is that nature has had much longer timescales to establish equilibrium during diamond growth than is possible in the laboratory. Unfortunately, the natural sample approach often lacks key information, including the temperature at which the diamonds used for calibration formed and the chemical composition of the diamond-growth medium. Such information is required for a full understanding of the fractionation factor that is being estimated. In some cases, especially in connection with nitrogen isotope fractionations, natural sample approaches take on greater importance as no reliable experimental studies or rigorous theoretical calculations have yet been done.

Equilibrium carbon isotope fractionation factors related to diamond

The C-isotope fractionation factors most relevant to this chapter are those between diamond and possible diamond-growth media, including CO_2-, CH_4- or carbonate-bearing fluids/melts and, at more reducing deeper mantle conditions, carbide-bearing melts/fluids and minerals.

Experiments. To our knowledge, there are only two published experimental studies directly involving diamond that attempted to calibrate equilibrium C-isotope fractionation factors for that mineral (Reutsky et al. 2015a; Bureau et al. 2018). In the Reutsky et al. (2015a) experiments, the breakdown of a sodium oxalate starting material at high P–T (6.3–7.5 GPa, 1300–1700 °C) in the diamond stability field produced a mixture of diamond, sodium carbonate melt and CO_2. The authors inferred that CO_2, which was present as a separate fluid phase after the experiment, was entirely dissolved in the carbonate melt at experimental conditions. Accordingly, 1/3 of the total carbon in the carbonate melt/fluid phase was dissolved CO_2. Reutsky et al. (2015a) interpreted the isotopic data from four of their experiments to record equilibrium C-isotope fractionations between carbonate fluid/melt and diamond, which could be represented by the equation: $\Delta^{13}C_{\text{carbonate melt/fluid–diamond}} = 7.38 \times 10^6/T^2$ (T in Kelvin).

The starting materials for the Bureau et al. (2018) experiments consisted of varying mixtures of oxides, carbonates and seed diamonds along with H_2O and dissolved salts. These were subjected to *P–T* conditions in the diamond stability field of 7.5 GPa and 1400 °C. The experimental run products, which were complex and included newly-grown diamond, were analyzed isotopically by NanoSIMS. It should be noted that this technique allows very small sample volumes to be analyzed but has large analytical uncertainties of > 1‰. Bureau et al. reported a $\Delta^{13}C_{\text{carbonate fluid–diamond}} = +2.8$‰ at 1400 °C. Given that the Reutsky et al. (2015a) and Bureau et al. (2018) experiments did not meet either of the two criteria required for demonstrating the establishment of isotopic equilibrium (new phases must not form; experiments should be reversed), the accuracy of the resulting fractionation factors must be evaluated in light of theoretical calculations and data derived from better-constrained experimental studies on related systems.

Well-constrained C-isotope exchange experiments have been conducted in three systems indirectly related to diamond formation, CO_2–calcite (Chacko et al. 1991; Scheele and Hoefs 1992; Rosenbaum 1994), calcite–graphite (Deines and Eggler 2009; Kueter et al. 2019a) and CO_2–CH_4 (Horita 2001; Kueter et al. 2019b). In terms of the CO_2–calcite system, the experimental study that most closely met the criteria for the demonstration of equilibrium is that of Rosenbaum (1994). Similarly, the high-temperature (1200–1400 °C) calcite–graphite experiments of Deines and Eggler (2009) used those two minerals as starting materials (i.e., no growth of new minerals during the experiments) and reversed the equilibrium factor with companion experiments at each temperature. The experiments of Kueter et al. (2019a) in the carbonate–graphite system were of a different style than those of Deines and Eggler in that they used starting materials comprising organic matter (tartaric acid and sucrose) and a mixture of $CaCO_3$ and Na_2CO_3, which decomposed under experimental conditions to form graphite and carbonate melt. As such, these are synthesis experiments that cannot in and of themselves unambiguously demonstrate that true isotopic equilibrium has been achieved. The two experimental studies in the CO_2–CH_4 system collectively investigated a broad range of temperatures (200–1000 °C), using a Ni catalyst to facilitate isotopic exchange between the gas species (Horita 2001; Kueter et al. 2019b).

C-isotope experiments were also carried out between graphite and Fe_3C (Satish-Kumar et al. 2011) and between Fe_3C and Fe-C melt (Reutsky et al. 2015b), with some of the latter experiments crystallizing diamond in addition to Fe_3C. Both of these experimental studies involved the crystallization of new phases during the course of the experiments, which leads to some ambiguity as to whether the measured isotopic fractionations represent equilibrium values. A refitting of the Satish-Kumar et al.'s (2011) data points to a straight line in which the fractionation factor is forced to go to a value of 0 at infinite temperature results in the following equation: $\Delta^{13}C_{\text{graphite–Fe}_3\text{C}} = 12.2 \times 10^6/T^2$. Reutsky et al. (2015b) measured a $\Delta^{13}C_{\text{Fe}_3\text{C-FeC melt}} \sim +2$‰ at 6.3 GPa and 1400 °C. They also measured a $\Delta^{13}C_{\text{diamond-Fe}_3\text{C}} = \sim +5$‰ but, because their experiments were intentionally polythermal (1600–1400 °C) and diamond formed earlier in the crystallization sequence than Fe_3C, the authors did not interpret this +5‰ value to reflect an equilibrium fractionation factor.

Theoretical calculations. Theory enables the calculation of isotope reduced partition function ratios, commonly referred to as β-factors, for individual fluid or mineral species. The β-factor calculations either use measured spectroscopic data for species as input for statistical mechanical computations or are based on a first-principles, lattice dynamics approach. These β-factors can then be used to compute isotopic fractionation factors between species. More specifically, the fractionation between species *a* and *b* at a given temperature can be represented as $\alpha_{a\text{-}b} = \beta_a / \beta_b$ or as $\Delta_{a\text{-}b} = 1000 \ln \beta_a - 1000 \ln \beta_b$.

Many calculations of C-isotope β-factors have been done for CO_2 (e.g., Bottinga 1968; Richet et al. 1977; Chacko et al. 1991; Polyakov and Kharlashina 1995) and calcite (Bottinga 1968; Chacko et al. 1991; Deines 2004; Schauble et al. 2006) and have yielded quite comparable results (mostly within ~ 0.2‰ at high temperature), despite differences in input data and calculation methodology[4]. Deines (2004) and Schauble et al. (2006) also did β-factor calculations for two other carbonate minerals relevant to the mantle, magnesite and dolomite. Fewer high-temperature β-factor calculations have been done for CH_4 than for CO_2 but the two available studies yielded very comparable results (Bottinga 1969a; Richet et al. 1977). Here, we have chosen to use the calculations of Chacko et al. (1991) for CO_2 and calcite, Schauble et al. (2006) for magnesite and dolomite and Richet et al. (1977) for CH_4.

Two sets of C-isotope β-factor calculations have been done for graphite and diamond, a pioneering study by Bottinga (1969b) and a later study by Polyakov and Kharlashina (1995). Significantly different calculation methodologies and types of input data were used in the two studies but they produced very similar β-factors that are within 0.3 and 0.1‰ of each other for graphite and diamond, respectively, at $T \geq 800$ °C. Polyakov and Kharlashina (1994) investigated the pressure dependence of β-factors (the β-factors for all phases increase with pressure) and noted that β-factors for graphite are more strongly affected by pressure than those of either diamond or calcite. As a consequence, although diamond is slightly enriched in ^{13}C relative to graphite at ambient pressure, that small degree of ^{13}C partitioning is predicted to reverse at higher pressure (i.e., graphite becomes the more ^{13}C-enriched phase).

Recently, β-factor calculations have also been done for carbide minerals (Fe_3C and SiC–Horita and Polyakov 2015; Fe_3C–Liu et al. 2019). The two sets of calculations disagree somewhat in their β-factors for Fe_3C but both indicate that carbides should be strongly depleted in ^{13}C relative to all the other carbon species described above. For instance, Liu et al.'s (2019) calculations indicate $\Delta^{13}C_{MgCO_3\text{-}Fe_3C} = +6.1‰$ at 15 GPa and 1500 °C compared to $\Delta^{13}C_{CaCO_3\text{-}Fe_3C} = +6.7‰$ ($\Delta^{13}C_{MgCO_3\text{-}CaCO_3} = +0.3‰$ at 1500 °C) at that *P–T* condition according to Horita and Polyakov (2015). It is not clear which of these two studies provides the more accurate β-factors for Fe_3C but we have chosen here to use the values of Horita and Polyakov as only they provide equations for reproducing their β-factor calculations as a function of temperature.

Comparison of experiment and theory. The data from the experimental studies, particularly the well-constrained fractionation data in the CO_2–calcite, calcite–graphite and CO_2-CH_4 systems, can be used to assess the validity of the theoretical calculations of β-factors for CO_2, CH_4, calcite and graphite, and indirectly, also the reliability of the calculations for diamond. The theoretical calculations are in reasonable agreement with all the experimental data in the CO_2–calcite system but the best constrained experimental datum in that system, that at 900 °C by Rosenbaum (1994) (2.70 ± 0.18‰ (1σ)), is in near perfect agreement with the fractionation at that temperature (2.68‰) derived from β-factor calculations for CO_2 and calcite by Chacko et al. (1991). The excellent agreement between experiment and theory indicates that the approximations inherent to the calculations, especially that for the solid phase, calcite, are valid.

The correspondence between theory and experiment is not quite as good for the CO_2–CH_4 system. As noted by both Horita (2001) and Kueter et al. (2019b), a theoretically-derived fractionation curve based on the calculations of Richet et al. (1977) is similar to but displaced to slightly smaller fractionations than their experimental data. Here, we have left the β-factor calculations for CO_2 as is and applied a multiplicative factor (0.9846) to the β-factors of

[4] The β-factor calculations of Bottinga (1968) contained an error, which was corrected by Chacko et al. (1991). The corrected Bottinga (1968) calculations, those of Chacko et al. (1991) and Schauble et al. (2006) give virtually identical high-temperature C-isotope β-factors for calcite whereas those of Deines (2004) give values about 3% lower than the other studies cited here.

CH_4 so as to minimize the weighted sum of squares deviation of the calculations from the experimental data points. This small (~ 1.5%) correction to the β-factors of CH_4 improves the fit of the calculations to the experimental data but maintains the basic shape of the fractionation curve prescribed by theory.

Theory and experiment can also be compared in the calcite–graphite system. The reversed experiments of Deines and Eggler (2009), conducted at 2 GPa, indicate $\Delta^{13}C_{\text{calcite-graphite}}$ of +1.34 ± 0.17‰ and +1.09 ± 0.03‰ at 1200 and 1400 °C, respectively. These data correspond almost exactly with the fractionations of 1.35 and 1.05‰ obtained by combining the β-factors for calcite (Chacko et al. 1991) and graphite (Polyakov and Kharlashina 1995) calculated for a pressure of 2 GPa. The theoretical calculations also agree with the results of the 1 GPa synthesis experiments of Kueter et al. (2019a), which indicate fractionations of 1.4 ± 0.2‰ and 1.1 ± 0.2‰ at 1300 and 1500 °C, respectively, compared to calculated fractionations of 1.32 and 1.04‰ at 1 GPa and those temperatures. This excellent agreement between theory and experiment strongly suggests that theoretical calculations for graphite are accurate. Moreover, given that the calculation methodology and input data for the diamond calculations are completely analogous to those for graphite (Polyakov and Kharlashina 1995), it can reasonably be inferred that the β-factors for diamond are also likely to be accurate.

Given the demonstrated ability of the theoretical calculations to predict fractionation factors involving CO_2, calcite and graphite (and by analogy diamond), it is instructive to critically evaluate the diamond-related fractionation factors reported in the experimental studies of Reutsky et al. (2015a) and Bureau et al. (2018). The former study proposed the fractionation equation: $\Delta^{13}C_{\text{carbonate melt/fluid–diamond}} = 7.38 \times 10^6/T^2$ based on their experiments in which diamond crystallized from a melt/fluid comprising 2/3 sodium carbonate and 1/3 dissolved CO_2. The theoretical calculations indicate that the C-isotope fractionation between a melt/fluid containing calcium carbonate[5] and dissolved CO_2 in 2:1 proportions and diamond can be described by: $\Delta^{13}C_{\text{Ca-carbonate melt/fluid–diamond}} = 4.0 \times 10^6/T^2$. The temperature coefficient for this theoretically-based fractionation equation is nearly a factor of 2 smaller than that given by the equation of Reutsky et al. (2015a). Similarly, the 1400 °C carbonate-diamond fractionation factor indicated by the theoretical calculations ($\Delta^{13}C_{CaCO_3\text{–diamond}}$ = +1.2‰) is more than a factor of 2 smaller than that reported by Bureau et al. (2018) ($\Delta^{13}C_{\text{carbonate fluid–diamond}}$ = +2.8‰). For the reasons discussed above, it is highly unlikely that the theoretical calculations are wrong to this degree. Rather, we conclude that the two experimental studies, both of which involved isotopic exchange associated with new mineral growth, record kinetic rather than equilibrium C-isotope fractionations. As discussed further in the section *Kinetics* below, chemical reactions in which isotopic fractionations are kinetically controlled generally favor concentration of the light isotope (^{12}C) in the reaction products. As such, rapid synthesis of diamond from carbonate fluids as occurred in both sets of experiments will lead to crystallization of diamond that is anomalously ^{12}C-enriched and, in turn, carbonate–diamond fractionation factors that are spuriously large relative to equilibrium values.

The accuracy of the β-factor calculations for iron carbide (Fe_3C) cannot be rigorously assessed on the basis of the available experimental data. The synthesis experiments of Satish-Kumar et al. (2011) in the graphite-Fe_3C system recorded a $\Delta^{13}C_{\text{graphite–}Fe_3C}$ = +3.64‰ at 5 GPa and 1500 °C, which can be compared to calculated $\Delta^{13}C_{\text{diamond–}Fe_3C}$ at that *P–T* condition of ~ +5.5‰ (Horita and Polyakov 2015) and $\Delta^{13}C_{\text{diamond–}Fe_3C}$ = +4.6‰ at 15 GPa and 1500 °C (Liu et al. 2019). Because increasing pressure produces a larger increase in the β-factors of graphite than diamond (see above), the fractionation between graphite and Fe_3C is predicted

[5] The calculations of Deines (2004) indicate that sodium carbonate (Na_2CO_3) has a slightly lower affinity for ^{13}C than calcite. The fractionation between a sodium carbonate melt (with 33% dissolved CO_2) and diamond can be described by: $\Delta_{\text{Na-carbonate melt/fluid–diamond}} = 3.7 \times 10^6/T^2$.

to be larger than that between diamond and Fe_3C at high pressure (Polyakov and Kharlashina 1994) and so the discrepancy between experiment and calculation is quite large. Given that synthesis-style experiments cannot demonstrate the attainment of true isotopic equilibrium, it is unclear whether it is the experiments or the calculations that are in error.

Recommended C-isotope fractionation factors. Following the reasoning and criteria discussed above, Table 3 presents equations for calculating what we believe to be the best equilibrium C-isotope fractionation factors currently available for diamond-related systems. This compilation is provided for convenience but the reader is urged to cite the original authors if these fractionation factors are used. A spreadsheet (Calc_C_N-isotope-fractionation-factors.xlsm) for calculating these fractionation factors as a function of temperature is provided online at https://doi.org/10.7939/DVN/XZNF6V.

Figure 18 plots these fractionation factors as a function of $1/T^2$. Relative to diamond, CO_2 and carbonates are enriched in ^{13}C (positive $\Delta^{13}C_{\text{phase-diamond}}$) whereas CH_4 and carbides are depleted in ^{13}C (negative $\Delta^{13}C_{\text{phase-diamond}}$). Also shown in the figure is the fractionation between diamond and the so-called water-maximum fluid, which comprises dominantly H_2O along with equal parts CO_2 and CH_4. This fluid favors ^{13}C relative to diamond but slightly less so than carbonates. The curve describing the fractionation between diamond and Fe_3C must be regarded as tentative as it is the only one not corroborated by robust experimental fractionation data. One potential test of these diamond–Fe_3C fractionations is based on the natural sample data of Mikhail et al. (2014), who reported a $\Delta^{13}C_{\text{diamond–Fe}_3\text{C}} = +7.2 \pm 1.3‰$, derived from what they interpreted to be syngenetic iron carbide inclusions in two Jagersfontein diamonds. Assuming the two phases formed in C-isotope equilibrium, this diamond-Fe_3C fractionation corresponds to a temperature of 1256 ± 137 °C according to the equations of Table 3. This is a plausible temperature for diamonds originating in the deep lithosphere or formed during subduction of an oceanic slab into the asthenosphere and transition zone. However, other calibrations of this fractionation (e.g., Satish-Kumar et al. 2011; Liu et al. 2019) would also yield plausible (but lower) temperatures.

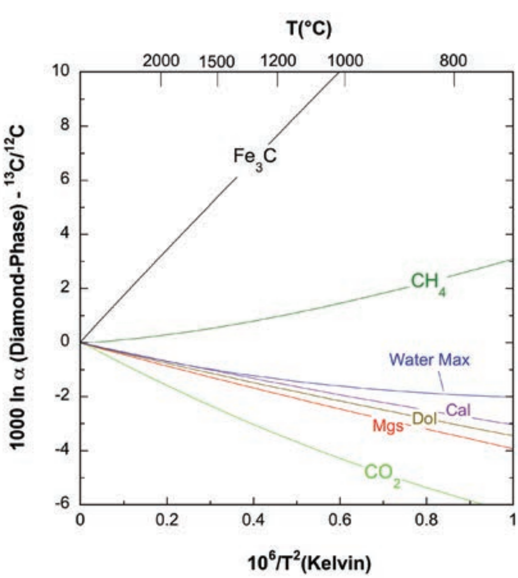

Figure 18. Summary of carbon isotope fractionation factors related to diamond plotted versus $10^6/T^2$ (T in Kelvin). The fractionation curves are based on calculations of β factors for the various phases (sources of β-factor calculations given in Table 3). Mgs = magnesite; Dol = dolomite; Cal = calcite. 'Water max' fluid is a water-rich fluid comprising equal amounts of CO_2 and CH_4 (see text).

As emphasized above, fractionation factors vary little with pressure, and the β-factors of Table 3 are those based on calculations done for ambient pressure conditions. The β-factors of

Table 3. Carbon isotope β-factors for species relevant to diamond.

Species	C_0	C_1	C_2	C_3	C_4	C_5	C_6
CO_2	–0.079	30.551	40.120	59.435	57.452	30.238	65.049
CH_4	0.086	20.234	31.262	48.914	47.887	25.030	53.071
calcite	0.001	25.180	15.383	13.297	9.5195	4.2857	8.5026
magnesite	0.020	25.948	14.000	7.6798	2.3338	0.23526	–0.09332
dolomite	0.020	25.436	13.525	7.3632	2.2372	0.23045	–0.07713
Fe_3C	0.000	4.5140	2.7791	0.01299	0.0000	0.0000	0.0000
diamond	0.000	21.649	9.790	5.2834	1.8790	0.30747	0.0000

Note: C-isotope β-factors reported here as 1000 ln β, which can be computed for each phase/species using the following expression: $1000 \ln \beta = C_0 + C_1 x - C_2{\times}10^{-1} x^2 + C_3{\times}10^{-2} x^3 - C_4{\times}10^{-3} x^4 + C_5{\times}10^{-4} x^5 - C_6{\times}10^{-6} x^6$, where $x = 10^6/T^2$ and T is temperature in Kelvin. The equations are applicable at temperatures between 25 and 10000 °C, except the equation for Fe_3C, which is only valid above 450 °C. These equations are polynomial fits to β-factor calculations reported in the following sources: CO_2 and calcite (Chacko et al. 1991); magnesite and dolomite (Schauble et al. 2006); diamond (Polyakov and Kharlashina 1995); Fe_3C (Horita and Polyakov 2015); CH_4 – the β-factors of Richet et al. (1977) multiplied by a factor of 0.9846 (see text). The C-isotope fractionation factor between any two carbon-bearing species a and b at a particular temperature is given by the arithmetic difference in their 1000 ln β values ($\Delta^{13}C_{a\text{-}b} = 1000 \ln \alpha_{a\text{-}b} = 1000 \ln \beta_a - 1000 \ln \beta_b$) at that temperature.

all phases increase with pressure (Polyakov and Kharlashina 1994) but at somewhat different rates depending on the properties of the phase. As a consequence, there is a small change in the magnitude of fractionation factors with increasing pressure, which only becomes detectable at extreme pressure. For example, Horita and Polyakov (2015) estimate that at 1500 °C, $\Delta^{13}C_{\text{diamond–}Fe_3C}$ increases from +5.38 to +5.85‰ as pressure increases from 0.001 GPa (surface pressure) to 30 GPa and $\Delta^{13}C_{\text{diamond-}CaCO_3}$ increases from −1.07 to −1.16‰ over that same pressure interval. These small pressure effects on the magnitude of fractionation factors (typically < 0.3 percent change per GPa) should not be significant for most purposes.

We would add one cautionary note regarding the preferred fractionation factors listed in Table 3. These fractionation factors are based on theoretical calculations or experiments in relatively simple chemical systems (e.g., CO_2–calcite) and thus do not consider the complex nature of diamond-forming mantle fluids/melts. Although fractionations are dominantly controlled by the vibrational characteristics of the simple fluid species carrying the element of interest (e.g., CO_2, CH_4, CO_3^{2-}), the presence of other dissolved constituents in the fluid phase can have second-order effects on the fractionation behavior of the simple fluid species. The exact magnitude of these second-order effects is difficult to ascertain but a crude maximum estimate can be obtained by considering the impact of different cations on C-isotope fractionations in carbonate minerals, whose fractionation behavior is largely determined by the vibrational characteristics of the CO_3^{2-} anion. Theoretical calculations indicate that changing the cation bonded to the carbonate anion from Mg to alkalis (strongest and weakest affinities for ^{13}C, respectively) has < ~ 0.5‰ effect on fractionations at a typical diamond-forming temperature of 1150 °C (Deines 2002; Schauble et al. 2006). Therefore, we anticipate that the presence of other dissolved species in natural diamond-forming fluids will only have a relatively small impact on the fractionation equations of Table 3.

Equilibrium nitrogen isotope fractionation factors related to diamond

As was the case with C-isotopes, the N-isotope fractionation factors most pertinent to this chapter are those between diamond and likely N-bearing species in diamond-growth media. Many workers have proposed that N_2 and NH_3 are the two dominant N-fluid species in the upper mantle under more oxidizing and reducing conditions, respectively (e.g., Deines et al. 1989; Li and Keppler 2014; Sokol et al. 2017). However, on the basis of laboratory experiments or theoretical calculations, other N-bearing species have also been suggested, including NH_2^+ and NH_2^- (Mysen 2018, 2019) and NH_4^+ (Mikhail and Sverjensky 2014). In addition, at the more reducing conditions of the deep mantle, N may exist in the form of a nitride-bearing melt or mineral.

To our knowledge, no experiments aimed specifically at calibrating equilibrium N-isotope fractionation factors between diamond and potential N-bearing species in diamond-growth media have been carried out. The available fractionation factors are derived either from theoretical calculations or extracted from natural sample datasets.

Theoretical calculations. The first attempt at constraining N-isotope fractionations for diamond was that of Deines et al. (1989), who based their estimate on Richet et al.'s (1977) N-isotope β-factor calculations for N_2, NH_3 and HCN. In particular, the β-factors of HCN were taken as an analogue for the fractionation behavior of the C-N bond in diamond. Petts et al. (2015) followed the same general theoretical approach as Deines et al. (1989) but used β-factor calculations for the CN^- molecule (rather than HCN) as the analogue for N in diamond. Both studies concluded that diamond would be depleted in ^{15}N relative to the likely upper mantle N fluid species. Petts et al. (2015) reported the following sequence in terms of affinity for ^{15}N relative to ^{14}N: $NH_4^+ > N_2 > NH_3 > CN^-$ (Fig. 19). They also calculated N-isotope fractionation factors between the CN^- diamond analogue and these N-bearing fluid species of −1 to −4‰ at temperatures between 1000–1300 °C. No theoretical calculations have been done for the specific NH_2 or nitride species that may exist in the mantle. However, Hanschmann (1981) did report β-factor calculations for NH_2CH_3 and BN at a selected number of temperatures below 727 °C. These calculations indicate that NH_2^- fractionates N-isotopes broadly like N_2 and that boron nitride is depleted in ^{15}N relative to the CN^- diamond analogue.

It should be noted that the β-factor calculations for the HCN and CN^- gas molecules are, at best, crude analogues for the N-isotope fractionation behavior of diamond. For instance, carbon and nitrogen in these gas molecules are connected by a strong triple bond compared to a weaker single bond in diamond. Other things being equal, bond strength generally correlates with a substance's relative affinity for the heavy isotope, which predicts that the weaker C–N bond in diamond would have a lower affinity for ^{15}N than either HCN or CN^- (Petts et al. 2015). On the other hand, condensed phases can partition isotopes differently than gases of the same composition (e.g., Horita and Wesolowski 1994), which may cause an isotopic effect in the opposite direction. That is, N in the solid phase diamond may have a stronger affinity for the heavy isotope than predicted by calculations on the HCN or CN^- gas molecules. Despite these uncertainties, the general prediction of the calculations is that diamond would favor the light nitrogen isotope relative to most N fluid species in the mantle. It appears that nitrides are the only currently known mantle N species that is likely to have a lower affinity for ^{15}N than diamond.

Natural sample calibrations. Several studies have attempted to extract N-isotope fractionation factors from data acquired on natural diamonds. This approach, which was pioneered by Thomassot et al. (2007) and also used by Palot et al. (2014) and Petts et al. (2015), is a bootstrap method based on co-variations in C- and N-isotope compositions and N-contents, either within a single diamond or within a suite of diamonds that are inferred to be co-genetic. The method implicitly assumes that the observed isotopic and elemental variations are the product of a closed-system (i.e., fluid-limited) Rayleigh fractionation process and that isotopic and chemical equilibrium is always maintained between the rim of the growing diamond and the growth medium. It also assumes that diamond is the only C- and N-bearing phase crystallizing from the growth medium (i.e., no other C- or N-bearing carbonate, silicate or nitride phases are co-crystallizing with diamond). Finally, the method assumes knowledge of the C-isotope fractionation factor between diamond and that growth medium. The papers by Cartigny et al. (2001), Thomassot et al. (2007), Smart et al. (2011) and Petts et al. (2015) provide details of the procedure. In essence, the slope of data arrays in $\delta^{13}C$ versus N abundance plots, combined with the known C-isotope fractionation factor between the growth medium and diamond ($\Delta^{13}C_{diamond-fluid}$) can be used to derive a diamond–fluid N partition coefficient (K_N). Armed with K_N and $\Delta^{13}C_{diamond–fluid}$ values, the slope of co-variations between $\delta^{13}C$ and $\delta^{15}N$ can be used to deduce $\Delta^{15}N_{diamond–fluid}$, the N-isotope fractionation factor between the growth medium and diamond.

To implement this approach, Thomassot et al. (2007) carried out high-precision, bulk isotopic and elemental analysis of 59 diamonds extracted from a single, highly diamondiferous peridotite xenolith recovered from the Premier kimberlite (*Cullinan mine*) of South Africa. They interpreted the trends in their data to reflect Rayleigh-style fractionation of diamond from a single batch of fluid rather than two-component mixing of fluids with different isotopic compositions and N abundances. They also inferred that their data trends were best explained if the early-formed diamond had relatively high $\delta^{13}C$- and $\delta^{15}N$-values and N-contents, which progressively evolved to lower values during fractional crystallization of diamond from the growth medium. In an equilibrium process, evolution of diamond to lower $\delta^{13}C$-values requires crystallization from a reducing (e.g., CH_4-rich) fluid. Moreover, the trend towards decreasing $\delta^{15}N$-values implies that $\Delta^{15}N_{diamond–fluid}$ is positive (Thomassot et al. computed K_N ~ 2 and $\Delta^{15}N_{diamond–fluid}$ ~ +1.2‰). In turn, a positive value for $\Delta^{15}N_{diamond–fluid}$ (see above) requires that these diamonds crystallized from a nitride-bearing growth medium (c.f., Fig. 19) or a growth medium containing some other, heretofore unknown N species with a lower affinity for ^{15}N than diamond.

Smart et al. (2011) and Petts et al. (2015) conducted detailed ion microprobe (SIMS) analyses of isotopic and N abundance zoning profiles in a gem-quality diamond recovered from an eclogite xenolith from the Jericho kimberlite of northern Canada. The core zone of this diamond shows smooth rimward increases in both $\delta^{13}C$- and $\delta^{15}N$-values coupled to a decrease in N concentrations. Broadly similar zoning patterns are seen in diamonds from Marange (Smit et al. 2016). In the case of the Jericho diamond, the increase in $\delta^{13}C$-values was interpreted to reflect crystallization of the diamond from an oxidizing, carbonate-bearing fluid/melt ($\Delta^{13}C_{diamond–fluid} = -1.7$‰ at 1100 °C) (Smart et al. 2011; Petts et al. 2015). Notably, the shift in $\delta^{15}N$-values observed in the core zone of this diamond is ~ 8.5 times larger than the shift in $\delta^{13}C$-values over the same interval. From these data trends, Petts et al. (2015) extracted a $K_N \geq 4.4$ (i.e., N is highly compatible in diamond relative to this growth medium) and a $\Delta^{15}N_{diamond–fluid} = -4.0 \pm 1.2$‰ ($2\sigma$). The numerical accuracy of this fractionation factor determination depends on the validity of the various assumptions noted above, namely that isotopic and chemical equilibrium was maintained between the growth medium and the diamond rim and that the

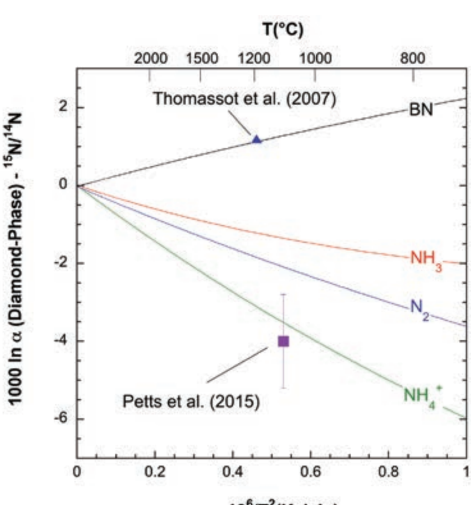

Figure 19. Summary of nitrogen isotope fractionation factors related to diamond plotted versus $10^6/T^2$ (T in Kelvin). The fractionation curves are based on calculations of β-factors for NH_4^+, N_2, NH_3 and CN^- by Petts et al. (2015) and BN by Hanschmann (1981). In these calculations, CN^- is taken to be an analogue for the N-isotope fractionation behavior of diamond. Also shown are two estimates of the N-isotope fractionation factor between the growth medium and diamond by Thomassot et al. (2007) and Petts et al. (2015) derived from analyses of natural diamonds. See text for discussion.

C-isotope fractionation factor between the diamond and the growth medium was −1.7‰. It is safe to conclude from this analysis, however, that the sign of $\Delta^{15}N_{diamond–fluid}$ must be negative for this diamond and also that the magnitude of $\Delta^{15}N_{diamond–fluid}$ must be a relatively large in order to account for the much bigger shift in $\delta^{15}N$ compared to $\delta^{13}C$-values.

Recommended N-isotope fractionation factors. There is much more uncertainty regarding equilibrium N-isotope than C-isotope fractionation factors for diamond. The two detailed natural sample studies that have been carried out have proposed opposite signs for $\Delta^{15}N_{diamond–fluid}$. More systematic studies on natural diamonds should be carried out to see if a dominant fractionation pattern and direction emerges. It is recommended, however, that these studies be based on detailed documentation of zoning profiles in individual diamonds rather than the bulk analysis of multiple diamonds as it is much easier to unambiguously determine the direction of isotopic and elemental fractionation with the former approach. In terms of theoretical estimates, a first-principles, lattice dynamics determination of β-factors for N-bearing diamond is clearly preferable to calculations based on gas molecule diamond proxies such as HCN or CN^-. Such first-principles calculations, although challenging, should be attempted.

In the interim, Table 4 and the on-line spreadsheet (Calc_C_N-isotope-fractionation-factors.xlsm at https://doi.org/10.7939/DVN/XZNF6V) presents equations for reproducing the N-isotope calculations reported by Petts et al. (2015) for N_2, NH_3, NH_4^+ and the diamond proxy, CN^-. The table also presents a polynomial fit to the β-factor calculations for BN by Hanschmann (1981), which should provide a general indication of how nitride-bearing fluids or melts may fractionate N-isotopes relative to diamond.

Table 4. Nitrogen isotope β-factors for species relevant to diamond.

Species	C_0	C_1	C_2	C_3	C_4	C_5	C_6
NH^{4+}	–0.044	188.20	352.73	610.15	632.58	342.59	74.349
N_2	0.014	153.77	227.38	332.47	311.22	158.20	32.941
NH_3	0.054	140.35	274.93	490.58	518.25	284.11	62.186
CN^-	0.009	110.10	135.48	175.35	151.81	73.265	14.706
BN	0.000	83.403	83.659	70.669	11.188	–24.428	–11.308

Note: N-isotope β-factors reported here as 1000 ln β, which can be computed for each gas molecule s using the following expression: $1000 \ln \beta = C_0 + C_1x - C_2{\times}10^{-1} x^2 + C_3{\times}10^{-2} x^3 - C_4{\times}10^{-3} x^4 + C_5{\times}10^{-4} x^5 - C_6{\times}10^{-6} x^6$, where $x = 10^6/T^2$ and T is temperature in Kelvin. The CN^- gas molecule is taken to be a diamond analogue. The equations are applicable at temperatures between 0 and 5000 °C. These equations are polynomial fits to β-factor calculations for NH_4^+, N_2, NH_3 and CN^- by Petts et al. (2015) and for boron nitride (BN) by Hanschmann (1981).

Kinetic effects

As is the case with equilibrium fractionation, kinetic fractionation processes can also generate systematic and continuous changes in the isotopic and elemental compositions of diamonds. Kinetic (i.e., non-equilibrium) isotopic fractionation corresponds to a unidirectional process, which, in contrast to equilibrium fractionation, is not reversible. For chemical reactions in which isotopic fractionation is kinetically controlled, the products of the reaction are typically depleted in the heavy isotope relative to the reactants because bonds in the reactants made with the light isotope are weaker and therefore more reactive than those made with the heavy isotope. However, cases of inverse kinetic isotope fractionation also exist in which the products are enriched in the heavy isotope (see Casciotti 2009).

That kinetic rather than equilibrium isotope fractionation can occur during diamond growth is well known from laboratory experiments, including some of the C-isotope experimental studies discussed above. In addition, strong sector zoning in $\delta^{15}N$-values was observed in a synthetic diamond grown at elevated pressure-temperature conditions (Boyd et al. 1988). Sector zoning refers to crystallographically-controlled differences in chemical or isotopic composition within different parts (sectors) of the same crystal. Diamond is in fact the first mineral for which isotope-sector zoning was reported. The finding that cubic and octahedral growth sectors of a synthetic diamond could differ by ~ 45‰ (Boyd et al. 1988) calls into question the use of diamond to infer the $\delta^{15}N$-values of mantle fluids and to assess the origin of nitrogen and, by implication, carbon in diamonds. Two subsequent studies on natural mixed-habit (with cuboid and octahedral growth sectors) diamonds, however, found $\delta^{15}N$ values within error along the [100] and [111] growth directions (Bulanova et al. 2002; Cartigny et al. 2003) and concluded that kinetic isotope fractionation during sector growth is not relevant to natural diamond formation. The very detailed study of Howell et al. (2015b) generally confirmed the above conclusion by noting differences in N-isotope composition between cuboid and octahedral growth sectors of only 0.4 to 1.0‰, i.e., within or just slightly exceeding the reported analytical uncertainty. These data were therefore taken as evidence that nitrogen uptake in natural diamond is not associated with significant kinetic isotope effects and that isotopic variations can generally be interpreted assuming the establishment of isotopic equilibrium between the diamond-forming medium and diamond.

Contrary to this conclusion, two recent studies argue that the C-isotope and by implication the N-isotope compositions of natural diamonds are largely controlled by kinetic isotope fractionation processes (Reutsky et al. 2017; Kueter et al. 2020). The conclusions of these important studies, if correct and widely applicable, would fundamentally alter our interpretation of isotopic and elemental co-variations in diamonds. As such, the two studies are discussed in detail below.

Reutsky et al. (2017) model. Reutsky et al. based their interpretations on zoning profiles observed in two gem-quality cuboid placer diamonds from the Yakutia region of Russia combined with kinetic modeling of these zoning profile data. The core zones of these diamonds are characterized by rimward decreases in $\delta^{13}C$-values coupled to decreasing N abundances; $\delta^{15}N$-values show no obvious zoning trend over the same core-zone interval. The rims of these diamonds have low N-contents, which also correspond to a precipitous drop in $\delta^{15}N$ to values as low as –63‰. If correct, this would be the lowest $\delta^{15}N$-value ever reported for diamonds. The present authors are not convinced of the accuracy of these extreme $\delta^{15}N$-values, which were obtained on low N-content diamond using the SIMS analytical technique. The $^{14}N–^{12}C$ peak, which is used to monitor the abundance of ^{14}N in SIMS diamond analyses, is isobaric with the $^{13}C–^{13}C$ peak. Although the two peaks are nominally resolved at the instrument mass resolution setting used by Reutsky et al. (2017), the tail of the much larger $^{13}C–^{13}C$ peak still contributes appreciably to the $^{14}N–^{12}C$ peak in the case of very low N-content (< 50 ppm) diamond (Stern et al. 2014). Analyses of such low N diamond by SIMS can therefore result in the measurement of spuriously low $\delta^{15}N$-values unless a non-routine analytical protocol is followed with the instrument operated at a much higher mass resolution (R.A. Stern, personal communication 2020).

Setting aside potential difficulties with the N-isotope analyses at the rims of these Yakutian placer diamonds, Reutsky et al. (2017) propose an innovative kinetic model for the origin of the correlated C-isotope and N-content zoning profiles observed in the core zones of their diamonds. The impetus for suggesting a kinetic rather than an equilibrium model for these diamonds stems from the observation of rimward decreases in $\delta^{13}C$-values. In an equilibrium scenario, a trend towards lower $\delta^{13}C$-values requires diamond precipitation from a reduced (e.g., CH_4) fluid as these are the only known fluid species that partition ^{12}C relative to diamond. However, previous studies had reported the presence of micro-carbonate inclusions in the Yakutian placer diamonds examined by Reutsky et al. (2017), which would imply that these diamonds crystallized from an oxidized fluid.

To resolve this paradox, Reutsky et al. (2017) proposed a decreasing linear growth rate (DLGR) model, originally developed in the material sciences for trace-element uptake during crystal growth (Burton et al. 1953). The model assumes that the diamond-forming fluid maintains a constant C-isotope composition throughout diamond growth and attributes the development of compositional zoning in diamond to a decrease in its linear growth rate as crystal size increases. That is, the model assumes that the volume growth rate of diamond remains constant, which in turn requires that the linear growth rate (the rate at which individual crystal faces move outward from their starting point) continuously decreases because the surface areas of crystal faces are getting larger during diamond growth. According to the DLGR model, the effective diamond–fluid C-isotope fractionation factor is zero when the crystal first forms and the linear growth rate is fast (i.e., initially no C-isotope fractionation occurs between diamond and fluid) but becomes larger as this growth rate decreases. More specifically, the effective fractionation factor progressively approaches the equilibrium fractionation factor as the linear growth rate decreases and should theoretically equal the equilibrium fractionation factor when the linear growth rate goes to zero. Because the model assumes that the fluid's isotopic composition remains constant throughout diamond growth, the increase in the magnitude of the effective fractionation factor with decreasing linear growth rate results in a progressively changing C-isotope composition of the newly-grown diamond rim. Counterintuitively, the model predicts rimward decreases in the δ^{13}C-values of diamond crystallizing from an oxidized fluid and rimward increases in the δ^{13}C-values of diamond crystallizing from a reduced fluid, which is opposite to what is predicted by the equilibrium model. In the case of the studied Yakutian placer diamonds, which are inferred to have precipitated from an oxidized (carbonate) fluid, crystallization led to progressively decreasing δ^{13}C-values in the diamond.

Reutsky et al. (2017) explain the observed rimward decrease in the N-content of their diamonds in an analogous way. There is no preferential partitioning of N between diamond and its parental fluid during the early stages of crystal growth when the linear growth rate is fast (i.e., $K_N = 1$) but the N partition coefficient progressively approaches the equilibrium value as the linear growth rate slows. Such a scenario would result in a trend towards decreasing N-content during diamond growth provided that the equilibrium K_N-value is < 1 (i.e., N behaves incompatibly in diamond).

The following lines of evidence suggest that, even if the DLGR model is valid for the particular Yakutia diamonds that Reutsky et al. (2017) studied, it is unlikely to be broadly applicable to natural diamonds. If correct, the constraints of the DLGR model should apply to all growing diamonds. That is, all diamonds should experience a progressive decrease in their linear growth rates as they increase in size because that phenomenon is an inevitable consequence of the constant volume growth rate assumption inherent to the model. Accordingly, if the model is generally applicable, C-isotope zoning profiles should be very common if not ubiquitous in natural diamonds. That prediction, however, is at odds with the observation that most diamonds that have been investigated to date do not show appreciable C-isotope zoning (see sections *Introduction* and *Diamond through time*). Although problematic for the DLGR model, the lack of isotopic zoning in many diamonds can readily be accommodated by the equilibrium fractional crystallization model by invoking a fluid-dominated (i.e., the fluid is effectively an infinite reservoir that does not change its isotopic composition as diamond precipitates) rather than a fluid-limited (i.e., where diamond crystallization induces isotopic shifts in the residual fluid) process. Only in the latter scenario will diamond crystallization lead to significant changes in the fluid isotopic composition and in turn the development of isotopic zoning profiles in the diamond. With the DLGR model, a fluid-limited system would produce reversals in C-isotope zoning profiles. In other words, for diamond crystallization from an oxidized fluid, δ^{13}C-values would first decrease and then increase (or visa-versa) as crystallization proceeds because of the combined effects of both changing fractionation factor and changing fluid isotopic composition during diamond crystallization. Such smooth (rather that abrupt reversals across growth zone boundaries) and systematic reversals in zoning profiles have not yet been documented in natural diamonds.

Although Reutsky et al. (2017) applied the DLGR model to gem-quality placer diamonds, their model and indeed kinetic models in general are more likely applicable to rapidly-grown fibrous diamonds than to slowly-grown gem diamonds (Sunagawa 1990). However, the available data suggest that C-isotope zoning is even less common in fibrous diamonds than in gem diamonds (namely δ^{13}C-values down to a minimum of ~ −8‰ at the core of fibrous diamonds increasing up to ~ −5‰ towards the outer rim; e.g. Boyd et al. 1992). We conclude therefore that while the DLGR model may be applicable, in some instances, to diamond growth on laboratory timescales, it does not provide a general explanation for the origin of zoning profiles in either fibrous or gem-quality natural diamonds.

Kueter et al. (2020) model. Like Reutsky et al. (2017), Kueter et al. (2020) also suggest that kinetic rather than equilibrium processes may control C-isotope compositions during diamond growth but propose a different kinetic model to account for their observations. The model is based on experiments in which stearic acid ($C_{18}H_{36}O_2$), sealed in a gold capsule, was rapidly decomposed at 0.2 GPa and 800 °C to form a mixture comprising primarily solid elemental carbon and CH_4 gas, along with lesser amounts of H_2O, H_2, and various other trace gases. Diffusion of H_2 gas out of the gold capsule over time promoted oxidation of the CH_4 to elemental carbon globules by the reaction: $CH_4 = C + H_2$. Under equilibrium conditions, elemental carbon (graphite) partitions ^{13}C relative to methane and, as a result, graphite precipitation should drive residual CH_4 to progressively more ^{13}C-depleted compositions. In a time-series set of experiments extending in duration from 30 seconds to 50 hours, Kueter et al. (2020) documented exactly the opposite trend; the δ^{13}C-values of CH_4 continuously increased with reaction progress. They attributed this finding to a kinetic isotope fractionation in which the weaker ^{12}C–H bonds in CH_4 preferentially broke down to form elemental carbon, which caused the residual CH_4 to become more ^{13}C-enriched. The C-isotope data from the time-series experiments were modeled to extract a kinetic graphite–CH_4 fractionation factor of −6.2 ± 0.3‰, which contrasts sharply with the equilibrium fractionation factor at 800 °C ($\Delta^{13}C_{\text{graphite-}CH_4}$ = +2.2‰). Kueter et al. (2020) speculated that an analogous, kinetically-controlled process involving methane oxidation may occur during natural diamond formation and could potentially explain why the great majority of diamond C-isotope profiles that do exhibit systematic variation show a trend to increasing δ^{13}C-values even though the mantle is thought to be dominated by relatively reduced fluids.

To assess the relevance of their short timescale experiments to the much longer timescale growth of natural diamonds, Kueter et al. (2020) applied the growth-entrapment (GE) model of Watson and Liang (1995) and Watson (1996, 2004), which was originally developed to explain the origin of sector zoning in natural crystals. The GE model proposes that an interplay between the growth rate of the crystal (V) and the diffusion rate (D_i) of a narrow near-surface layer of half-width l determines if partitioning equilibrium will be established between the surface of the growing crystal and the growth medium. If the crystal growth rate is too fast or diffusivity in the surface layer too slow, a disequilibrium (i.e., kinetic) partitioning of elements or isotopes between the crystal and the growth medium can become entrapped at the crystal surface and later preserved within the growing crystal. The GE model defines a non-dimensional parameter, the growth Péclet number ($Pe = V{*}l/D_i$), which determines if a kinetic partitioning will likely be recorded in the crystal. Specifically, if the value of Pe is > ~1, entrapment of a kinetic partitioning is likely.

Using the growth rate of carbon globules in their experiments (~ 10^{-12} m/s) in combination with an estimated surface layer half-width (1 nm) and diffusivity (~ 10^{-32} m^2/s), Kueter et al. (2020) calculated a Pe number of ~ 10^{11}, which indicates that, as observed, kinetic rather than equilibrium fractionation of C-isotopes was inevitable in their experiments. Applying the GE model to the growth of natural diamonds is more challenging but Kueter et al. made the following bounding calculation. Using Koga et al.'s (2005) experimentally-determined estimate of carbon lattice diffusion rate in diamond ($D = 4.5 \times 10^{-30}$ m^2/s) at 1100 °C, a typical lithospheric diamond-formation temperature, they computed that a crystal growth rate of $V \leq \sim 10^{-21}$ m/s would be required to obtain a growth Péclet number low enough ($Pe \leq 1$) to attain C-isotope equilibration at the diamond rim. At that growth rate, it would take > 3 billion years to form a 250 µm-radius diamond crystal. Thus, if correct, these calculations would effectively preclude the establishment of C-isotope and by implication N-isotope equilibrium during the growth of natural diamonds.

We would offer the following critique of this model calculation. The calculation assumed that the diffusion rate of carbon in the surface layer would be the same as that determined by Koga et al. (2005) for carbon diffusion within a well-formed diamond crystal. However, as noted by Watson and Liang (1995) and elaborated by Watson (2004), the diffusion rate of the surface layer is likely faster and possibly many orders of magnitude faster than the diffusion rate within the crystal lattice. Without quantitative knowledge of the surface-layer diffusion rate, it is not possible to do a robust GE calculation constraining whether isotopic equilibrium is likely to be established during natural diamond growth.

Several observations may be helpful in framing the question. At the carbon globule growth rate of Kueter et al.'s experiments, a 1 mm-radius crystal could be grown in < 40 yr. The time required for lithospheric diamonds to grow is not known but timescales of 10^5 to 10^7 yr do not seem unreasonable. Indeed, sizable pockets of fluid are known to persist in stable continental crust for billions of years (Holland et al. 2013). If similar, long-lived fluid pockets exist in cratonic mantle, crystallization times of minerals in these pockets, driven by either simple cooling or redox reactions, could be quite protracted. For example, a growth rate of $V = 10^{-17}$ m/s allows a 1 mm-radius crystal to form in ~ 3.5 million years. At that growth rate, attaining $Pe \leq 1$ requires $D \geq \sim 10^{-26}$ m^2/s for the surface layer, which is about 3.5–4 orders of magnitude faster than the lattice diffusion rate for carbon in diamond at 1100 °C and roughly equivalent to the lattice diffusion rate at 1315 °C (Koga et al. 2005). It is not certain if such diffusivities for the surface layer are reasonable but the absence of clear examples of C- or N-isotope sector zoning in natural diamonds suggests that surface layer diffusivities must be significantly higher than lattice diffusivities; otherwise, isotopic sector zoning would be common in natural diamonds.

The isotopic composition of natural diamonds and their internal zoning patterns are helpful in assessing the general applicability of the Kueter et al. (2020) kinetic model. If the isotopic composition of gem diamonds is kinetically controlled, then for typical temperatures of diamond formation (~1150 °C), the kinetic CH_4-diamond C-isotope fractionation factor would be +4.7‰ (Kueter et al. 2020). Accordingly, the cores of gem diamonds crystallizing from fluids with a mantle-like C-isotope composition of −5‰ should have δ^{13}C-values of about −10 to −9‰. Such low δ^{13}C-values are atypical for peridotitic diamonds and zonation trends increasing outwards from distinctly ^{13}C-depleted cores are even rarer. These observations suggest that the kinetic fractionation factor of Kueter et al. is much too large to account for the average C-isotope compositions of peridotitic diamonds unless one supposes that the mantle fluids responsible for the formation of these diamonds have δ^{13}C-values of −1 to 0‰.

A comparison of isotopic zoning patterns in gem diamonds versus those in fibrous diamonds is also useful in evaluating Kueter et al.'s (2020) model and specifically their proposal that the isotopic compositions of many diamonds are determined by a kinetic fractionation process during crystallization from methane-rich fluids. As noted previously, kinetic isotope effects, if applicable, are more likely to be evident in rapidly-grown fibrous diamonds. For instance, if surface layer diffusion rates were fast enough to allow the establishment of isotopic equilibrium during formation of slowly-grown gem diamonds but not in rapidly-grown fibrous diamonds then diamond formation from CH_4-rich fluids would drive fractionation trends in opposite directions in the two cases; toward lower and higher δ^{13}C-values in gem and fibrous diamonds, respectively. In addition, assuming that gem and fibrous diamonds are, on average, formed from similar C-isotope composition fluids, the early crystallized diamond in the fractionation sequence would be markedly different in the case of diamond precipitation from methane-rich fluids because of the opposite signs of the kinetic and equilibrium diamond–fluid fractionation factors. Even in the case of diamond formation from oxidized fluids where the signs of kinetic and equilibrium fractionation factors should be the same, it seems likely from Kueter et al.'s (2020) results that the magnitude of the kinetic fractionation factor would be significantly larger, which should again lead to detectable differences in the $\delta^{13}C$-values of the first crystallized gem versus fibrous diamonds. The available data do not indicate systematic differences in the fractionation trends or isotopic compositions of gem and fibrous diamonds (Weiss et al. 2022, this volume). This observation suggests either that the isotopic compositions of *both* gem and fibrous diamonds are controlled by kinetic processes or *neither* are kinetically controlled. The evidence detailed in the paragraphs above suggests that the former scenario is unlikely.

In summary, it is our view that, at present, there is no compelling evidence to indicate that the C- or N-isotope compositions of natural diamonds are largely due to kinetic rather than equilibrium fractionation processes. Nevertheless, the exceedingly slow diffusion rates of carbon and nitrogen in diamonds make kinetic isotope effects a possibility, certainly during diamond growth on laboratory timescales but perhaps also on geological timescales. Further search for clear disequilibrium features, such as isotopic sector zoning in mixed habit diamonds, is recommended as these may help to determine if natural diamond growth rates are near a critical threshold such that second-order variations in these growth rates will determine whether diamonds grow in isotopic equilibrium with the growth medium.

Mixing of fluids

Mixing of fluids with one carrying oxidized (CO_2 or CO_3^{2-}) and the other reduced carbon species (CH_4, C_2H_6) and/or H_2 will cause redox reactions that produce diamond (or graphite) and water (e.g., reactions 8 and 10 in Deines 1980 and reactions 1 and 2 below). The same principle applies if a reduced fluid infiltrates a carbonate-bearing mantle substrate. This process can be associated with large variations in stable isotopic composition and nitrogen content of precipitated diamond if the fluids derive from isotopically and compositionally distinct sources (e.g., mixing of reduced mantle-derived and oxidized subduction-derived fluids). As discussed in the *Introduction* and further below, most natural diamonds show fairly limited internal variation in their carbon isotope composition across continuously grown sections (marked by an absence of hiatuses in CL images), suggesting that mixing between extreme end-member fluids does not usually occur at the site of diamond formation. Gradual mixing of distinct fluids or recharge through fresh pulses of isotopically similar (but not identical) fluid, however, likely cause at least some of the seemingly chaotic fluctuations observed even on the level of individual homogenous growth zones that involve switches from increasing to decreasing (or vice versa) $\delta^{13}C$ and/or N-content. Good examples can be found in a profile across a small (< 1 mm) diamond of unknown paragenesis from Aviat on the Rae Craton (AV6-111; Peats et al. 2012), in the George Creek (Colorado) diamond plates studied by Fitzsimons et al. (1999), the homogenous core zone of eclogitic diamond A46 from Argyle (analytical spots 1–5) and two homogenous zones of harzburgitic diamond DBP-460_7 from Kimberley/'*De Beers Pool*' (analytical spots 1–6 and 7–10; the latter two diamonds from Supplementary Table 1 of Howell et al. 2020). The small scale and complexity of these potential mixing relationships, however, has so far precluded the successful development of numerical mixing models. For a more detailed discussion of fluid mixing based on combined He–N–C isotope data, see Jacob and Mikhail (2022, this volume).

Isochemical precipitation of diamond and Rayleigh isotope fractionation in multi-component systems

Conventional models of diamond precipitation in the course of redox reactions between carbon-bearing fluids or melts and peridotitic or eclogitic diamond substrates are built on the premise that such mantle rocks contain sufficient iron that can be shifted between the divalent and trivalent states to buffer the redox state of infiltrating fluids or melts. In other words, in these models diamond precipitates because the oxygen fugacity of the fluid is buffered by the host rocks. Yet, for the most important diamond substrate, strongly depleted cratonic harzburgites (yielding ~ 56% of all mined diamonds; Stachel and Harris 2008), this premise does not apply. Even very minor amounts of infiltrating fluid or melt, capable of delivering or removing less than 50 ppm O_2, are sufficient to completely overwhelm the buffering capacity of such iron-, garnet- and pyroxene-poor rocks (Luth and Stachel 2014).

As a result of the high solidus temperature of cratonic harzburgites (Wyllie 1987), together with the lower temperatures of the lithospheric mantle relative to the asthenosphere, percolating melts should generally freeze in harzburgite whilst COH (carbon-hydrogen-oxygen) fluids will be able to pass through. For such COH fluids, redox neutral precipitation of diamond during either cooling or ascent (i.e., cooling and depressurization) was recently developed as an alternative mode of diamond formation (Luth and Stachel 2014; Stachel and Luth 2015) and is briefly reviewed here. In this model, diamond formation can occur as a consequence of two oxygen-conserving reactions:

$$CO_2 + CH_4 = 2C + 2H_2O \tag{1}$$

or

$$2C_2H_6 = 3CH_4 + C \tag{2}$$

The former occurs in response to cooling (isobaric or along a geotherm) and the latter in response to depressurization. Only reaction (1) is capable of creating significant diamond endowment (> 1 ppm or > 5 carats per ton) at constant depth (the requirement for a diamond mantle source) at low fluid–rock ratios. Reaction (1) also is more consistent with oxygen fugacity measurements on cratonic peridotites (e.g., Stagno et al. 2013), which predict that at typical diamond-forming pressure–temperature conditions, coexisting COH fluids would be at or near the water maximum (> 90 mol% H_2O) and contain minor amounts of both CO_2 and CH_4 (Luth and Stachel 2014; Stachel and Luth 2015).

During diamond precipitation following reaction (1), carbon isotopes fractionate between diamond and the two carbon species in the fluid (CO_2 and CH_4). The relative proportions of CO_2 and CH_4 in the fluid are expressed as XCO_2 (molar $CO_2/[CO_2{+}CH_4]$). Except for the case of equal proportions of CO_2 and CH_4 in the initial fluid ($XCO_2 = 0.5$), XCO_2 evolves during diamond crystallization to either higher or lower values. For initial fluids that are CO_2 dominated ($XCO_2 > 0.5$), XCO_2 increases as diamond crystallization proceeds, leading to progressively more negative values for the diamond–fluid carbon isotope fractionation factor ($\Delta^{13}C_{\text{diamond–fluid}}$). Conversely, for methane-dominated fluids ($XCO_2 < 0.5$), XCO_2 decreases with diamond crystallization, which leads to progressively less negative and eventually positive $\Delta^{13}C_{\text{diamond–fluid}}$ values. The equations to model Rayleigh isotope fractionation in a multi-component system (RIFMS) were developed by Ray and Ramesh (2000). Assuming a mantle-like carbon isotope composition of the initial fluid ($\delta^{13}C$ of −5‰) and typical conditions for peridotitic diamond formation (1140 °C and 5 GPa), Stachel et al. (2017) used the RIFMS equations to model diamond precipitation following reaction (1) for XCO_2 from 0.89 (corresponding to the upper fO_2 limit of diamond stability at these *PT* conditions) to 0.10. In these calculations, the bulk diamond–fluid carbon isotope fractionation factor ($\Delta^{13}C_{\text{diamond–fluid}}$) scales with the relative proportions of CO_2 and CH_4 (i.e., XCO_2 and $1 - XCO_2$ respectively), each being multiplied by their respective fractionation factor, i.e., $\Delta^{13}C_{\text{diamond–fluid}} = XCO_2 \times \Delta^{13}C_{\text{diamond-}CO_2} + (1 - XCO_2) \times \Delta^{13}C_{\text{diamond-}CH_4}$. Except when $XCO_2 = XCH_4$, XCO_2 will vary as diamond precipitates and so will $\Delta^{13}C_{\text{diamond–fluid}}$. As illustrated in Figure 20, precipitated diamond invariably evolves along parallel trends, showing the same small increases in $\delta^{13}C$-values with fractionation up to the point at which either CO_2 or CH_4 becomes exhausted in the fluid. The absolute $\delta^{13}C$-values of diamond are, however, highly sensitive to XCO_2 and increase by 3.7‰ as XCO_2 decreases from 0.89 to 0.10 (Stachel et al. 2017).

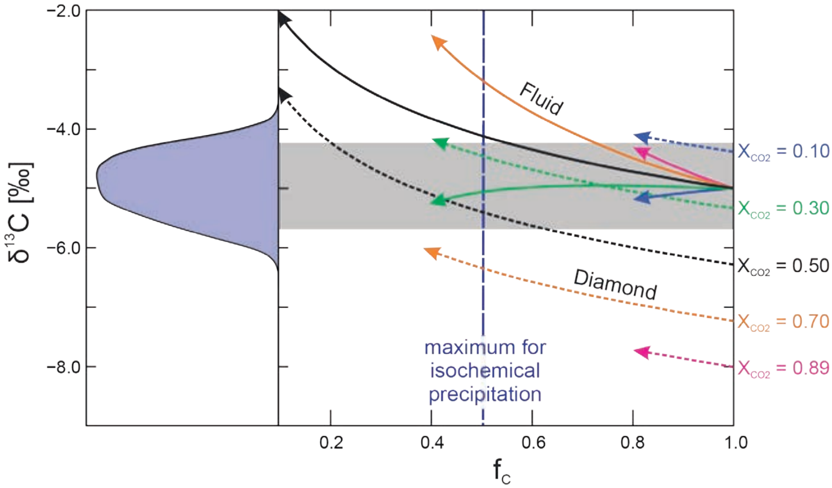

Figure 20. Evolution in carbon stable isotope composition of near water-maximum COH fluids and diamonds precipitated from such fluids during Rayleigh isotope fractionation in a multicomponent system (RIFMS; Ray and Ramesh 2000). Isotope fractionation during the diamond forming reaction $CO_2 + CH_4 = 2C + 2H_2O$ was modeled at a temperature-pressure condition of 1140 °C/5 GPa (Stachel et al. 2017). The evolution of the fluids is shown as **solid lines**, starting from an initial $\delta^{13}C$ of −5‰ (mantle value) at $f_C = 1$, with f_C being the remaining fraction of carbon-bearing species in the fluid. The evolution of precipitating diamonds is shown as **dashed lines**, matching the color of the associated fluid. XCO_2 (molar CO_2/[CO_2+CH_4]) indicates the relative proportions of the two diamond-forming carbon species in the fluid. Except for the case of $XCO_2 = 0.5$, the relative proportions of CO_2 and CH_4 evolve during diamond precipitation towards exhaustion of the minor species, at which point diamond formation stops. Isobaric cooling of a fluid, as the driver of isochemical diamond precipitation, is unlikely to exceed ~ 200 °C, limiting f_C to ≥ 0.5 (**vertical blue dashed line**). The **grey band** corresponds to the interquartile range in $\delta^{13}C$ for harzburgitic diamonds worldwide (Table 1). The distribution shown in **light blue** is a probability density function combining diamonds precipitated at four discrete XCO_2 values (0.4, 0.3, 0.2 and 0.1) and provides a good match for the distribution of $\delta^{13}C$-values in peridotitic diamonds worldwide (Fig. 2).

Isobaric cooling of fluid released, e.g., from hot intrusions of proto-kimberlite into ambient deep lithospheric mantle, likely will not exceed a ~ 200 °C temperature interval. As the amount of carbon precipitated isochemically from the fluid following reaction (1) scales with the temperature decrease, at most 50% ($f_C = 0.5$) of the carbon species in the fluid will precipitate as diamond (Stachel and Luth 2015). Based on this limit, diamond internal variations due to RIFMS processes will be smaller than 1‰. Also based on the limit $f_C \geq 0.5$, only fluids with XCO_2 between 0.4 to 0.1 precipitate diamond with carbon isotope compositions that fall between the 25th (−5.7‰) and 75th quartile (−4.2‰) for harzburgitic diamonds worldwide (shown as grey band in Fig. 20). Calculating a probability density function for all $\delta^{13}C$-values obtained from models for XCO_2 of 0.4, 0.3, 0.2 and 0.1 (calculated in f_C increments of 0.001, until either $f_C = 0.5$ or the point of CO_2 exhaustion was reached) indicates good agreement with the worldwide diamond distribution. As some fluctuation in the initial carbon isotope composition of diamond-forming fluids is likely, the variability in XCO_2 of ascending COH fluids may be even smaller than the modeled range from 0.4 to 0.1, in order to achieve the observed tight mode in the harzburgitic diamond distribution.

The isochemical diamond precipitation model of Luth and Stachel (2014) applies to harzburgitic diamond substrates below their solidus temperature. The model may, however, have applicability to lherzolitic and eclogitic diamond substrates as well (Luth 2017): in such rocks the influx of a hydrous fluid initiates melting, associated with strong partitioning of water from the fluid into the melt phase, which then should force diamond precipitation from the residual carbon-oversaturated COH fluid. This proposal awaits further detailed evaluation.

The calculations of Luth and Stachel (2014) are based on the thermodynamic model for pure COH fluids of Zhang and Duan (2009). Recent experimental work at pressures between 3 and 6 GPa showed, however, that at sub-solidus temperature conditions hydrous fluids contain up to ~40 wt% dissolved solids[6] (Adam et al. 2014; Kessel et al. 2015). The high solute content of the experimental fluids resembles that of high-density-fluids (HDFs) observed as inclusions in diamond (Navon 1991; Klein-BenDavid et al. 2009; Weiss et al. 2015, 2022, this volume). Whilst such high solute contents may affect the model of Luth and Stachel (2014) on a detailed level (potentially shifting fluid speciation and carbon solubility in *PT* space), the principle of isochemical diamond precipitation, during either isobaric cooling or ascent along a geotherm, is expected to remain valid. Based on the experimental work of Stagno and Frost (2010), HDFs derived from near-water maximum COH fluids in equilibrium with diamond (i.e., representing fO_2 conditions ~ ½ log unit more reducing than the enstatite + magnesite = olivine + diamond [EMOD] equilibrium) may carry a significant content of dissolved carbonate (equivalent to up to 20 mol% of CO_2), which then may allow for an additional oxygen conserving diamond-forming reaction between methane and dissolved carbonate to occur during cooling. As a variant of the isochemical precipitation model (Luth and Stachel 2014), a possible diamond-forming reaction involving a carbonated near-water maximum fluid passing through subsolidus peridotite is:

$$2MgCO_3 + 2CH_4 + Mg_2Si_2O_6 = 4C + 4H_2O + 2Mg_2SiO_4 \tag{3}$$

In this reaction, the sole role of the diamond substrate (the host silicate rock) is to accommodate liberated MgO through the conversion of orthopyroxene to olivine.

A question not explicitly addressed by the isochemical precipitation model is the impact of diamond precipitation from near-water maximum COH fluids on the water budget of the affected substrates. Diamondiferous peridotite xenoliths contain 25 ppm (125 ct/ton) of diamond on average, ranging up to 5500 ppm (Viljoen et al. 2004). During cooling by 200 °C (see above), a water-maximum COH fluid precipitates about 0.8 mol% diamond, which is equivalent to about 0.5 wt% diamond (see Fig. 15 of Stachel and Luth 2015). A diamond content of 25 ppm thus requires that the diamond substrates interacted with at least 0.5 wt% (5000 g/ton) fluid. Hydrous HDFs are documented as thin (≤ 1.5 μm) films around silicate and oxide inclusions (Nimis et al. 2016) and as primary fluid inclusions in both fibrous and smooth-surfaced monocrystalline diamonds (Jablon and Navon 2016). Mineral inclusions in diamond, however, are generally anhydrous (Matveev and Stachel 2009; Novella et al. 2015) and measured water contents in typical diamond source rocks (depleted cratonic peridotites) from the Kaapvaal Craton are low (< 80 ppm in olivine; Peslier et al. 2010). Metasomatism and associated diamond precipitation through essentially dry melts (<0.1 wt% H_2O in equilibrium with anhydrous olivine inclusions in diamond; Novella et al. 2015) is considered unlikely, as such dry melts cannot percolate through depleted cratonic peridotites that for normal geotherms are below their anhydrous solidus temperature. Thus, the observed low water contents can only relate to dehydrogenation of the peridotitic diamond substrates subsequent to diamond formation, likely caused by incipient melting (Matveev and Stachel 2009; Wang et al. 2021) or through more gradual upward migration of volatiles driven by continuous input of heat from the convecting mantle. Available data for the speed of hydrogen diffusion through diamond suggest re-equilibration of initially hydrous inclusions with anhydrous substrates may occur on the scale of days to thousands of years (Matveev and Stachel 2009; Cherniak et al. 2018).

[6] Dissolved solids are all non-COH (+ halogens + S) constituents of a fluid, irrespective if they are dissolved as ions or neutral species.

Diamond formation driven by pH changes in ionic fluids

Based on calculations conducted at 900 °C and 5 GPa using the Deep Earth Water (DEW) model, Sverjensky and Huang (2015) suggested that diamond may form in response to decreasing pH during interaction of an ionic hydrous fluid with coesite-bearing eclogite. Similar to the isochemical precipitation model outlined in the previous section, diamond formation via the destruction of formate ($HCOO^-$) and propionate ($C_2H_5COO^-$) occurs at nearly constant oxygen fugacity (Sverjensky and Huang 2015). Whilst constituting an appealing alternative to conventional models of diamond formation in settings with a geothermal gradient lower than the cratonic average (40 mW/m^2 model geotherm of Hasterok and Chapman 2011) and at depths near the graphite–diamond transition, geothermobarometric studies (e.g., Stachel and Luth 2015; Nimis 2022, this volume) indicate that pressure–temperature conditions of eclogitic diamond formation typically fall above the hydrous solidus of eclogite (Kessel et al. 2005), i.e., eclogitic diamond formation generally occurs in the presence of a melt, where the DEW model no longer applies. From a stable isotope perspective, although the diamond–fluid carbon isotope fractionation factors for most of the minor carbon species in the modeled fluids are unknown, CO_2, which is by far the most abundant carbon species in the fluid, should dominate the bulk fractionation factor and thus the isotope effects will be similar to diamond precipitation from an oxidizing fluid composed of neutral species (see above and Fig. 18).

Similar calculations using the DEW model to determine the speciation of fluids in equilibrium with peridotite (Sverjensky et al. 2014), indicated a non-ionic carbon speciation (CO_2, CH_4 and CO), in agreement with conventional models (e.g., Zhang and Duan 2009). This is of particular relevance as the isochemical precipitation model reviewed in the preceding section strictly applies only to strongly depleted peridotite (harzburgite).

Diamond through time—*in situ* carbon and nitrogen isotope data for diamonds with Paleoarchean to Meso/Neoproterozoic formation ages

Howell et al. (2020) conducted a large *in situ* study of the carbon isotope composition of diamond through time with the goal of examining possible temporal changes in mantle carbon speciation. In total, 908 carbon isotope measurements were obtained via multi-collector SIMS on fragments of 88 peridotitic and 56 eclogitic diamonds, with known formation ages ranging from the Paleoarchean (maximum age: 3.5 Ga) to the Mesoproterozoic (minimum age: 1.0 Ga). The key outcomes of the Howell et al. (2020) study are:

1. Cathodoluminescence imaging indicated that nearly half the diamonds formed during pulsed or episodic growth. Nevertheless, the observed variability in $\delta^{13}C$ (measured as absolute difference between highest and lowest value in single samples) was small in both peridotitic (mean: 0.8‰) and eclogitic diamonds (mean: 1.6‰). This limited variability across diamond fragments clearly implies that the heritage dataset of conventional bulk stable isotope analyses, obtained using diamond fragments ≤1 mg, is valid and its continued use is well justified.

2. No systematic trends in $\delta^{13}C$ or systematic co-variations of $\delta^{13}C$ and nitrogen content were observed in any of the 144 diamonds analyzed. This implies that kinetic fractionation effects, e.g., due to decreasing growth rates during outward growth (Reutsky et al. 2017), are uncommon, if they occur at all. Equally, Rayleigh fractionation during diamond growth is evidently uncommon. In view of the mild isotope effects of RIFMS (maximum variation in $\delta^{13}C$ during isobaric cooling by 200 °C is 0.9‰ but typically will be less; see Fig. 20), minor fractionations could remain unrecognized, but in general, the absence of coherent trends in the studied samples indicates that diamond formation rarely occurs under fluid-limited conditions where fractionation trends would be more apparent. An absence of fractionation trends in precipitated diamonds, and by inference in their parental fluids, however, does not imply that carbon isotopes are not fractionated between diamond and fluid.

3. No systematic variation is apparent in the mantle carbon isotope record since 3.5 Ga (Fig. 21). Local variability aside, from the Paleoarchean to the Mesoproterozoic the modes (not shown; see Howell et al. 2020 instead) for both peridotitic and eclogitic diamonds correspond to the mantle value of −5‰.

For nitrogen isotope measurements the worldwide database is less mature and, consequently, allows only for a preliminary assessment of possible variations through time. Combining bulk isotope analyses from literature with averages for SIMS traverses (in part calculated separately for distinct core and rim zones for clearly zoned diamonds) obtained on the same samples used for the Howell et al. (2020) study, $\delta^{15}N$-values associated with age information are available for 249 peridotitic and 97 eclogitic diamonds. For details on diamond formation ages, see Howell et al. (2020). From this data set, three broad age groups are established: (1) Archean (4.0–2.5 Ga; 144 peridotitic and 37 eclogitic), (2) Paleoproterozoic (<2.5–1.6 Ga; 71 peridotitic and 38 eclogitic) and (3) Meso- (<1.6–1.0 Ga) to Neoproterozoic diamonds (<1.0–0.54 Ga; 34 peridotitic and 23 eclogitic). Due to a strong bias of certain age groups to individual mines, the information derived from Figure 22 must be interpreted with some caution. For peridotitic diamonds, average and median values remain reasonably constant through time (e.g., median values of −0.8, +1.8 and −3.2‰ from oldest to youngest group), with the caveat that the Meso- to Neoproterozoic dataset only consists of diamonds from two locations, 1.4 Ga (Smit et al. 2010) diamonds from Ellendale 4 and 9, and 0.7 Ga (Aulbach et al. 2018) diamonds from Victor with quite disparate $\delta^{15}N$ characteristics (Ellendale being ^{15}N-enriched and Victor ^{15}N-depleted).

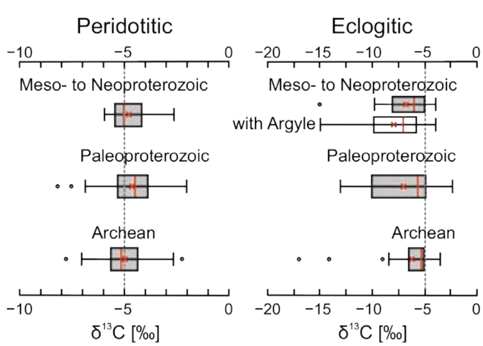

Figure 21. Carbon isotope composition ($\delta^{13}C$) of peridotitic (**left**) and eclogitic suite diamonds (**right**), grouped according to formation age. Median values (**red lines**), averages (**red crosses**), 25th to 75th percentiles (interquartile range; **boxes**) and ranges (**whiskers**) are shown. Outliers are indicated as **small circles**. The **blue dashed line** indicates the mantle value of about −5‰ (Deines 2002). Based on the carbon isotope data set of Howell et al. (2020), obtained on diamonds used in inclusion-dating studies or with otherwise constrained ages, and 22 additional analyses of Neoproterozoic diamonds from the Victor Mine. For Meso- to Neoproterozoic diamonds of the eclogitic suite two distributions are shown, one including diamonds from Argyle (labelled "with Argyle") and one (above) with eclogitic diamonds from Orapa, Jwaneng and Victor only. An apparent trend of decreasing mean and median $\delta^{13}C$ values with time disappears when the Argyle data set is excluded.

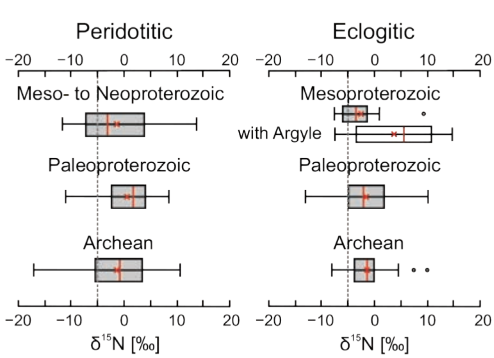

Figure 22. Nitrogen isotope composition ($\delta^{15}N$) of peridotitic (**left**) and eclogitic suite diamonds (**right**), grouped according to formation age. Median values (**red lines**), averages (**red crosses**), 25th to 75th percentiles (interquartile range; **boxes**) and ranges (**whiskers**) are shown. Outliers are indicated as **small circles**. The **blue dashed line** indicates the assumed mantle value of −5 (± 2)‰ (Cartigny and Marty 2013). For Mesoproterozoic diamonds of the eclogitic suite two distributions are shown, one including diamonds from Argyle (labelled "with Argyle") and one (above) with 1 Ga old eclogitic diamonds from Orapa and Jwaneng only.

For eclogitic diamonds, Figure 22 appears to indicate a strong increase in $\delta^{15}N$ in Mesoproterozoic diamonds, but this increase in the average (from −1.3 and −1.6 to +3.7‰, for Archean, Paleoproterozoic and Mesoproterozoic diamonds, respectively) and median $\delta^{15}N$-values (from −1.5 and −2.1 to +5.6‰) relates exclusively to the strongly ^{15}N-enriched eclogitic diamond suite from Argyle (mean of +9.5‰ and median of +10.7‰), whereas approximately 1 Ga diamonds from Orapa and Jwaneng document continuity in $\delta^{15}N$ through time (mean of −2.6‰ and median of −3.5‰).

Despite the limitations of the current data set, the above observations imply that the mantle source(s) for nitrogen in diamond did not undergo significant isotopic evolution between about 3.5 and 0.7 Ga.

ORIGIN OF LARGE RANGES IN $\delta^{13}C$ AND $\delta^{15}N$— THE RELATIVE ROLES OF MANTLE, SEDIMENT AND OCEANIC CRUST

As reviewed in the *Introduction* to this chapter, the explanation of ^{13}C-depleted carbon, observed principally in eclogitic, but also in websteritic and some peridotitic diamonds, as being sourced from subducted organic matter still remains a subject of scientific debate. To add further constraints, recent research increasingly included nitrogen isotope data for diamond, together with oxygen and sulfur isotope compositions determined for silicate and sulfide inclusions, respectively. When the first reliable isotope determinations of nitrogen in diamond became available for the different source parageneses (Boyd et al. 1987; Cartigny et al. 1997, 1998), a problem arose for the recycled sediment model in that the expected strictly positive $\delta^{15}N$-values (see Cartigny and Marty 2013, their Fig. 1 for the $\delta^{15}N$-distribution of both recent and ancient sediments) that characterize sediment-derived nitrogen were absent in the majority (~ 70%) of diamonds with low $\delta^{13}C$-values that were supposed to be indicative of sediment recycling (Cartigny 2005). Based on the expanded data set presented here, this relationship has changed given that ~ 70% (16 out of 22 samples) of diamonds with $\delta^{13}C < -15‰$ have positive $\delta^{15}N$ values (Fig. 8).

The recycled origin for C in eclogitic diamonds was bolstered by the observation of mass-independent sulfur isotope fractionation in sulfide inclusions of eclogitic diamonds (Farquhar et al. 2002; Thomassot et al. 2009; Smit et al. 2019b) and their near absence in peridotitic diamonds (Cartigny et al. 2009). Such fractionations only originated during Archean atmospheric processes and hence are restricted to Archean sediments, thereby providing a direct link between eclogitic inclusions in diamond and subduction of Archean sediments. The recycling model was further reinforced by the observation of prominent ^{18}O-enrichment ($\delta^{18}O > +6‰$, up to 16‰; $\delta^{18}O_{mantle}$ being taken as falling between +5 and +6‰) in eclogitic silicate inclusions, contained in diamonds with $\delta^{13}C$-values distinctly lower than the mantle range (Lowry et al. 1999; Schulze et al. 2003, 2013; Ickert et al. 2013; Zedgenizov et al. 2016). Questions arise from $\delta^{18}O$-values > +10‰ and up to +16‰, observed for coesite inclusions in diamond, as such high $\delta^{18}O$-values are exceedingly rare in both sediments and altered-oceanic crust. Cartigny et al. (2014) pointed out that the curvature of possible binary mixing trends in $\delta^{13}C$–$\delta^{18}O$ space between a mantle and a recycled component requires a lower carbon content in the recycled component, which is counter-intuitive in view of the low ratio of $C_{Mantle}/C_{Oceanic\ Crust}$ (~ 1/50, as deduced from C_{Mantle} of ~ 50 ppm of Marty 2012 and $C_{Oceanic\ Crust}$ of ~2000 ppm of Li et al. 2019). Simple binary mixing of a mantle and crustal component with fixed carbon concentrations, $\delta^{13}C$ and $\delta^{18}O$ is, however, not necessarily implied by the observed co-variations in $\delta^{13}C$ and $\delta^{18}O$. Instead, Ickert et al. (2013) proposed that only the most intensely altered, topmost parts of altered oceanic crust (AOC), with $\delta^{18}O \geq 6‰$, contain sufficiently high concentrations of primary organic carbon to allow for the growth of ^{13}C-depleted diamonds, whereas diamond formation in deeper AOC, associated with lower carbon contents and

$\delta^{18}O$-values, is dominated by infiltrating mantle fluids/melts, with carbon contents typically on the wt% level (e.g., Stachel and Luth 2015). Yet, this model is not universally accepted, as carbonates with high $\delta^{13}C$ are abundant in topmost parts of AOC, requiring carbonate removal by subsolidus decarbonation or partial melting reactions to precede diamond formation.

Models invoking the derivation of all C-isotope variability via within-mantle isotopic fractionation of asthenospherically-derived carbon-bearing fluids (Galimov 1991; Javoy et al. 1986) suffered from the difficulty in explaining the abundant circumstantial evidence of other signatures of crustal recycling in eclogites from both radiogenic and stable isotopes (Pearson et al. 2003; Jacob 2004). Attempts to reconcile subducted eclogitic substrates with mantle-derived carbon and nitrogen in diamonds called on the exclusive introduction of these components during metasomatic diamond growth (e.g., Thomassot et al. 2009) but suffered from the impracticability of generating the highly ^{13}C-depleted tail of the eclogitic diamond distribution through fractionation of mantle fluids (see section *Introduction*). Hence, while there is little doubt that carbon is subducted into the mantle, as evident from the mass balance and C-isotope composition of subduction zone volcanics (Mattey et al. 1984; Kelemen and Manning 2015; Plank and Manning 2019), disentangling the effects of subduction, mantle processes and fluid/melt evolution, and to develop a unifying theory to explain the C- and N-isotope data in particular, remained a major problem.

Early criticism of the requirement for subducted crustal carbon in diamonds generally focused on the inability of binary mixing to create the observed frequency distribution for $\delta^{13}C$-values in eclogitic diamonds (e.g., Javoy et al. 1986; Deines et al. 1991), while at the same time overlooking the likely mantle carbon input to the system. In addition, the inherent isotopic variability of any of the mixing endmembers involved makes the discovery of well-defined mixing trends, even between two endmembers, unlikely.

Building on an existing body of work on C- and N-isotope variability in AOC, including the observation of strongly ^{13}C-depleted values (Shilobreeva et al. 2011), Li et al. (2019) further investigated this reservoir as a source of the isotopically light carbon in diamonds and examined likely mixing relations in C–N isotope space. Given this model is among the most recent, here we review its strengths and weaknesses. In their model, Li et al. (2019) suggest that in addition to an asthenosphere-derived mantle component ($\delta^{13}C$ and $\delta^{15}N$ ~ −5‰), at least three AOC-hosted reservoirs are involved (Fig. 17) that together can explain the complex and varied C–N isotope variation in eclogitic diamonds. A key assumption in the model is the decoupling of the sources for carbon and nitrogen in these reservoirs, leading to the observed decoupling in their C- and N-isotope signatures. Li et al. (2019) implicated roles for metamorphic equivalents of: (1) "normal" marine carbonate, i.e., chemical sediment precipitated within AOC with a mean $\delta^{13}C$-value of ~ 0‰, together with clays formed by low-T alteration, with positive $\delta^{15}N$-values of up to +16‰; (2) biogenic carbonate (± organic matter) in AOC with a $\delta^{13}C$-value of ~ −30‰, again combined with low-T clays ($\delta^{15}N$ values of up to +16‰); and (3) AOC altered at relatively high temperatures, containing no carbonate or organic matter (i.e., negligible C) but ^{15}N-depleted clay ($\delta^{15}N$-values of −16 to −12‰), levering the N-isotope composition with little effect on the C-isotope composition. Mixing these three endmembers with a mantle component is a more satisfactory way of explaining the complex C–N isotope systematics of diamonds than considering sedimentary carbon alone (Fig. 17). All three AOC components will have some degree of isotopic heterogeneity making for a complex scatter of data—as observed. In addition, there may also be inhomogeneity in the isotope composition of mantle-derived nitrogen, with deep-rooted mantle plumes carrying a ^{15}N-enriched signature ($\delta^{15}N$ of +3 ± 2‰; Dauphas and Marty 1999; Marty and Dauphas 2003; Labidi et al. 2020) derived from ancient, deeply subducted material or possibly tapping primordial heterogeneities preserving strongly ^{15}N depleted signatures.

The model of Li et al. (2019) has significant advantages in being able to derive the C-, N- and O-isotope signatures of diamonds and their silicate inclusions in a spatially compact package, without requiring isotopically light carbon of exclusively organic-sediment origin to counterintuitively migrate stratigraphically downwards into the altered oceanic crust that constitutes the eclogitic diamond substrates. Instead, isotopically light and heavy C is an intrinsic component of altered oceanic crust that contains varied O-isotope signatures plus isotopically varied nitrogen being derived from secondary clays that may have light or heavy N-isotope compositions, depending on the temperature of AOC alteration.

The re-equilibration of isotopically distinct carbon in carbonate and reduced carbon, however, remained unaddressed. Also, the distribution and total range of δ^{13}C-values observed for diamonds and for AOC are not a perfect match, with high δ^{13}C-values (up to +5‰) being abundant in AOC and δ^{13}C-values below about −25‰ being very rare (e.g., Shilobreeva et al. 2011; Li et al. 2019). The suggested δ^{13}C-value of −30‰ for the biogenic carbonate—low-*T* clay end-member (Li et al. 2019; C2 in Fig. 17) already incorporates the inevitable metamorphic devolatilization of subducting slabs that drives the remaining carbonate to more negative δ^{13}C-values. For rare (2.4%) eclogitic diamonds with δ^{13}C-values below −30‰, AOC is an unlikely carbon source. Like biogenic carbonate, organic matter from the bio-alteration of igneous oceanic crust does not extend to such extreme levels of ^{13}C depletion (Banerjee et al. 2006; Kruber et al. 2008). Accordingly, while the model of Li et al. (2019) is attractive for explaining much of the apparently disparate C–N-isotope data for eclogitic diamonds, a role for isotopically light C within terrigenous or shelf sediments (average δ^{13}C of sedimentary organic carbon over the last 3.5 b.y. is −26 ± 7‰; Schidlowski 2001) is likely needed to explain diamond δ^{13}C-values below −30‰. For diamond δ^{13}C-values of about −40‰, as observed at the Jericho mine, involvement of methane in the formation of kerogen precursors for sedimentary organic carbon is required (Schidlowski 2001; Smart et al. 2011). Sedimentary inputs are also implied by the presence of anomalous Δ^{33}S variations in sulfides included within diamonds (Farquhar et al. 2002; Thomassot et al. 2009; Smit et al. 2019b). ODP drilling of forearc sediments shows that the down-going sediment inventory can be dominated by both terrigenous sediment and carbonate, whereas the carbon flux to arc magmas is dominated by the carbonate signal (Plank and Manning 2019). Subduction of some sediment along with oceanic crust into the deeper convecting mantle is demanded by modeling of the Hf–Nd isotope systematics of ocean island basalts (Chauvel et al. 2008).

A further open question that currently is very difficult to address is the role of isotope fractionation in creating some of the variance observed in Figure 17. Of the 335 combined C- and N-isotope analyses of eclogitic diamonds in our database, 239 (71%) fall into the C-isotope mantle range (δ^{13}C between −7 and −3‰). During diamond precipitation in a fluid-limited system, the N-isotope composition of diamond varies by an order of magnitude more than the carbon isotope composition (Mikhail et al. 2014; Hogberg et al. 2016; see also discussion of isotope fractionation above). Consequently, for the dominant population of eclogitic diamonds with a mantle-like C-isotope composition, elevated δ^{15}N-values (≥ 0‰) may be interpreted to represent either mixing of C and N derived from the mantle and from AOC (combinations of low temperature clay with either normal or biogenic carbonate, at $N/C_{Mantle} \ll N/C_{AOC}$; see Fig. 17) or the much stronger evolution of N-isotopes (due to a larger isotope fractionation factor or a lower residual fraction of nitrogen) during Rayleigh fractionation. We note, however, that the match between the δ^{15}N frequency distribution for eclogitic diamonds and the relative proportions of the expected AOC reservoirs is not perfect and that Rayleigh isotope fractionation, at least during diamond precipitation, appears to occur only rarely (see above). Furthermore, no coupled δ^{13}C–δ^{15}N–δ^{18}O dataset for AOC exist yet and the Li et al. (2019) model is based on a data set that was assembled from several studies. An important next step, therefore, is to collect a comprehensive isotopic dataset for AOC and to document its evolution during metamorphic re-equilibration and devolatilization.

Despite these currently unaddressed questions, Li et al. (2019) for the first time connected the broad ranges in observed C- and N-stable isotope signatures, their paragenetic association and their relationship to observed O-isotope variations and identified a combination of at least five major sources acting in various combinations:

1. Asthenosphere-derived typical mantle fluids carrying the "canonical" mantle C- and N-isotope signatures, possibly with a distinct N-isotope signature for deeper "plume mantle" sources (Dauphas and Marty 1999; Marty and Dauphas 2003).
2. Subducted shallow igneous oceanic crust that originally was altered at low temperatures, causing precipitation of biogenic and/or normal carbonate together with formation of clay.
3. Subducted deeper igneous oceanic crust that originally was altered at higher temperatures, including the formation of clay.
4. Subducted marine carbonate sediment with varying detrital clay contributions
5. Subducted terrigenous sediment containing kerogenous carbon.

The signature of this menu of widely varying C- and N-isotopes is enhanced by additional petrogenetic processes such as decarbonation reactions and isotopic fractionations.

FUTURE DIRECTIONS

To address the open questions discussed in this review, future research into the following topics would be beneficial:

- The speciation and partitioning behavior of nitrogen (K_N diamond–fluid) during diamond precipitation needs to be addressed experimentally over a range of oxygen fugacities.
- Nitrogen isotope fractionation factors between diamond and the various possible nitrogen species in diamond-forming fluids need to be investigated experimentally or with rigorous theoretical calculations.
- Elemental and isotopic partitioning data for nitrogen would allow to make full use of a rich dataset of nitrogen concentration measurements and a growing dataset of $\delta^{15}N$ analyses of diamond. For the relative rare cases where clear covariations between $\delta^{13}C$ and N-content occur, based on partitioning data the concentration of nitrogen in the fluid or the speciation of nitrogen could be constrained.
- Continued search for isotopic or elemental zoning patterns in individual diamonds (e.g., sector zoning) that can unequivocally be ascribed to kinetic isotope fractionation processes.
- Improved spatial resolution of stable isotope analyses could reveal hitherto unrecognized fractionation trends on the μm to sub-μm level.
- More extensive coupled C- and N-isotope studies need to be performed on altered oceanic crust and mantle, in the form of fracture-zone peridotites, to better evaluate the extent of coupling or decoupling of C- and N-isotopes in subducting slabs. This should be accompanied by experimental studies of the isotopic effects of devolatilization of these slabs.
- More extensive thermodynamic data relevant to fluid speciation at deep lithospheric mantle and asthenosphere / transition zone pressures would aid in understanding isotopic variations in diamonds formed in these environments. In particular,

the thermodynamic model for COH fluids in the mantle (Zhang and Duan 2009) needs to be expanded to include the role of dissolved solids.

- The observation of distinct features (higher N-content, lower N-aggregation state, more restricted range of $\delta^{13}C$-values) of sulfide-bearing diamonds relative to silicate-included diamonds from the same locality and of the same paragenesis needs to be studied in more detail to evaluate if sulfide-included diamonds have specific characteristics or if these differences just represent multiple generations of diamonds, with one being more sulfide-rich.

ACKNOWLEDGMENTS

We are grateful to the late Erik Hauri for being an ardent supporter of diamond research under the Deep Carbon Observatory banner. It was also Erik who pushed us hard to get the large database of stable isotope and nitrogen data for diamond that comes with this paper out into the public domain. Kelsey Graversen (University of Alberta) is sincerely thanked for conducting tedious and detailed error-checking of the database and for adding the DOIs for all references to the spreadsheet. Emilie Thomassot still found a few more wrong entries and we thank her for that. A special thanks to Richard Stern, managing director of the Canadian Centre for Isotopic Microanalysis, for supporting the research summarized in this review over the years through analytical developments and a trove of highest quality analyses. Juske Horita, Sami Mikhail and Zachary Sharp are thanked for their constructive input as reviewers. Karen Smit as our editor went above and beyond to get this chapter in good shape.

REFERENCES

Adam J, Locmelis M, Afonso JC, Rushmer T, Fiorentini ML (2014) The capacity of hydrous fluids to transport and fractionate incompatible elements and metals within the Earth's mantle. Geochem Geophys Geosystems 15:2241–2253

Akagi T, Masuda A (1988) Isotopic and elemental evidence for a relationship between kimberlite and Zaire cubic diamonds. Nature 336:665–667

Appora-Gnekindy I (1998) Etude expérimentale du fractionnement isotopique du carbone et de l'oxygène dans les systèmes CO_2–carbonate liquides: Application aux contextes carbonatiques. PhD thesis, Institut de Physique du Globe de Paris, 351p

Aubaud C, Pineau F, Hekinian R, Javoy M (2006) Carbon and hydrogen isotope constraints on degassing of CO_2 and H_2O in submarine lavas from the Pitcairn hotspot (South Pacific). Geophys Res Lett 33: L02308

Aulbach S, Creaser RA, Stachel T, Heaman LM, Chinn IL, Kong J (2018) Diamond ages from Victor (Superior Craton): Intra-mantle cycling of volatiles (C, N, S) during supercontinent reorganisation. Earth Planet Sci Lett 490:77–87

Badziag P, Verwoerd WS, Ellis WP, Greiner NR (1990) Nanometre-sized diamonds are more stable than graphite. Nature 343:244–245

Banerjee NR, Furnes H, Muehlenbachs K, Staudigel H, de Wit M (2006) Preservation of ~3.4–3.5 Ga microbial biomarkers in pillow lavas and hyaloclastites from the Barberton Greenstone Belt, South Africa. Earth Planet Sci Lett 241:707–722

Beyssac O, Chopin C (2003) Comment on "Diamond, former coesite and supersilicic garnet in metasedimentary rocks from the Greek Rhodope: a new ultrahigh-pressure metamorphic province established" by E.D. Mposkos and D.K. Kostopoulos–Earth Planet. Sci. Lett. 192 (2001) 497–506. Earth Planet Sci Lett 214:669–674

Bottinga Y (1968) Calculations of fractionation factors for carbon and oxygen isotopic exchange in the system calcite–carbon dioxide–water. J Phys Chem 72:800–808

Bottinga Y (1969a) Calculated fractionation factors for carbon and hydrogen isotope exchange in the system calcite–carbon dioxide–graphite–methane–hydrogen–water vapor. Geochim Cosmochim Acta 33:49–64

Bottinga Y (1969b) Carbon isotope fractionation between graphite, diamond and carbon dioxide. Earth Planet Sci Lett 5:301–307

Boyd FR, Pokhilenko NP, Pearson DG, Mertzman SA, Sobolev NV, Finger LW (1997) Composition of the Siberian cratonic mantle: evidence from Udachnaya peridotite xenoliths. Contrib Mineral Petrol 128:228–246

Boyd SR, Pillinger CT (1994) A preliminary-study of $^{15}N/^{14}N$ in octahedral growth form diamonds. Chem Geol 116:43–59

Boyd SR, Mattey DP, Pillinger CT, Milledge HJ, Mendelssohn M, Seal M (1987) Multiple growth events during diamond genesis: an integrated study of carbon and nitrogen isotopes and nitrogen aggregation state in coated stones. Earth Planet Sci Lett 86:341–353
Boyd SR, Pillinger CT, Milledge HJ, Mendelssohn MJ, Seal M (1988) Fractionation of nitrogen isotopes in a synthetic diamond of mixed-crystal habit. Nature 331:604–607
Boyd SR, Pillinger CT, Milledge HJ, Mendelssohn MJ, Seal M (1992) C and N isotopic composition and the infrared absorption spectra of coated diamonds: evidence for the regional uniformity of CO_2–H_2O rich fluids in lithospheric mantle. Earth Planet Sci Lett 109:633–644
Boyd SR, Pineau F, Javoy M (1994) Modelling the growth of natural diamonds. Chem Geol 116:29–42
Brey GP, Bulatov V, Girnis A, Harris JW, Stachel T (2004) Ferropericlase–a lower mantle phase in the upper mantle. Lithos 77:655–663
Bulanova GP, Pearson DG., Hauri EH, Griffin BJ (2002) Carbon and nitrogen isotope systematics within a sector-growth diamond from the Mir kimberlite, Yakutia. Chem Geol 188:105–123
Bureau H, Remusat L, Esteve I, Pinti DL, Cartigny P (2018) The growth of lithospheric diamonds. Sci Adv 4:eaat1602
Burgess R, Cartigny P, Harrison D, Hobson E, Harris J (2009) Volatile composition of microinclusions in diamonds from the Panda kimberlite, Canada: Implications for chemical and isotopic heterogeneity in the mantle. Geochim Cosmochim Acta 73:1779–1794
Burton JA, Prim RC, Slichter WP (1953) The distribution of solute in crystals grown from the melt. Part I. Theoretical. J Chem Phys 21:1987–1991
Cartigny P (2005) Stable isotopes and the origin of diamond. Elements 1:79–84
Cartigny P (2010) Mantle-related carbonados? Geochemical insights from diamonds from the Dachine komatiite (French Guiana). Earth Planet Sci Lett 296:329–339
Cartigny P, Marty B (2013) Nitrogen isotopes and mantle geodynamics: The emergence of life and the atmosphere-crust–mantle connection. Elements 9:359–366
Cartigny P, Boyd SR, Harris JW, Javoy M (1997) Nitrogen isotopes in peridotitic diamonds from Fuxian, China: the mantle signature. Terra Nova 9:175–179
Cartigny P, Harris JW, Javoy M (1998) Eclogitic diamond formation at Jwaneng: No room for a recycled component. Science 280:1421–1424
Cartigny P, Harris JW, Javoy M (2001) Diamond genesis, mantle fractionations and mantle nitrogen content: a study of $\delta^{13}C$–N concentrations in diamonds. Earth Planet Sci Lett 185:85–98
Cartigny P, Harris JW, Taylor A, Davies R, Javoy M (2003) On the possibility of a kinetic fractionation of nitrogen stable isotopes during natural diamond growth. Geochim Cosmochim Acta 67:1571–1576
Cartigny P, Stachel T, Harris JW, Javoy M (2004) Constraining diamond metasomatic growth using C- and N-stable isotopes: examples from Namibia. Lithos 77:359–373
Cartigny P, Farquhar J, Thomassot E, Harris JW, Wing B, Masterson A, McKeegan K, Stachel T (2009) A mantle origin for Paleoarchean peridotitic diamonds from the Panda kimberlite, Slave Craton: Evidence from ^{13}C-, ^{15}N- and $^{33,34}S$-stable isotope systematics. Lithos 112:852–864
Cartigny P, Palot M, Thomassot E, Harris JW (2014) Diamond formation: a stable isotope perspective. Annu Rev Earth Planet Sci 42:699–732
Casciotti KL (2009) Inverse kinetic isotope fractionation during bacterial nitrite oxidation. Geochim Cosmochim Acta 73:2061–2076
Chacko T, Mayeda TK, Clayton RN, Goldsmith JR (1991) Oxygen and carbon isotope fractionations between CO_2 and calcite. Geochim Cosmochim Acta 55:2867–2882
Chacko T, Cole DR, Horita J (2001) Equilibrium oxygen, carbon and hydrogen isotope fractionation factors applicable to geological systems. Rev Mineral Geochem 43:1–81
Chauvel C, Lewin E, Carpentier M, Arndt N, Marini JC (2008) The role of recycled oceanic basalt and sediment in generating the Hf-Nd mantle array. Nat Geosci 1:64–67
Cherniak DJ, Watson EB, Meunier V, Kharche N (2018) Diffusion of helium, hydrogen and deuterium in diamond: Experiment, theory and geochemical applications. Geochim Cosmochim Acta 232:206–224
Chinn IL, Perritt SH, Stiefenhofer J, Stern RA (2018) Diamonds from Orapa Mine show a clear subduction signature in SIMS stable isotope data. Mineral Petrol 112:197–207
Chopin C (2003) Ultrahigh-pressure metamorphism: tracing continental crust into the mantle. Earth Planet Sci Lett 212:1–14
Chrenko RM, Tuft RE, Strong HM (1977) Transformation of the state of nitrogen in diamond. Nature 270:141–144
Clayton RN, Goldsmith JR, Karel KJ, Mayeda TK, Newton RC (1975) Limits on the effect of pressure on isotopic fractionation. Geochim Cosmochim Acta 39:1197–1201
Craig H (1953) The geochemistry of the stable carbon isotopes. Geochim Cosmochim Acta 3:53–92
Craven JA, Harte B, Fisher D, Schulze DJ (2009) Diffusion in diamond. I. Carbon isotope mapping of natural diamond. Mineral Mag 73:193–200
Daulton TL, Ozima M (1996) Radiation-induced diamond formation in uranium-rich carbonaceous materials. Science 271:1260–1263

Dauphas N, Marty B (1999) Heavy nitrogen in carbonatites of the Kola Peninsula: A possible signature of the deep mantle. Science 286:2488–2490
Davies GR, Nixon PH, Pearson DG, Obata M (1993) Tectonic implications of graphitized diamonds from the Ronda, peridotite massif, southern Spain. Geology 21:471–474
Davies RM, Griffin WL, O'Reilly SY, Andrew AS (2003) Unusual mineral inclusions and carbon isotopes of alluvial diamonds from Bingara, eastern Australia. Lithos 69:51–66
De Corte K, Cartigny P, Shatsky VS, Sobolev NV, Javoy M (1998) Evidence of fluid inclusions in metamorphic microdiamonds from the Kokchetav massif, northern Kazakhstan. Geochim Cosmochim Acta 62:3765–3773
De Corte K, Cartigny P, Shatsky VS, Sobolev NV, Javoy M (1999) Characteristics of microdiamonds from UHPM rocks of the Kokchetav massif (Kazakhstan). *In:* Proc 7th Int Kimberlite Conf Vol. 1, Gurney JJ et al. (eds) Red Roof Design, Cape Town, p 174–182
De Stefano A, Kopylova MG, Cartigny P, Afanasiev V (2009) Diamonds and eclogites of the Jericho kimberlite (Northern Canada). Contrib Mineral Petrol 158:295–315
Deines P (1980) The carbon isotopic composition of diamonds: relationship to diamond shape, color, occurrence and vapor composition. Geochim Cosmochim Acta 44:943–961
Deines P (2002) The carbon isotope geochemistry of mantle xenoliths. Earth Sci Rev 58:247–278
Deines P (2004) Carbon isotope effects in carbonate systems. Geochim Cosmochim Acta 68:2659–2579
Deines P, Eggler DH (2009) Experimental determination of carbon isotope fractionation between $CaCO_3$ and graphite. Geochim Cosmochim Acta 73:7256–7274
Deines P, Haggerty SE (2000) Small-scale oxygen isotope variations and petrochemistry of ultradeep (> 300 km) and transition zone xenoliths. Geochim Cosmochim Acta 64:117–131
Deines P, Gurney JJ, Harris JW (1984) Associated chemical and carbon isotopic composition variations in diamonds from Finsch and Premier kimberlite, South-Africa. Geochim Cosmochim Acta 48:325–342
Deines P, Harris JW, Spear PM. Gurney JJ (1989) Nitrogen and ^{13}C content of Finsch and Premier diamonds and their implications. Geochim Cosmochim Acta 53:1367–1378
Deines P, Harris JW, Robinson DN, Gurney JJ, Shee SR (1991) Carbon and oxygen isotope variations in diamond and graphite eclogites from Orapa, Botswana, and the nitrogen-content of their diamonds. Geochim Cosmochim Acta 55:515–524
Deines P, Stachel T, Harris JW (2009) Systematic regional variations in diamond carbon isotopic composition and inclusion chemistry beneath the Orapa kimberlite cluster, in Botswana. Lithos 112:776–784
Donnelly CL, Stachel T, Creighton S, Muehlenbachs K, Whiteford S (2007) Diamonds and their mineral inclusions from the A154 South pipe, Diavik Diamond Mine, Northwest Territories, Canada. Lithos 98:160–176
Dobrzhinetskaya LF, O'Bannon EF III, Sumino H (2022) Non-cratonic diamonds from UHP metamorphic terranes, ophiolites and volcanic sources. Rev Mineral Geochem 88:191–256
Eggler DH, Baker DR (1982) Reduced volatiles in the system C–O–H: Implications for mantle melting, fluid formation and diamond genesis. In: High pressure research in geophysics. Akimoto S, Manghnani MH (eds) Center for Academic Publications, Tokyo, p 237–250
Evans T, Qi Z (1982) The kinetics of the aggregation of nitrogen atoms in diamond. Proc R Soc London A381:159–178
Evans T, Harris JW (1989) Nitrogen aggregation, inclusion equilibration temperatures and the age of diamonds. In Kimberlites and Related Rocks. Proc 4th Int Kimberlite Conf, GSA Spec Publ 14 Vol. 2, Ross J et al. (eds) Blackwell, Carlton, p. 1001–1006
Farquhar J, Wing BA, McKeegan KD, Harris JW, Cartigny P, Thiemens MH (2002) Mass-independent sulfur of inclusions in diamond and sulfur recycling on early Earth. Sci 298:2369–2372
Fitzsimons ICW, Harte B, Chinn IL, Gurney JJ, Taylor WR (1999) Extreme chemical variation in complex diamonds from George Creek, Colorado: a SIMS study of carbon isotope composition and nitrogen abundance. Mineral Mag 63:857–878
Fitzsimons ICW, Harte B, Clark RM (2000) SIMS stable isotope measurement: counting statistics and analytical precision. Mineral Mag 64:59–83
Fraley C, Raftery AE (2002) Model-based clustering, discriminant analysis, and density estimation. J Am Stat Assoc 97:611–631
Frost DJ, McCammon CA (2008) The redox state of Earth's mantle. Annu Rev Earth Planet Sci 36:389–420
Galbraith RF (2005) Statistics for Fission Track Analysis. Chapman and Hall/CRC, Boca Raton, Florida
Galimov EM (1991) Isotope fractionation related to kimberlite magmatism and diamond formation. Geochim Cosmochim Acta 55:1697–1708
Garai J, Haggerty SE, Rekhi S, Chance M (2006) Infrared absorption investigations confirm the extraterrestrial origin of carbonado diamonds. Astrophys J 653:L153–L156
Giuliani A, Kamenetsky VS, Phillips D, Kendrick MA, Wyatt BA, Goemann K (2012) Nature of alkali-carbonate fluids in the sub-continental lithospheric mantle. Geology 40:967–970
Green BL, Collins AT, Breeding CM (2022) Diamond spectroscopy, defect centers, color, and treatments. Rev Mineral Geochem 88:637–688

Gurney JJ, Harris JW, Rickard RS (1984) Silicate and oxide inclusions in diamonds from the Orapa Mine, Botswana. *In*: Kimberlites II: the mantle and crust-mantle relationships. Kornprobst J (ed) Elsevier, Amsterdam, p 3–9
Haggerty SE (2014) Carbonado: Physical and chemical properties, a critical evaluation of proposed origins, and a revised genetic model. Earth Sci Rev 130:49–72
Hanschmann G (1981) Berechnung von Isotopieeffekten auf quantenchemischer Grundlage am Beispiel stickstoffhaltiger Moleküle. ZFI-Mitteilungen 41:19–39
Harris JW, Hawthorne JB, Oosterveld MM (1986) A comparison of characteristics of diamonds from Orapa and Jwaneng kimberlite pipes in Botswana. Extended Abstr 4th Int Kimperlite Conf Geol Soc Australia Spec Publ 16:395–397
Harris JW, Smit KV, Fedortchouk Y, Moore M (2022) Morphology of monocrystalline diamond and its inclusions. Rev Mineral Geochem 88:119–166
Harte B (2010) Diamond formation in the deep mantle: the record of mineral inclusions and their distribution in relation to mantle dehydration zones. Mineral Mag 74:189–215
Harte B, Otter M, McKeegan K (1992) Carbon isotope measurements on diamonds. Chem Geol 101:177–183
Harte B, Fitzsimons ICW, Harris JW, Otter ML (1999) Carbon isotope ratios and nitrogen abundances in relation to cathodoluminescence characteristics for some diamonds from the Kaapvaal Province, S-Africa. Mineral Mag 63:829–856
Harte B, Taniguchi T, Chakraborty S (2009) Diffusion in diamond. II. High-pressure-temperature experiments. Mineral Mag 73:201–204
Hasterok D, Chapman DS (2011) Heat production and geotherms for the continental lithosphere. Earth Planet Sci Lett 307:59–70
Hauri EH, Pearson DG, Bulanova GP, Milledge HJ (1999) Microscale variations in C and N isotopes within mantle diamonds revealed by SIMS. *In:* Proc 7th Int Kimberlite Conf Vol 1. Gurney JJ et al. (eds) Red Roof Design, Cape Town, p 341–347
Hogberg K, Stachel T, Stern RA (2016) Carbon and nitrogen isotope systematics in diamond: Different sensitivities to isotopic fractionation or a decoupled origin? Lithos 265:16–30
Holland G, Lollar B, Li L et al. (2013) Deep fracture fluids isolated in the crust since the Precambrian era. Nature 497:357–360
Horita J (2001) Carbon isotope exchange in the system CO_2–CH_4 at elevated temperatures. Geochim Cosmochim Acta 65:1907–1919
Horita J, Polyakov VB (2015) Carbon-bearing iron phases and the carbon isotope composition of the deep Earth. PNAS 112:31–36
Horita J, Wesolowski DJ (1994) Liquid–vapor fractionation of oxygen and hydrogen isotopes of water from the freezing to the critical temperature. Geochim Cosmochim Acta 58:3425–3437
Hough RM, Gilmour I, Pillinger CT, Arden JW, Gilkes KWR, Yuan J, Milledge HJ (1995) Diamond and silicon-carbide in impact melt rock from the Ries impact crater. Nature 378:41–44
Howell D, O'Neill CJ, Grant KJ, Griffin WL, O'Reilly SY, Pearson NJ, Stern RA, Stachel T (2012) Platelet development in cuboid diamonds: insights from micro-FTIR mapping. Contrib Mineral Petrol 164:1011–1025
Howell D, Griffin WL, Yang J, Gain S, Stern RA, Huang JX, Jacob DE, Xu X, Stokes AJ, O'Reilly SY, Pearson NJ (2015a) Diamonds in ophiolites: Contamination or a new diamond growth environment? Earth Planet Sci Lett 430:284–295
Howell D, Stern RA, Griffin WL, Southworth R, Mikhail S, Stachel T (2015b) Nitrogen isotope systematics and origins of mixed-habit diamonds. Geochim Cosmochim Acta 157:1–12
Howell D, Stachel T, Stern RA, Pearson DG, Nestola F, Hardman MF, Harris JW, Jaques AL, Shirey SB, Cartigny P, Smit KV (2020) Deep carbon through time: Earth's diamond record and its implications for carbon cycling and fluid speciation in the mantle. Geochim Cosmochim Acta 275:99–122
Huss GR (2005) Meteoritic nanodiamonds: Messengers from the stars. Elements 1:97–100
Ickert RB, Stachel T, Stern RA, Harris JW (2013) Diamond from recycled crustal carbon documented by coupled $\delta^{18}O$–$\delta^{13}C$ measurements of diamonds and their inclusions. Earth Planet Sci Lett 364:85–97
Jacob DE (2004) Nature and origin of eclogite xenoliths from kimberlites. Lithos 77:295–316
Jacob DE, Mikhail S (2022) Polycrystalline diamonds from kimberlites: Snapshots of rapid and episodic diamond formation in the lithospheric mantle. Rev Mineral Geochem 88:167–190
Jablon BM, Navon O (2016) Most diamonds were created equal. Earth Planet Sci Lett 443:41–47
Javoy M, Pineau F, Iiyama I (1978) Experimental-determination of isotopic fractionation between gaseous CO_2 and carbon dissolved in tholeiitic magma–preliminary study. Contrib Mineral Petrol 67:35–39
Javoy M, Pineau F, Allegre CJ (1982) Carbon geodynamic cycle. Nature 300:171–173
Javoy M, Pineau F, Demaiffe D (1984) Nitrogen and carbon isotopic composition in the diamonds of Mbuji Mayi (Zaïre). Earth Planet Sci Lett 68:399–412
Javoy M, Pineau F, Delorme H (1986) Carbon and nitrogen isotopes in the mantle. Chem Geol 57:41–62
Johnson CN, Stachel T, Muehlenbachs K, Stern RA, Armstrong JP, EIMF (2012) The micro-/macro-diamond relationship: A case study from the Artemisia kimberlite (Northern Slave Craton, Canada). Lithos 148:86–97

Kagi H, Fukura S (2008) Infrared and Raman spectroscopic observations of Central African carbonado and implications for its origin. Euro J Mineral 20:387–393

Kaiser W, Bond L (1959) Nitrogen, a major impurity in common type I diamonds. Phys Rev 115:857–863

Kamiya Y, Lang AR (1964) On the structure of coated diamonds. Philos Mag 11:347–356

Kelemen PB, Manning CE (2015) Reevaluating carbon fluxes in subduction zones, what goes down, mostly comes up. PNAS 112:E3997–E4006

Kessel R, Ulmer P, Pettke T, Schmidt MW, Thompson AB (2005) The water-basalt system at 4 to 6 GPa: Phase relations and second critical endpoint in a K-free eclogite at 700 to 1400 degrees C. Earth Planet Sci Lett 237:873–892

Kessel R, Pettke T, Fumagalli P (2015) Melting of metasomatized peridotite at 4–6 GPa and up to 1200 °C: an experimental approach. Contrib Mineral Petrol 169:1–19

Kieffer SW (1982) Thermodynamics and lattice vibrations of minerals: 5. Application to phase equilibria, isotopic fractionation, and high-pressure thermodynamic properties. Rev Geophys Space Phys 20:827–849

Kjarsgaard BA, de Wit M, Heaman LM, Pearson DG, Stiefenhofer J, Janusczcak N, Shirey SB (2022) A review of the geology of global diamond mines and deposits. Rev Mineral Geochem 88:1–118

Klein-BenDavid O, Logvinova AM, Schrauder M, Spetius ZV, Weiss Y, Hauri EH, Kaminsky FV, Sobolev NV, Navon O (2009) High-Mg carbonatitic microinclusions in some Yakutian diamonds—a new type of diamond-forming fluid. Lithos 112 Suppl 2:648–659

Klein-BenDavid O, Pearson DG, Nowell GM, Ottley C, McNeill JCR, Cartigny P (2010) Mixed fluid sources involved in diamond growth constrained by Sr–Nd–Pb–C–N isotopes and trace elements. Earth Planet Sci Lett 289:123–133

Knoche R, Sweeney RJ, Luth RW (1999) Carbonation and decarbonation of eclogites: the role of garnet. Contrib Mineral Petrol 135:332–339

Koeberl C, Masaitis VL, Shafranovsky GI, Gilmour I, Langenhorst F, Schrauder M (1997) Diamonds from the Popigai impact structure, Russia. Geology 25:967–970

Koga KT, Van Orman JA, Walter MJ (2003) Diffusive relaxation of carbon and nitrogen isotope heterogeneity in diamond: a new thermochronometer. Phys Earth Planet Sci 139:35–43

Koga KT, Walter MJ, Nakamura E, Kobayashi K (2005) Carbon self-diffusion in a natural diamond. Phys Rev B 72:024108

Korsakov AV, Rezvukhina OV, Jaszczak JA, Rezvukhin DI, Mikhailenko DS (2019) Natural graphite cuboids. Minerals 9:110

Koval'skiy VV, Galimov EM, Prokhorov VS (1972) Isotopic composition of carbon from colored Yakutian diamonds. Trans (Doklady) USSR Acad Sci 203:118–119 (translated from Doklady Akademii Nauk SSSR, 1982, 203:1440–1442)

Krebs MY, Pearson DG, Stachel T, Stern RA, Nowicki T, Cairns S (2016) Using microdiamonds in kimberlite diamond grade prediction: a case study of the variability in diamond population characteristics across the size range 0.2 to 3.4 mm in Misery kimberlite, Ekati Mine, NWT, Canada. Econ Geol 111:503–525

Kruber C, Thorseth IH, Pedersen RB (2008) Seafloor alteration of basaltic glass: Textures, geochemistry, and endolithic microorganisms. Geochem Geophys Geosystems 9:12

Kueter N, Lilley MD, Schmidt MW, Bernasconi SM (2019a) Experimental carbonatite/graphite carbon isotope fractionation and carbonate/graphite geothermometry. Geochim Cosmochim Acta 253:290–306

Kueter N, Schmidt MW, Lilley MD, Bernasconi SM (2019b) Experimental determination of equilibrium CH_4–CO_2–CO carbon isotope fractionation factors (300–1200 °C). Earth Planet Sci Lett 506:64–75

Kueter N, Schmidt MW, Lilley MD, Bernasconi SM (2020) Kinetic carbon isotope fractionation links graphite and diamond precipitation to reduced sources. Earth Planet Sci Lett 529:115848

Labidi J, Barry PH, Bekaert DV, et al. (2020) Hydrothermal ^{15}N–^{15}N abundances constrain the origins of mantle nitrogen. Nature 580:367–371

Lavoisier A-L (1776) Second mémoire sur la destruction du diamant au grand verre brûlant de Tschirnausen, connu sous le nom de Lentille du Palais royal, Mémoires de l'Académie royale des sciences. 1772 II:591–616

Leech M, Ernst WG (1998) Graphite pseudomorphs after diamond? A carbon isotope and spectroscopic study of graphite cuboids from the Maksyutov Complex, south Ural Mountains, Russia. Geochim Cosmochim Acta 62:2143–2154

Li K, Li L, Pearson DG, Stachel T (2019) Diamond isotope compositions indicate altered igneous oceanic crust dominates deep carbon recycling. Earth Planet Sci Lett 516:190–201

Li Y, Keppler H (2014) Nitrogen speciation in mantle and crustal fluids. Geochim Cosmochim Acta 129:13–32

Liu J, Wang W, Yang H, Wu Z, Hu MY, Zhao J, Bi W, Alp EE, Dauphas N, Liang W, Chen B, Lin JF (2019) Carbon isotopic signatures of super-deep diamonds mediated by redox chemistry. Geochem Perspec Lett 10:51–55

Lowry D, Mattey DP, Harris JW (1999) Oxygen isotope composition of syngenetic inclusions in diamond from the Finsch Mine, RSA. Geochim Cosmochim Acta 63:1825–1836

Luth RW (1993) Diamonds, eclogites, and the oxidation state of the Earth's mantle. Science 261:66–68

Luth RW (2017) Diamond formation during parital melting in the Earth's mantle. Geol Soc Am 129th Annual Meeting, Seattle, abstract # 20–6

Luth RW, Stachel T (2014) The buffering capacity of lithospheric mantle: implications for diamond formation. Contrib Mineral Petrol 168:1–12

Luth RW, Palyanov YN, Bureau H (2022) Experimental petrology applied to natural diamond growth. Rev Mineral Geochem 88:755–808

Marty B (2012) The origins and concentrations of water, carbon, nitrogen and noble gases on Earth. Earth Planet Sci Lett 313–314:56–66
Marty B, Dauphas N (2003) The nitrogen record of crust–mantle interaction and mantle convection from Archean to present. Earth Planet Sci Lett 206:397–410
Matsuhisa Y, Goldsmith JR, Clayton RN (1978) Mechanisms of hydrothermal crystallization of quartz at 250 °C and 15 kbar. Geochim Cosmochim Acta 42:173–182
Mattey DP (1991) Carbon-dioxide solubility and carbon isotope fractionation in basaltic melt. Geochim Cosmochim Acta 55:3467–3473
Mattey DP, Carr RH, Wright IP, Pillinger CT (1984) Carbon isotopes in submarine basalts. Earth Planet Sci Lett 70:196–206
Mattey DP, Taylor WR, Green DH, Pillinger CT (1990) Carbon isotopic fractionation between CO_2 vapor, silicate and carbonate melts–an experimental-study to 30 kbar. Contrib Mineral Petrol 104:492–505
Matveev S, Stachel T (2009) Evaluation of kimberlite diamond potential using FTIR spectroscopy of xenocrystic olivine. Lithos 112:36–40
McCandless TE, Gurney JJ (1997) Diamond eclogites: Comparison with carbonaceous chondrites, carbonaceous shales, and microbial carbon-enriched MORB. Geol Geofiz 38:371–381
McDade P, Harris JW (1999) Syngenetic inclusions bearing diamonds from Letseng-La-Terai, Lesotho. *In:* Proc 7th Int Kimberlite Conf Vol 2. Gurney JJ et al. (eds) Red Roof Design, Cape Town, p 557–565
Meyer HOA (1987) Inclusions in diamond. *In:* Mantle Xenoliths. Nixon PH (ed) John Wiley and Sons Ltd., Chichester, p 501–522
Meyer HOA, Boyd FR (1972) Composition and origin of crystalline inclusions in natural diamonds. Geochim Cosmochim Acta 36:1255–1273
Milledge HJ, Mendelssohn MJ, Seal M, Rouse JE, Swart PK, Pillinger CT (1983) Carbon isotopic variation in spectral type II diamonds. Nature 303:791-792
Mikhail S, Howell D (2016) A petrological assessment of diamond as a recorder of the mantle nitrogen cycle. Am Mineral 101:780–787
Mikhail S, Sverjensky DA (2014) Nitrogen speciation in upper mantle fluids and the origin of Earth's nitrogen-rich atmosphere. Nat Geosci 7:816–819
Mikhail S, Verchovsky AB, Howell D, Hutchison MT, Southworth R, Thomson AR, Warburton P, Jones AP, Milledge HJ (2014) Constraining the internal variability of the stable isotopes of carbon and nitrogen within mantle diamonds. Chem Geol 366:14–23
Moore RO, Gurney JJ (1985) Pyroxene solid solution in garnets included in diamond. Nature 318:553–555
Mysen B (2018) Mass transfer in the Earth's interior: fluid–melt interaction in aluminosilicate–C–O–H–N systems at high pressure and temperature under oxidizing conditions. Prog Earth Planet Sci 5:6
Mysen B (2019) Nitrogen in the Earth: abundance and transport. Prog Earth Planet Sci 6:38
Navon O (1991) High internal-pressures in diamond fluid inclusions determined by infrared-absorption. Nature 353:746–748
Navon O, Hutcheon ID, Rossman GR, Wasserburg GJ (1988) Mantle-derived fluids in diamond micro-inclusions. Nature 355:784–789
Nimis P (2022) Pressure and temperature data for diamonds. Rev Mineral Geochem 88:533–566
Nimis P, Alvaro M, Nestola F, Angel RJ, Marquardt K, Rustioni G, Harris JW, Marone F (2016) First evidence of hydrous silicic fluid films around solid inclusions in gem-quality diamonds. Lithos 260:384–389
Nier AO (1947) A mass spectrometer for isotope and gas analysis. Rev Sci Instrum18:398–411
Nier AO, Gulbransen EA (1939) Variations in the relative abundance of the carbon isotopes. J Am Chem Soc 61:697–698
Nisbet EG, Mattey DP, Lowry D (1994) Can diamonds be dead bacteria. Nature 367:694–694
Novella D, Bolfan-Casanova N, Nestola F, Harris JW (2015) H_2O in olivine and garnet inclusions still trapped in diamonds from the Siberian craton: Implications for the water content of cratonic lithosphere peridotites. Lithos 230:180–183
O'Neil JR (1986) Theoretical and experimental aspects of isotopic fractionation. Rev Mineral 16:1–40
O'Neill HS, Rubie DC, Canil D, Geiger CA, Ross CR, Seifert F, Woodland AB (1993) Ferric iron in the upper mantle and in transition zone assemblages: Implications for relative oxygen fugacities in the mantle. *In:* Evolution of the Earth and Planets. Vol 74. Am Geophys Union Geophys Monograph Ser, p 73–88
Palot M, Cartigny P, Harris JW, Kaminsky FV, Stachel T (2012) Evidence for deep mantle convection and primordial heterogeneity from nitrogen and carbon stable isotopes in diamond. Earth Planet Sci Lett 357–358:179–193
Palot M, Pearson DG, Stern RA, Stachel T, Harris JW (2013) Multiple growth events, processes and fluid sources involved in diamond genesis: A micro-analytical study of sulphide-bearing diamonds from Finsch mine, RSA. Geochim Cosmochim Acta 106:51–70
Palot M, Pearson DG, Stern RA, Stachel T, Harris JW (2014) Isotopic constraints on the nature and circulation of deep mantle C–H–O–N fluids: Carbon and nitrogen systematics within ultra-deep diamonds from Kankan (Guinea). Geochim Cosmochim Acta 139:26–46
Palot M, Pearson DG, Stachel T, Stern RA, Le Pioufle A, Gurney JJ, Harris JW (2017) The transition zone as a host for recycled volatiles: Evidence from nitrogen and carbon isotopes in ultra-deep diamonds from Monastery and Jagersfontein (South Africa). Chem Geol 466:733–749

Pearson DG, Davies GR, Nixon PH, Milledge HJ (1989) Graphitized diamonds from a peridotite massif in Morocco and implications for anomalous diamond occurrences. Nature 338:60–62

Pearson DG, Davies GR, Nixon PH, Mattey DP (1991) A carbon isotope study of diamond facies pyroxenites and associated rocks from the Beni Bousera Peridotite, North Morocco. J Petrol Spec Vol 2:175–189

Pearson DG, Canil D, Shirey SB (2003) Mantle samples included in volcanic rocks: xenoliths and diamonds. Chapter 5 *In*: Treatise on Geochemistry vol. 2:171–275. Elsevier, Amsterdam

Pearson DG, Brenker FE, Nestola F, McNeill J, Nasdala L, Hutchison MT, Matveev S, Mather K, Silversmit G, Schmitz S, Vekemans B (2014) Hydrous mantle transition zone indicated by ringwoodite included within diamond. Nature 507:221–224

Peats J, Stachel T, Stern RA, Muehlenbachs K, Armstrong J (2012) Aviat diamonds: a window into the deep lithospheric mantle beneath the northern Churchill Province, Melville Peninsula, Canada. Can Mineral 50:611–624

Peslier AH, Woodland AB, Bell DR, Lazarov M (2010) Olivine water contents in the continental lithosphere and the longevity of cratons. Nature 467:78–81

Petts DC, Chacko T, Stachel T, Stern RA, Heaman LM (2015) A nitrogen isotope fractionation factor between diamond and its parental fluid derived from detailed SIMS analysis of a gem diamond and theoretical calculations. Chem Geol 410:188–200

Plank T, Manning CE (2019) Subducting carbon. Nature 574:343–352

Pokhilenko NP, Sobolev NV, Reutsky VN, Hall AE, Taylor LA (2004) Crystalline inclusions and C isotope ratios in diamonds from the Snap Lake/King Lake kimberlite dyke system: evidence of ultradeep and enriched lithospheric mantle. Lithos 77:57–67

Polyakov VB, Kharlashina NN (1994) Effect of pressure on equilibrium isotopic fractionation. Geochim Cosmochim Acta 58:4739–4750

Polyakov VB, Kharlashina NN (1995) The use of heat-capacity data to calculate carbon-isotope fractionation between graphite, diamond, and carbon-dioxide—a new approach. Geochim Cosmochim Acta 59:2561–2572

Ray JS, Ramesh R (2000) Rayleigh fractionation of stable isotopes from a multicomponent source. Geochim Cosmochim Acta 64:299–306

Regier ME, Pearson DG, Stachel T, Luth RW, Stern RA, Harris JW (2020) The lithospheric-to-lower-mantle carbon cycle recorded in superdeep diamonds. Nature 585:234–238

Reutsky VN, Harte B, EIMF, Borzdov YM, Palyanov YN (2008) Monitoring diamond crystal growth, a combined experimental and SIMS study. Eur J Mineral 20:365–374

Reutsky V, Borzdov Y, Palyanov Y, Sokol A, Izokh O (2015a) Carbon isotope fractionation during experimental crystallization of diamond from carbonate fluid at mantle conditions. Contrib Mineral Petrol 170:41

Reutsky V, Borzdov YM, Palyanov YN (2015b) Carbon isotope fractionation during high pressure and high temperature crystallization of Fe-C melt. Chem Geol 406:18–24

Reutsky VN, Shiryaev AA, Titkov SV, Wiedenbeck M, Zudina NN (2017) Evidence for large scale fractionation of carbon isotopes and of nitrogen impurity during crystallization of gem quality cubic diamonds from placers of North Yakutia. Geochem Int 55:988–999

Richardson SH, Gurney JJ, Erlank AJ, Harris JW (1984) Origin of diamonds in old enriched mantle. Nature 310:198–202

Richardson SH, Erlank AJ, Hart SR (1985) Kimberlite-borne garnet peridotite xenoliths from old enriched subcontinental lithosphere. Earth Planet Sci Lett 75:116–128

Richardson SH, Harris JW, Gurney JJ (1993) Three generations of diamonds from old continental mantle. Nature 366:256–258

Richet P, Bottinga Y, Javoy M (1977) A review of hydrogen, carbon, nitrogen, oxygen, sulphur, and chlorine stable isotope fractionation among gaseous molecules. Annu Rev Earth Planet Sci 5:65–110

Robert F, Rejou-Michel A, Javoy M (1992) Oxygen isotopic homogeneity of the Earth: new evidence. Earth Planet Sci Lett 108:1–9

Robertson R, Fox JJ, Martin AE (1934) Two types of diamond. Philos Trans R S (London), Ser A 232:463–535

Robinson DN, Scott JA, Van Niekerk A, Anderson VG (1989) The sequence of events reflected in the diamonds of some southern African kimberlites. *In:* Kimberlites and Related Rocks: Their Mantle/Crust Setting, Diamonds, and Diamond Exploration, GSA Spec Publ 14. Vol 2. Ross J et al. (eds) Blackwell, Carlton, p 990–1000

Rohrbach A, Schmidt MW (2011) Redox freezing and melting in the Earth's deep mantle resulting from carbon-iron redox coupling. Nature 472:209–212

Rohrbach A, Ghosh S, Schmidt MW, Wijbrans CH, Klemme S (2014) The stability of Fe–Ni carbides in the Earth's mantle: Evidence for a low Fe–Ni–C melt fraction in the deep mantle. Earth Planet Sci Lett 388:211–221

Rosenbaum JM (1994) Stable isotope exchange between carbon dioxide and calcite at 900 °C. Geochim Cosmochim Acta 58:3747–3753

Rudge JF (2008) Finding peaks in geochemical distributions: A re-examination of the helium-continental crust correlation. Earth Planet Sci Lett 274:179–188

Rumble D, Miller MF, Franchi IA, Greenwood RC (2007) Oxygen three-isotope fractionation lines in terrestrial silicate minerals: An inter-laboratory comparison of hydrothermal quartz and eclogitic garnet. Geochim Cosmochim Acta 71:3592–3600

Satish-Kumar M, So H, Yoshimo T, Mutsumi K, Hiroi Y (2011) Experimental determination of carbon isotope fractionation between iron carbide melt and carbon: ^{12}C-enriched carbon in the Earth's core? Earth Planet Sci Lett 310:340–348

Sautter V, Haggerty SE, Field S (1991) Ultradeep (>300 kilometers) ultramafic xenoliths—petrological evidence from the transition zone. Science 252:827–830

Schauble EA, Ghosh P, and Eiler JM (2006) Preferential formation of ^{13}C–^{18}O bonds in carbonate minerals, estimated using first-principles lattice dynamics. Geochim Cosmochim Acta 70:2510–2529

Scheele N, Hoefs J (1992) Carbon isotope fractionation between calcite, graphite and CO_2: An experimental study. Contrib Mineral Petrol 112:35–4

Schidlowski M (2001) Carbon isotopes as biogeochemical recorders of life over 3.8 Ga of Earth history: evolution of a concept. Precambrian Res 106:117–134

Schulze DJ, Harte B, Valley JW, Brenan JM, Channer DMD (2003) Extreme crustal oxygen isotope signatures preserved in coesite in diamond. Nature 423:68–70

Schulze DJ, Harte B, Edinburgh Ion Microprobe Facility staff, Page FZ, Valley JW, Channer DM, Jaques AL (2013) Anticorrelation between low δ^{13}C of eclogitic diamonds and high δ^{18}O of their coesite and garnet inclusions requires a subduction origin. Geology 41:455–458

Shatsky VS, Zedgenizov DA, Ragozin AL, Kalinina VV (2014) Carbon isotopes and nitrogen contents in placer diamonds from the NE Siberian craton: implications for diamond origins. Euro J Mineral 26:41–52

Shilobreeva S, Martinez I, Busigny V, Agrinier P, Laverne C (2011) Insights into C and H storage in the altered oceanic crust: Results from ODP/IODP Hole 1256D. Geochim Cosmochim Acta 75:2237–2255

Smit KV, Timmerman S, Aulbach S, Shirey SB, Richardson SH, Phillips D, Pearson DG (2022) Geochronology of diamonds. Rev Mineral Geochem 88:567–636

Shiryaev AA, Gaillard F (2014) Local redox buffering by carbon at low pressures and the formation of moissanite–natural SiC. Euro J Mineral 26:53–59

Simakov SK (2010) Metastable nanosized diamond formation from a C–H–O fluid system. J Mater Res 25:2336–2340

Simakov SK (2011) Nanodiamond formation in natural processes from fluid systems at low *P–T* parameters. Doklady Earth Sci 436:148–151

Slodkevich VV (1980) Polycrystalline aggregates of octahedral-shaped graphite. Doklady Akademii Nauk SSSR 253:697–700 (in Russian)

Slodkevich VV (1983) Graphite pseudomorphs after diamond. Int Geol Rev 25:497–514

Smart KA, Chacko T, Stachel T, Muehlenbachs K, Stern RA, Heaman LM (2011) Diamond growth from oxidized carbon sources beneath the Northern Slave Craton, Canada: A δ^{13}C–N study of eclogite-hosted diamonds from the Jericho kimberlite. Geochim Cosmochim Acta 75:6027–6047

Smart KA, Tappe S, Stern RA, Webb SJ, Ashwal LD (2016) Early Archaean tectonics and mantle redox recorded in Witwatersrand diamonds. Nat Geosci 9:255–259

Smirnov GI, Mofolo MM, Lerotholi PM, Kaminsky FV, Galimov EM, Ivanovskaya IN (1979) Isotopically light carbon in diamonds from some kimberlite pipes in Lesotho. Nature 278:630–630

Smit KV, Shirey SB, Richardson SH, le Roex AP, Gurney JJ (2010) Re–Os isotopic composition of peridotitic sulphide inclusions in diamonds from Ellendale, Australia: Age constraints on Kimberley cratonic lithosphere. Geochim Cosmochim Acta 74:3292–3306

Smit KV, Shirey SB, Stern RA, Steele A, Wang W (2016) Diamond growth from C–H–N–O recycled fluids in the lithosphere: Evidence from CH_4 micro-inclusions and δ^{13}C–δ^{15}N–N content in Marange mixed-habit diamonds. Lithos 265:68–81

Smit KV, Stachel T, Luth RW, Stern RA (2019a) Evaluating mechanisms for eclogitic diamond growth: An example from Zimmi Neoproterozoic diamonds (West African craton). Chem Geol 520:21–32

Smit KV, Shirey SB, Hauri EH, Stern RA (2019b) Sulfur isotopes in diamonds reveal differences in continent construction. Science 364:383–385

Smith EM, Shirey SB, Nestola F, Bullock ES, Wang JH, Richardson SH, Wang WY (2016) Large gem diamonds from metallic liquid in Earth's deep mantle. Science 354:1403–1405

Sobolev NV (1977) Deep-seated inclusions in kimberlites and the problem of the composition of the upper mantle. (Translated from the Russian edition, 1974) AGU, Washington

Sobolev NV, Shatsky VS (1990) Diamond inclusions in garnets from metamorphic rocks–a new environment for diamond formation. Nature 343:742–746

Sobolev NV, Lavrent'ev YG, Pokhilenko NP, Usova LV (1973) Chrome-rich garnets from the kimberlites of Yakutia and their paragenesis. Contrib Mineral Petrol 40:39–52

Sobolev NV, Galimov EM, Ivanovskaya IN, Yefimova ES (1979) Isotopic composition of carbon from diamonds containing crystalline inclusions (in Russian). Doklady Akademii Nauk SSSR 249:1217–1220

Sokol AG, Palyanov YN, Tomilenki AA, Bul'bak TA, Palyanova GA (2017) Carbon and nitrogen speciation in nitrogen-rich C-O-H-N fluids at 5.5–7.8 GPa. Earth Planet Sci Lett 460:234–243

Stachel T (2014) Diamond. Mineral Assoc Canada Short Course Ser 44:1–28

Stachel T, Harris JW (1997) Syngenetic inclusions in diamond from the Birim field (Ghana)—A deep peridotitic profile with a history of depletion and re-enrichment. Contrib Mineral Petrol 127:336–352

Stachel T, Harris JW (2008) The origin of cratonic diamonds–Constraints from mineral inclusions. Ore Geol Rev 34:5–32

Stachel T, Luth RW (2015) Diamond formation—Where, when and how? Lithos 220–223:200–220
Stachel T, Brey GP, Harris JW (2000a) Kankan diamonds (Guinea) I: from the lithosphere down to the transition zone. Contrib Mineral Petrol 140:1–15
Stachel T, Harris JW, Brey GP, Joswig W (2000b) Kankan diamonds (Guinea) II: lower mantle inclusion parageneses. Contrib Mineral Petrol 140:16–27
Stachel T, Brey GP, Harris JW (2005) Inclusions in sublithospheric diamonds: Glimpses of deep Earth. Elements 1:73–78
Stachel T, Harris JW, Muehlenbachs K (2009) Sources of carbon in inclusion bearing diamonds. Lithos 112:625–637
Stachel T, Chacko T, Luth RW (2017) Carbon isotope fractionation during diamond growth in depleted peridotite: Counterintuitive insights from modelling water-maximum CHO fluids as multi-component systems. Earth Planet Sci Lett 473:44–51
Stachel T, Aulbach S, Harris JW (2022) Mineral inclusions in lithospheric diamonds. Rev Mineral Geochem 88:307–392
Stagno V, Frost DJ (2010) Carbon speciation in the asthenosphere: Experimental measurements of the redox conditions at which carbonate-bearing melts coexist with graphite or diamond in peridotite assemblages. Earth Planet Sci Lett 300:72–84
Stagno V, Ojwang DO, McCammon CA, Frost DJ (2013) The oxidation state of the mantle and the extraction of carbon from Earth's interior. Nature 493:84–88
Stern RA, Palot M, Howell D, Stachel T, Pearson DG, Cartigny P, Oh A (2014) Methods and reference materials for SIMS diamond C- and N-isotope analysis. University of Alberta, Education and Research Archive. Canadian Centre for Isotopic Microanalysis, Research Report 14–01:1–87
Stixrude L, Lithgow-Bertelloni C (2007) Influence of phase transformations on lateral heterogeneity and dynamics in Earth's mantle. Earth Planet Sci Lett 263:45–55
Sunagawa I (1990) Growth and morphology of diamond crystals under stable and metastable conditions. J Cryst Growth 99:1156–1161
Sverjensky DA, Huang F (2015) Diamond formation due to a pH drop during fluid–rock interactions. Nat Commun 6:8702
Sverjensky DA, Stagno V, Huang F (2014) Important role for organic carbon in subduction-zone fluids in the deep carbon cycle. Nature Geosci 7:909–913
Swart PK, Pillinger CT, Milledge HJ, Seal M (1983) Carbon isotopic variation within individual diamonds. Nature 303:793–795
Tappert R, Stachel T, Harris JW, Muehlenbachs K, Ludwig T, Brey GP (2005) Diamonds from Jagersfontein (South Africa): messengers from the sublithospheric mantle. Contrib Mineral Petrol 150:505–522
Taylor WR, Jaques AL, Ridd M (1990) Nitrogen-defect aggregation characteristics of some Australian diamonds: Time-temperature constraints on the source regions of pipe and alluvial diamonds. Am Mineral 75:1290–1310
Thomassot E, Cartigny P, Harris JW, Viljoen KS (2007) Methane-related diamond crystallization in the Earth's mantle: Stable isotope evidences from a single diamond-bearing xenolith. Earth Planet Sci Lett 257:362–371
Thomassot E, Cartigny P, Harris JW, Lorand JP, Rollion-Bard C, Chaussidon M (2009) Metasomatic diamond growth: A multi-isotope study 13C, 15N, 33S, 34S of sulphide inclusions and their host diamonds from Jwaneng (Botswana). Earth Planet Sci Lett 282:79–90
Thomson AR, Kohn SC, Bulanova GP, Smith CB, Araujo D, Walter MJ (2014) Origin of sub-lithospheric diamonds from the Juina-5 kimberlite (Brazil): constraints from carbon isotopes and inclusion compositions. Contrib Mineral Petrol 168:1–29
Thomson AR, Walter MJ, Kohn SC, Brooker RA (2016) Slab melting as a barrier to deep carbon subduction. Nature 529:76–79
Timmerman S, Yeow H, Honda M, Howell D, Jaques AL, Krebs MY, Woodland S, Pearson DG, Avila JN, Ireland TR (2019) U–Th/He systematics of fluid-rich 'fibrous' diamonds–Evidence for pre- and syn-kimberlite eruption ages. Chem Geol 515:22–36
Tolansky S, Komatsu H (1967) Abundance of type 2 diamonds. Science 157:1173–1175
Urey HC (1947) The thermodynamic properties of isotopic substances. J Chem Soc 562–581
Valley JW, O'Neil JR (1981) $^{13}C/^{12}C$ exchange between calcite and graphite–a possible thermometer in Grenville marbles. Geochim Cosmochim Acta 45:411–419
Vermeesch P (2012) On the visualisation of detrital age distributions. Chem Geol 312–313:190–194
Viljoen KS, Dobbe R, Smit B, Thomassot E, Cartigny P (2004) Petrology and geochemistry of a diamondiferous lherzolite from the Premier diamond mine, South Africa. Lithos 77:539–552
Vinogradov AP, Kropotova OI, Usitinov VI (1965) Possible source of carbon in diamonds as indicated by the $^{12}C/^{13}C$ ratios. Geochem Int 2:495–503 (translated from Geokhimiya, 1965, n°1966, 1643–1651)
Vinogradov AP, Kropotov OI, Orlov YL, Grinenko VA (1966) Isotopic composition of diamond and carbonado crystals. Geochem Int 3:1123–1125
Walter MJ, Bulanova GP, Armstrong LS, Keshav S, Blundy JD, Gudfinnsson G, Lord OT, Lennie AR, Clark SM, Smith CB, Gobbo L (2008) Primary carbonatite melt from deeply subducted oceanic crust. Nature 454:622–625
Walter MJ, Thomson AR, Smith EM (2022) Geochemistry of silicate and oxide inclusions in sublithospheric diamonds. Rev Mineral Geochem 88:393–450

Wang Y-F, Qin J-Y, Soustelle V, Zhang J-F, Xu H-J (2021) Pyroxene does not always preserve its source hydrogen concentration: Clues from some peridotite xenoliths. Geochim Cosmochim Acta 292:382–408

Watson EB (1996) Surface enrichment and trace-element uptake during crystal growth. Geochim Cosmochim Acta 60:5013–5020

Watson EB (2004) A conceptual model for near-surface kinetic controls on the trace-element and stable isotope composition of abiogenic calcite crystals. Geochim Cosmochim Acta 68:1473–1488

Watson EB, Liang Y (1995) A simple model for sector zoning in slowly grown crystals: Implications for growth rate and lattice diffusion, with emphasis on accessory minerals in crustal rocks. Am Mineral 80:1179–1187

Weiss Y, McNeill J, Pearson DG, Nowell GM, Ottley CJ (2015) Highly saline fluids from a subducting slab as the source for fluid-rich diamonds. Nature 524:339–342

Weiss Y, Cazs J, Navon O (2022) Fluid inclusions in fibrous diamonds. Rev Mineral Geochem 88:475–532

Wickman FE (1956) The cycle of carbon and the stable carbon isotopes. Geochim Cosmochim Acta 9:136–153

Wiggers de Vries DF, Bulanova GP, De Corte K, Pearson DG, Craven JA, Davies GR (2013) Micron-scale coupled carbon isotope and nitrogen abundance variations in diamonds: Evidence for episodic diamond formation beneath the Siberian Craton. Geochim Cosmochim Acta 100:176–199

Wilson MR, Kjarsgaard BA, Taylor B (2007) Stable isotope composition of magmatic and deuteric carbonate phases in hypabyssal kimberlite, Lac de Gras field, Northwest Territories, Canada. Chem Geol 242:435–454

Wirth R, Rocholl A (2003) Nanocrystalline diamond from the Earth's mantle underneath Hawaii. Earth Planet Sci Lett 211:357–369

Wyllie PJ (1987) Metasomatism and fluid generation in mantle xenoliths. *In*: Mantle Xenoliths. Nixon PH (ed) John Wiley and Sons Ltd., Chichester, p 609–621

Xu XZ, Cartigny P, Yang JS, Dilek Y, Xiong FH, Guo GL (2018) Fourier transform infrared spectroscopy data and carbon isotope characteristics of the ophiolite-hosted diamonds from the Luobusa ophiolite, Tibet, and Ray-Iz ophiolite, Polar Urals. Lithosphere 10:156–169

Yaxley GM, Ghosh S, Kiseeva ES, Mallik A, Spandler C, Thomson AR, Walter MJ (2019) CO_2-rich melts in Earth. *In*: Deep Carbon: Past to Present. Orcutt BN, Daniel I, Dasgupta R, (eds). Cambridge University Press, Cambridge, p 129–162

Zedgenizov DA, Harte B (2004) Microscale variations of $\delta^{13}C$ and N content within a natural diamond with mixed-habit growth. Chem Geol 205:169–175

Zedgenizov D, Rubatto D, Shatsky V, Ragozin A, Kalinina V (2016) Eclogitic diamonds from variable crustal protoliths in the northeastern Siberian craton: Trace elements and coupled $\delta^{13}C$–$\delta^{18}O$ signatures in diamonds and garnet inclusions. Chem Geol 422:46–59

Zhang C, Duan Z (2009) A model for C–O–H fluid in the Earth's mantle. Geochim Cosmochim Acta 73:2089–2102